# Biofilm forming and swarming activities of *Bacillus cereus* modulated by multiclass compounds

**By**

**Abdul Rafay Rafiq**

**2020-GCUF-011107**

This report is submitted in partial fulfillment
of the requirements for the degree of

**BACHELOR OF SCIENCE**

**IN**

**BIOTECHNOLOGY**

**DEPARTMENT OF BIOINFORMATICS AND BIOTECHNOLOGY**

**GOVERNMENT COLLEGE UNIVERSITY, FAISALABAD**

**August 2024**

# Declaration

I carried out the work reported in this report, under the kind supervision of **Dr. Mohsin Tariq**, Assistant Professor, Department of Bioinformatics and Biotechnology, Government College University, Faisalabad, Pakistan.

I hereby declare that the title of the report is **"Biofilm forming and swarming activities of *Bacillus cereus* modulated by multiclass compounds"** and the contents of this report are the product of my own research and no part has been copied from any published source (except the references, standard mathematical or genetic models /equations /formulas /protocol, *etc*).

I further declare that this work has not been submitted for the award of any other degree/diploma. The University may take action if the information provided is found inaccurate at any stage.

Abdul Rafay Rafiq

2020-GCUF-011107

# Certificate By Supervisory Committee

We certify that the contents and form of the report submitted by Abdul Rafay Rafiq, Reg. No: 2020-GCUF-011107 has been found satisfactory and according to the prescribed format.

We recommend it to be processed for evaluation by the Internal Examiner for the award of degree.

**Supervisor**

Signature …….

Name:……...

Designation with Stamp……...

**Internal Examiner**

Signature …….

Name:……

Designation with Stamp……...

**Chairperson**

Signature …….

Name:……

Designation with Stamp……...

# Acknowledgments

I would like to acknowledge and give my warmest thanks to my supervisor, **Dr. Mohsin Tariq**, Assistant Professor at the Department of Bioinformatics and Biotechnology, Government College University, Faisalabad for his support and guidance. His mentorship has not only enriched my academic journey but also inspired me to strive for excellence.

I want to thank **Dr. Richard Losick**, Department of Molecular and Cellular Biology, Harvard University, Massachusetts Hall, Cambridge, USA, whose foundational research work and scientific advice enabled me to plan and carry out my own research.

Lastly, I dedicate this work to my parents, **Mohammad Rafiq** and **Rizwana Jamil**. Their boundless emotional and moral support, unwavering care, and tireless sacrifices have been my greatest source of strength. Without their endless encouragement and the immense resources, they provided, I would not have reached this milestone. Their love and dedication have been the foundation of my journey, and for that, I am eternally grateful.

**Abdul Rafay Rafiq**

# TABLE OF CONTENTS

**Declaration** ..... **ii**
**Certificate By Supervisory Committee** ..... **iii**
**Acknowledgments** ..... **iv**
**List of Figures** ..... **viii**
**List of Tables** ..... **x**
**List of Abbreviation** ..... **xi**
**Abstract** ..... **xiii**
**Chapter 1** ..... **1**
**Introduction** ..... **1**
1.1. Biofilm ..... 1
1.1.1. Steps of biofilm formation ..... 1
1.1.2. Biofilm and health sector ..... 1
1.1.3. Biofilm and industrial sector ..... 2
1.1.4. Biofilm and agricultural sector ..... 2
1.2. *Bacillus cereus* ..... 3
1.2.1. *Bacillus cereus* as a pathogen ..... 3
1.2.2. *Bacillus cereus* as an industrial issue ..... 4
1.2.3. *Bacillus cereus* as a PGPR ..... 4
1.3. Conditions for *B. cereus* biofilm formation ..... 5
1.3.1. Temperature ..... 5
1.3.2. Optimal PH ..... 5
1.3.3. Time ..... 5
1.3.4. Adherence surfaces for biofilm formation ..... 5
1.4. Chemical compounds affect biofilm formation and swarming ..... 5
1.5. Environmentally widespread compounds ..... 5
1.6. Aim of this study ..... 7
**Chapter 2** ..... **8**
**Literature review** ..... **8**
2.1 *Bacillus* genus ..... 8
2.1.1. Isolation of *Bacilli* ..... 8
2.1.2. Morphology of *Bacilli* ..... 8
2.1.3. *B. cereus* group ..... 8
2.2 *B. cereus* ..... 9

2.2.1. Conditions favorable for *B. cereus biofilm* ..... 9
2.2.2. Genomics behind *B. cereus* biofilm formation ..... 9
2.2.3. Swarming activity of *B. cereus* ..... 10
2.2.4. Biotic & abiotic surfaces colonized by biofilm forming *B. cereus* ..... 10
2.3 Analytical techniques for studying biofilm formation ..... 11
2.3.1 Microscopic techniques ..... 11
2.3.2 Spectroscopic techniques ..... 11
2.3.3 Quantitative techniques ..... 11
2.3.4 Molecular Approaches ..... 11
2.4 Techniques to eradicate biofilm ..... 12
2.4.1. Physical methods ..... 12
2.4.2 Chemical approaches ..... 12
2.4.3 Emerging technologies ..... 12
**Chapter 3 ..... 13**
**Materials & Methods ..... 13**
3.1 Stains and culture conditions ..... 13
3.2 Chemical preparations ..... 13
3.3 Abiotic surface adhesion test ..... 13
3.4 Biofilm culture ..... 13
3.5 Biofilm live weight determination ..... 14
3.6 Adherence visualization assay ..... 14
3.7 Swarming motility assay ..... 14
3.8 Statistical analyses ..... 15
**Chapter 4 ..... 16**
**Results ..... 16**
4.1 Distinct Biofilm morphotypes ..... 16
4.2 Abiotic surface adhesion test ..... 17
4.3 Biofilm Thickness ..... 22
4.4 Biofilm location characterization ..... 25
4.5 EPS encased bacteria OD600 ..... 29
4.6 Biofilm live weight ..... 33
4.7 Adherence visualization assay ..... 36
4.8 Swarming motility assay ..... 39
4.9 Statistical analysis ..... 46
**Chapter 5 ..... 50**

**Discussion** ..... **50**
**Conclusion** ..... **57**
**References** ..... **58**

# List of Figures


| Figure No | Title | Page No |
|---|---|---|
| **Figure 1.** | Distinct morphotypes of WGT1 and WGT2 formed on LB broth. | 16 |
| **Figure 2.** | Relative absorbance levels of biofilm formed by WGT1 at 570nm after multiclass compound treatments represented by bars. | 19 |
| **Figure 3.** | Relative absorbance levels of biofilm formed by WGT2 at 570nm after multiclass compound treatments represented by bars. | 19 |
| **Figure 4.** | Calorimetric representation of relative absorbance levels of WGT1 biofilm at 570 nm after multiple compound treatments. | 20 |
| **Figure 5.** | Calorimetric representation of relative absorbance of WGT2 biofilm at 570 nm after multiple compound treatments. | 21 |
| **Figure 6.** | Relative thickness of WGT1 biofilms measured in cm after multiclass compound treatments represented by bars. | 24 |
| **Figure 7.** | Relative thickness of WGT2 biofilms measured in cm after multiclass compound treatments represented by bars. | 24 |
| **Figure 8.** | Biofilms formed by WGT1 modulated by multiclass chemical treatments. | 27 |
| **Figure 9.** | Biofilms formed by WGT2 modulated by multiclass chemical treatments. | 28 |
| **Figure 10.** | Relative absorbance levels of WGT1 EPS bacterial population at 600nm represented by bars. | 32 |
| **Figure 11.** | Relative absorbance levels of WGT2 EPS bacterial population at 600nm represented by bars. | 32 |
| **Figure 12.** | Live weights of WGT1 biofilm modulated by multiclass compound treatments represented by bars. | 35 |
| **Figure 13.** | Live weights of WGT2 biofilm modulated by multiclass compound treatments represented by bars. | 35 |
| **Figure 14.** | Adherence of WGT1 influenced by multiclass compounds represented by stained regions. | 37 |
| **Figure 15.** | Adherence of WGT2 influenced by multiclass compounds represented by stained regions. | 38 |
| **Figure 16.** | Relative swarming diameters due to WGT1 motility affected by multiclass chemical treatments represented by bars. | 41 |

**Figure 17.** Relative swarming diameters due to WGT2 motility affected by multiclass chemical treatments represented by bars. .....41
**Figure 18.** WGT1 Swarming motility affected by multiclass compounds. .....42
**Figure 19.** WGT1 Swarming motility affected by multiclass compounds. .....43
**Figure 20.** WGT2 Swarming motility affected by multiclass compounds. .....44
**Figure 21.** WGT2 Swarming motility affected by multiclass compounds. .....45

# List of Tables


| Table No | Title | Page No |
|---|---|---|
| **Table 1.** | Relative absorbance levels of WGT1 and WGT2 biofilm formation at 570nm after multiclass compound treatments. | 18 |
| **Table 2.** | WGT1 and WGT2 Biofilm thickness in cm modulated by multiclass compound treatments. | 23 |
| **Table 3.** | Characterization of biofilms formed by WGT1 and WGT2 according to location. | 26 |
| **Table 4.** | EPS encased bacteria $OD_{600}$ of WGT1 and WGT2 biofilms modulated by multiclass chemical treatments. | 30 |
| **Table 5.** | Planktonic bacteria $OD_{600}$ of WGT1 and WGT2 biofilms modulated by multiclass chemical treatments | 31 |
| **Table 6.** | Live weights of WGT1 and WGT2 biofilms modulated by multiclass compound treatments. | 34 |
| **Table 7.** | Swarming motility of WGT1 and WGT2 modulated by multiclass compound treatments represented by increase or decrease in swarming diameter (cm). | 40 |
| **Table 8.** | Correlation among biofilm and swarming properties of WGT1. | 47 |
| **Table 9.** | Correlation among biofilm and swarming properties of WGT2. | 49 |

# List of Abbreviation

| Abbrevation | Full Form |
|---|---|
| $^{o}C$ | Degree centigrade |
| % | Percentage |
| µL | Microliter |
| AFM | Atomic force microscopy |
| Ag | Silver |
| AHL | Acyl-homoserine lactone |
| BSIs | Blood stream infections |
| CA-UTIs | Catheter-associated urinary tract infections |
| CLSM | Confocal laser scanning microscopy |
| cm | Centimeter |
| Cu | Copper |
| CV | Crystal violet |
| DNA | Deoxyribonucleic acid |
| EDTA | Ethylenediaminetetraacetic acid |
| EPS | Extracellular polymeric substance |
| FISH | Fluorescence in situ hybridization |
| flaA | Flagellin A gene |
| flaB | Flagellin B gene |
| FlhF | Flagellar biosynthesis regulator F |
| FTIR | Fourier-transform infrared |
| GCUF | Government College University, Faisalabad |
| h | Hours |
| $H_2S$ | Hydrogen sulfide |
| HAIs | Hospital-acquired infections |
| HCN | Hydrogen cyanide |
| K+ | |
| LAB | Lactic acid bacteria |
| LB | Luria-Bertani |
| MALDI-TOF mass spectrometry | Matrix-Assisted Laser Desorption/Ionization Time-of-Flight mass spectrometry. |
| $Mg^{2+}$ | Magnesium ions |
| min | Minutes |
| mL | Mili liter |
| $Mn^{2+}$ | Manganese ions |
| NaCl | Sodium Chloride |
| nm | Nanometer |
| OD | Optical Density |
| p | Probability value |
| PCR | Polymerase chain reaction |
| PET | Polyethylene terephthalate |
| PGPR | Plant growth-promoting rhizobacteria |

| | |
|---|---|
| PlcR | Pleiotropic regulator |
| PVC | Polyvinyl Chloride |
| qPCR | Quantitative polymerase chain reaction |
| QS | Quorum sensing |
| r | Correlation coefficient |
| RNA | Ribonucleic acid |
| SEM | Scanning electron microscopy |
| TiO2 | Titanium dioxide |
| V/V | Volume by volume |
| VAP | Ventilator-associated pneumonia |
| W/V | Weight by volume |
| ZnO | Zinc Oxide |

# Abstract

*Bacillus cereus*, a Gram negative, facultative anaerobic bacterium is a serious human pathogen, industrial contaminant and plant growth promoting rhizobacterium casting its shadow upon health, industrial and agricultural sector due to its biofilm forming ability. Biofilm is a multicellular colony of bacteria enclosed in a self-synthesized gel like extracellular polymeric substance (EPS). Therefore, exploitation and eradication of *B. cereus* biofilm forming ability is highly demanding. In this study we tested a variety of compounds which are widespread in environment for their modulating potential on *B. cereus* biofilms. Citric acid, copper sulfate, iron (III) chloride and malic acid demonstrated an inhibitory impact on biofilm parameters while rest of the compounds, chiefly promoted them. Multiple biofilm related parameters including abiotic surface adhesion represented by absorbance at 570 nm, biofilm thickness, biofilm live weight, biofilm location, EPS encased bacteria $OD_{600}$, flagellar adherence and swarming diameter were recorded and subjected to statistical correlation analyses. Positive and significant correlations were found among these parameters. Generally, *B. cereus* biofilms showed adaptive responses to environmental stimuli majorly different nutrients and exogenous chemical treatments. Biofilm promoting compounds can be developed into, biofilm inducing nutrient media for research and development; inoculants in biofertilizers for better colonization of root by PGPR; media used in industrial biofilm reactors for robust biofilm formation, to develop robust biofilms for bioremediation, Conversely, biofilm inhibiting compounds could be used in sanitizer formulations for eradicating undesirable biofilms.

# Chapter 1

# Introduction

## 1.1. Biofilm

Biofilms are multicellular communities of microorganisms that adhere to biotic or abiotic surfaces and are encased in a self-produced gel like extracellular polymeric substance (EPS) matrix (Bello et al., 2023). The EPS consists of multiple biomolecules, polysaccharides or exopolysaccharides which provide it its cohesion structural integrity; Protein components making 10-15% of total organic carbon and involved in cell adhesion, enzymatic activity, and intercellular communication i.e. amyloid fibers; Nucleic acids i.e. environmental DNA and RNA which contribute to structural stability; Phospholipids and molecules like humic substances, minerals, and various functional groups like phosphoric, carboxylic, hydroxyl, and amino groups (María Gabriela Paraje, 2023; Quinn et al., 2019; Suparna Dutta Sinha et al., 2021; Xue et al., 2024).

### 1.1.1. Steps of biofilm formation

The formation of a Biofilm generally takes place in a five step process : Initial attachment in which microbes attach to any surface through weak and reversible adhesion via van der Waals forces; Irreversible attachment through cell adhesion structures like pili; Microcolony formation characterized by cell division and recruitment of other microbes through quorum sensing (QS), this stage adds to growing biofilm; Maturation phase in which microbial cells within biofilm produce large amount of EPS which results into making up 50-60% total organic carbon of the biofilm; Dispersion characterized by enzymatic degradation of biofilm leading to microbial cellular detachment and dispersion to colonizing new surfaces, the stage marks the completion of biofilm life cycle (Armbruster & Parsek, 2018; Floyd et al., 2017; Pa et al., 2023).

### 1.1.2. Biofilm and health sector

Dealing with biofilms as a medical issue demands fabrication of novel eradication strategies due to increased risk of hospital-acquired infections (HAIs) i.e. ventilator-associated pneumonia (VAP), surgical site infections, catheter-associated urinary tract infections (CA-UTIs) and bloodstream infections (BSIs) (Assefa & Amare, 2022; Kenichiro Yaita et al., 2019; Sandra Pamela Cangui-Panchi et al., 2022). Biofilms robustly adhered onto the medical devices such as catheters, prosthetic joints, and dental unit water

lines, pacemakers, mechanical heart valves, and intrauterine device leading to persistent infections as well as device failure (Caldara et al., 2022; Del Pozo, 2017; Ma & Katzenmeyer-Pleuss, 2017). Biofilm associated chronic infections are not only difficult to treat but also cause persistent inflammation, tissue damage and diagnostic challenges. Biofilm forming pathogenic bacteria are not detected by conventional diagnostic methods and hence false negative results are produced (Di et al., 2022; Vestby et al., 2020). Pathogenic species of bacteria equipped with biofilm forming abilities are more resistant to antibiotics due to little or no antibiotic penetration and modulation of metabolic activities reducing their susceptibility to antibiotics (Abebe, 2020; Hall & Mah, 2017). Biofilm forming and drug resistant bacteria containing resistance genes can spread into the environment through hospital effluents and amplify the above-mentioned health concerns.

### 1.1.3. Biofilm and industrial sector

Biofilms also causes significant problems in industrial settings leading to economical loses. Biofilms formed on equipment surfaces in food industries produce enzymes notorious for food spoilage, off flavors and odors leading to food contamination and resultantly economic losses (Carrascosa et al., 2021; Machado et al., 2020; Odeyemi et al., 2020). Water quality and safety can be compromised due to biocorrosion, befouling and spread of toxic spores as well as waterborne pathogens caused by biofilm formed in water chillers and filtration systems (Chan et al., 2019). Dairy industries use milk processing equipment which if contaminated by biofilms, leads to spoilage of tons of gallons of milk products (Flint et al., 2020; Oliveira et al., 2019). Biocorrosive properties of biofilms can cause leakage in storage tanks in oil and gas industries leading to oil spillage, environmental contamination and reduced productivity (Elumalai et al., 2020; Vishwakarma, 2019). Inversely, Biofilms can be beneficially exploited in biofilm reactors: Biofilm reactors are specialized bioreactor systems designed to promote the growth and cultivation of microbial biofilms; these reactors have various applications i.e. Wastewater treatment, bioremediation of contaminated environments, biofuel production, fermentation and bioconversion processes (Ahmad et al., 2022; Dutta et al., 2022; Rao, 2023; Saini et al., 2023).

### 1.1.4. Biofilm and agricultural sector

Although biofilm is proven to be economically and medically harmful to certain medical and industrial settings, it is more like a beneficial trait to agriculture. EPS of biofilm can bind to and sequester salts like hence reducing their toxicity and availability to plants. Biofilm forming bacteria improve water retention in soil and mitigate osmotic stress

(Yasmeen et al., 2020). Biofilm-forming plant growth-promoting rhizobacteria (PGPR) stimulate antioxidant activity in plants mitigating oxidative damage (H.G. Gowtham et al., 2022). These PGPR have been found to promote growth of economically and nutritionally valuable crops like wheat. Maize, rice, tomatoes, potatoes and soybean (Iryna Kulkova et al., 2023). Certain biofilm forming bacteria also act as effective biocontrol agents. Biofilm formation by plant growth-promoting rhizobacteria (PGPR) can inhibit plant pathogens through several mechanisms: competitive exclusion by outcompeting pathogens for nutrients and space, and physically excluding them from plant surfaces due to protective EPS; antibiosis via antimicrobial compounds such as antibiotics, enzymes, and biosurfactants concentrated in the biofilm matrix; quorum quenching to disrupt pathogen signaling and virulence; induction of systemic resistance in the plant; and nutrient competition by efficient scavenging and sequestration of essential nutrients (Carezzano et al., 2023; Danish et al., 2024).

## 1.2. *Bacillus cereus*

*Bacillus cereus* is a Gram-positive, motile, spore-forming, biofilm forming, facultatively anaerobic, rod-shaped bacterium commonly found in soil, vegetation, and various raw as well as processed food products (McDowell et al., 2023).

### 1.2.1. *Bacillus cereus* as a pathogen

*B. cereus* is widely distributed in the environment and is known to cause two primary types of intestinal foodborne illnesses: emetic syndrome, which leads to nausea and vomiting, and diarrheal syndrome, characterized by abdominal pain and diarrhea. These illnesses are caused by the production of emetic toxins (cereulide) and diarrheal toxins (hemolysin BL, cytotoxin K), respectively (Griffiths & Schraft, 2017; Messelhäußer & Ehling-Schulz, 2018). Though often regarded as an opportunistic pathogen, *B. cereus* can also cause severe non intestinal infections, particularly in immunocompromised individuals. These include life-threatening bacteremia (Bianco et al., 2021) requiring prompt antibiotic treatment, severe eye infections like endophthalmitis (Zheng et al., 2024) that can lead to vision loss and need aggressive antimicrobial therapy, meningitis of the brain and spinal cord (M Rollán-Martínez Herrera et al., 2022) requiring prompt diagnosis and management, rapidly progressing pneumonia that can develop into acute respiratory distress syndrome, bone infections like osteomyelitis (Newman et al., 2022) leading to destruction and sepsis treatable with antibiotics, debridement, and sometimes surgery, rare but dangerous brain abscesses (Koizumi et al., 2020) needing antimicrobials and surgical drainage, serious skin

and soft tissue cellulitis (Malik-Tabassum et al., 2017) requiring prompt antibiotic therapy, and rare yet severe heart valve endocarditis (Fukushima et al., 2024) often necessitating prolonged antibiotics and potential valve replacement. *B. cereus*'s ability to form resilient spores and produce a range of virulence factors, including toxins and enzymes, enhances its adaptability and persistence in diverse environments, making it a significant foodborne and opportunistic pathogen.

### 1.2.2. *Bacillus cereus* as an industrial issue

*B. cereus* poses significant challenges to various industries due to its ability to form biofilms, leading to economic losses and food safety concerns. The bacterium's biofilm-forming capacity can cause corrosion in industrial settings, as seen in the study evaluating its corrosion behavior on Q235 carbon steel in simulated cooling water (Hu et al., 2022). Additionally, B. cereus is a common contaminant in dairy products, with up to 90% of its spores being resistant to cleaning, posing a serious concern for the dairy industry (Liu et al., 2020; Tirloni et al., 2022). Furthermore, the presence of B. cereus in food products can lead to food poisoning outbreaks (Jovanovic et al., 2021), emphasizing the importance of effective biofilm removal strategies in the food industry to prevent contamination and subsequent economic losses. Understanding the mechanisms of biofilm formation and the resilience of B. cereus spores is crucial for developing control methods and maintaining food safety standards in various industrial sectors.

### 1.2.3. *Bacillus cereus* as a PGPR

*B. cereus*, a plant growth-promoting rhizobacteria (PGPR), plays a crucial role in enhancing plant growth through various mechanisms, including biofilm formation. Studies have shown that *B. cereus* strains exhibit significant plant-stimulating traits such as indole-3-acetic acid (IAA) production, phosphate solubilization, and biocontrol activities against phytopathogens (Nagrale et al., 2023). Additionally, *B. cereus* strains have been found to promote plant growth under abiotic stresses like salinity, drought, and heavy metal pollution (Iryna Kulkova et al., 2023). Biofilm formation by *B. cereus* on plant roots is essential for successful colonization and activation of plant beneficial traits, ultimately leading to improved plant growth and development (Lin et al., 2022). Furthermore, *B. cereus* strains have been shown to modulate rhizospheric microbial community diversity, enhancing plant height, fresh weight, and nutritional quality of crops (Dong et al., 2023). Thereby, *B. cereus* demonstrates great potential as a biofertilizer and biocontrol agent, contributing to increased crop yield and improved soil ecosystem health.

## 1.3. Conditions for *B. cereus* biofilm formation

*B. cereus* shows adaptive biofilm formation in response to environmental stimuli. Studies have shown that *B. cereus* forms more robust biofilms under nutrient-limited conditions compared to rich media environments (Chateau et al., 2022; Qin et al., 2022).

### 1.3.1. Temperature

Temperature plays a role, as *B. cereus* forms robust biofilms at 37°C, whereas it does not sustain biofilm formation across a range of temperatures (Candela et al., 2011).

### 1.3.2. Optimal PH

Optimal PH for biofilm formation for *B. cereus* is 6.0-7.5(Candela et al., 2011).

### 1.3.3. Time

Biofilm formed over longer period of time i.e. 48 hours is reportedly less robust than biofilm made in shorter period of time i.e. 24 hours for some strains (Candela et al., 2011).

### 1.3.4. Adherence surfaces for biofilm formation

*B. cereus* produces biofilms on various surfaces, including polystyrene, glass wool, and stainless steel. The transition from a free-floating to a sessile lifestyle is triggered by the bacterium's encounter with suitable attachment surfaces (Majed et al., 2016). During biofilm formation, *B. cereus* assembles an extracellular matrix composed of DNA, proteins, and polysaccharides. Biosurfactant production is a key requirement for *B. cereus* biofilm formation, and this process may be directly or indirectly regulated by the pleiotropic regulator PlcR (Hsueh et al., 2006).

## 1.4. Chemical compounds affect biofilm formation and swarming

Several compounds have been previously shown to influence biofilm formation, Manganese ($Mn^{2+}$); Heme; Glucose; Glycerol; Sodium chloride (NaCl); Benzalkonium chloride and iron enhances the extent of biofilm formation in several bacterial species, (Gomes et al., 2021; Hussain et al., 2018; Kwon et al., 2017), while oxides like zinc oxide (Zno); titanium diocide ($Tio_2$), acids like Citric acid; Lactic acid, and heavy metals like copper (cu), Silver (Ag), Zinc (zn) inhibit biofilm formation (Leire Goñi-Ciaurriz & Itziar Vélaz, 2023; Li et al., 2020).

## 1.5. Environmentally widespread compounds

Ammonium oxalate is secreted by many fungal species (Dutton et al., 1993; Gadd, 1999; LAPEYRIE et al., 1987). Ammonium sulfate is a widely used nitrogen and sulfur chemical

fertilizer (Chien et al., 2011; Pei et al., 2020). Ascorbic acid is a common food additive and also used in pharmaceutical industries (Wang et al., 2018). Boric Acid is a common; pesticide for controlling cockroaches, ants, and termites; (Hadrup et al., 2021) and also a fungicide for protecting crop from fungal pathogens (Martinko et al., 2022). Calcium chloride is a de-icing agent used on sidewalks and roads for lowering freezing point of water preventing ice formation (Gerasimov et al., 2021). Citric acid is a preservative used preventing food spoilage and a root exudate secreted in rhizosphere by many plants (Jiao et al., 2022). Copper sulfate is a common fungicide (Tamm et al., 2022). D- Glucose is widely used sweetener used in vast range of application from industries to restaurants and home kitchen and it is preferred energy source for bacteria (Yu & Guo, 2022). Gelatin is a protein found in skin, bones and connective tissues of animals which usually end up as dead organic matter into the environment (Alipal, 2021). Glycine is the simplest amino acid which can act as carbon as well as nitrogen source for bacteria, glycine is present in all living beings making its exposure ubiquitous (Johnson & Cuellar, 2023). Iron (III) chloride is used to treat industrial waste, sewage water and to purify water (Alper Solmaz et al., 2024) from where it can be exposed to microbial community. Magnesium sulfate is commonly found in sea water (Kim et al., 2021) from where it spread though rivers then through streams and is also used in synthetic fertilizers for $Mg^{2+}$ being important for chlorophyl and photosynthesis (LI et al., 2021). Malic acid is used in formulations for house hold cleaning and disinfection purposes where it can leak out into environment and interact with microbial community (Hwang et al., 2022). Manganese sulfate is used in fertilizer formulations as $Mn^{2+}$ is an important micronutrient for plants (Isakova et al., 2024) and also for bacteria (Qin et al., 2023). Molybdenum Trioxide is employed in enzymatic biosensors for detection biological markers of quality, pathogens and contaminations in food products i.e. presence of xanthin as quality marker in fish (Lu et al., 2023; Sharma et al., 2023). Pectin is a structural component of plant cell wall and hence roots are covered with molecules of pectin which can interacts with rhizosphere microbial community (Haas et al., 2021). Potassium chloride is used potassium fertilizer formulation which when applied to soil interacts with microbial community. Potassium dihydrogen phosphate is also a fertilizer as it is a source of phosphate and phosphorus both of which are important for plant growth (Ma et al., 2021). Zinc oxide is used in cigarette filters for removing Hydrogen cyanide (HCN) and Hydrogen sulfide ($H_2S$) without affecting flavor, these cigarette filters are commonly discarded into the environment (Cui et al., 2024; Shao et al., 2021).

## 1.6. Aim of this study

The aim of this study is to determine the influence of organic acids, minerals, salts, metals, fertilizers, oxides, polysaccharides and sugars, amino acids and proteins- which claim a high degree of environmental exposure to bacteria- on biofilm forming and swarming activities of environmental isolates of *B. cereus* namely WGT1 and WGT2.

This study has multiple implications in multiple fields; compounds which promote robust biofilm formation can be used to formulate biofilm inducing nutrient media for culturing biofilms for research and development purposes; biofilm inducing chemicals can be used as inoculants in biofertilizers containing biofilm forming PGPR for strong adherence and colonization to plant roots; ironically chemicals which inhibit biofilm formation can be develop into sanitizers for eradication of undesirable biofilms; Biofilm enhancing chemicals can be used to develop robust and efficient biofilms inside biofilm reactors used in industries.

# Chapter 2

# Literature review

## 2.1 *Bacillus* genus

The genus "*Bacillus*" is a diverse group of spore-forming, rod-shaped, gram-positive bacteria widely found in soil and water. This genus contains over 266 named species and is a member of the phylum "*Bacillota*". *Bacillus* species have implications in both medical and biodefense aspects of microbiology (Borriss, 2020). Researchers have proposed several phylogenetic classification models for the genus *Bacillus*. One 2003 study divided *Bacillus* into 10 distinct clusters, including the nested genera *Paenibacillus, Brevibacillus, Geobacillus, Marinibacillus, and Virgibacillus*. Building on this, a 2008 analysis based on 16S and 23S rRNA sequences found that *Bacillus* is paraphyletic to the *Lactobacillales*, with species like *B. coahuilensis* grouping within this order. Advancing further, a 2010 gene concatenation study identified a more limited number of *Bacillus* groups with a comparable phylogenetic structure to the earlier proposals (Carroll et al., 2021). One clade contains *Bacillus anthracis, B. cereus, Bacillus mycoides, Bacillus pseudomycoides, Bacillus thuringiensis,* and *Bacillus weihenstephanensis* which are nearly genetically identical within 97% 16S identity and are considered a single species, but are classified separately for medical reasons (Carroll et al., 2021).

### 2.1.1. Isolation of *Bacilli*

*Bacillus* species are commonly isolated from soil samples by suspending the soil in water, heat-shocking the mixture to eliminate vegetative cells, and then culturing the remaining spores on agar plates. The resulting *Bacillus* colonies are often characterized by their white, large, spreading, and irregularly shaped morphology (Cho & Chung, 2020).

### 2.1.2. Morphology of *Bacilli*

*Bacillus* cells under microscope appear as elongated rods, usually containing oval endospores at one end of the cell. The endospore formation is the primary survival strategy for *Bacillus* species in harsh environments (Vittoria et al., 2023), Terminal endospores are features used to identify *Bacillus* species isolated from soil samples (Vittoria et al., 2023).

### 2.1.3. *B. cereus* group

Of the 34 species of *Bacillus,* the two most medically important are *B. anthracis*, the causative agent of anthrax, and *B. cereus*, which causes food poisoning. *B. cereus* is the

second most frequent human pathogen after *B. anthracis*. Other species that cause human disease include *Bacillus alvei*, *Bacillus megaterium, Bacillus coagulans, Bacillus laterosporus, Bacillus subtilis, Bacillus sphaericus, Bacillus circulans, Bacillus brevis, Bacillus licheniformis, Bacillus macerans, Bacillus pumilus, and Bacillus thuringiensis* (Ehling-Schulz et al., 2019). *B. cereus* is the most common intraocular pathogen, and *Bacillus* species are most commonly isolated in cases of penetrating nonsurgical trauma. Some *Bacillus* species are also harmful to plants and other organisms (Ehling-Schulz et al., 2019).

## 2.2 *B. cereus*

*B. cereus* has the ability to grow as both submerged and floating biofilms. Submerged biofilms attach to surfaces, while floating biofilms form at the air-liquid interface (Sanchez-Vizuete et al., 2022).

### 2.2.1. Conditions favorable for *B. cereus biofilm*

Several environmental factors influence *B. cereus* biofilm formation: sufficient nutrients, such as carbon sources including glucose, fructose, and sucrose, specific amino acids such as glutamic acid, arginine, and histidine, essential minerals like magnesium, calcium, and iron, and necessary vitamins such as biotin and thiamine are required for biofilm growth; *B. cereus* can form biofilms over a wide range of temperatures, typically between 10°C and 45°C; biofilm formation is favored in slightly acidic to neutral pH conditions, around pH 5.0 to 7.0; increased ionic strength, such as high salt concentrations, can enhance biofilm formation in some strains; and the physicochemical properties of the surface, such as hydrophobicity and roughness, influence the initial attachment of *B. cereus* cells (Candela et al., 2011; Chateau et al., 2022; Qin et al., 2022)..

### 2.2.2. Genomics behind *B. cereus* biofilm formation

Environmental factors trigger the expression of HK a-d operon, as a result HK a-d operon activates the expression of Spo0A a-m operon. Spo0A activates the expression of SinI which in turn regulates the expression of TasA, SipW and calY genes required amyloid fibers. TasA and sipW are located in a single operon on *B. cereus* genome while CalY is located downstream the TasA-SipW operon. SinI regulates the expression of these amyloid fibers associated genes by downregulating the expression of SinR which is a repressor for amyloid fibers associated genes namely TasA-SipW and CalY (Yan et al., 2017).

### 2.2.3. Swarming activity of *B. cereus*

Swarming is a flagellum-driven, social form of bacterial locomotion in which cells undergo a differentiation process to produce long, hyperflagellated swarmer cells that can coordinately migrate across surfaces. This motility mode confers an advantage for the colonization of natural and host surfaces, and can also contribute to the bacterium's virulence (Liu et al., 2020). Swarming triggers differential gene expression, with upregulation of flagellin genes i.e. flaA and flaB, K+ transport genes, and components of the enterotoxin hemolysin BL, enhancing the pathogenicity of the bacterium (Smith et al., 2020). Additionally, the protein FlhF plays a multifunctional role in *B. cereus*, influencing flagellation, swarming, protein secretion, and pathogenicity, as its depletion leads to altered extracellular protein profiles and reduced pathogenicity in infection models (Li et al., 2022). Furthermore, *B. cereus* swarming involves the induction of genes related to metabolism, membrane transport, sporulation, QS, antibiotic synthesis, and virulence, highlighting the ecological significance and potential role in colonization of environments and hosts (Park et al., 2019).

Swarming by *B. cereus* optimally occurs at temperatures ranging from 25 to 38°C. Under optimal growth conditions, some *B. cereus* strains develop characteristic colony patterns on swarming agar plates. The differentiation of *B. cereus* into swarmer cells involves changes in cell morphology, such as the production of longer and more flagella, as well as alterations in gene expression and protein secretion (Park et al., 2019).

### 2.2.4. Biotic & abiotic surfaces colonized by biofilm forming *B. cereus*

*B. cereus* has been found to form biofilms on various surfaces, both biotic and abiotic. Biotic surfaces where *B. cereus* can colonize and form biofilms include living plant tissues like leaves, seeds, and roots, as well as animal tissues such as skin and intestinal epithelium. On the other hand, abiotic surfaces where *B. cereus* can adhere and create biofilms encompass stainless steel, plastic, glass, conveyor belts, stainless steel pipes, storage tanks, silicone, polyethylene terephthalate (PET), Teflon, and aluminum (Kwon et al., 2017; Majed et al., 2016). This ability to form biofilms on a wide array of surfaces poses a significant concern, especially in food processing environments, as biofilms can serve as reservoirs for contamination and contribute to the persistence of *B. cereus* in these settings

## 2.3 Analytical techniques for studying biofilm formation

### 2.3.1 Microscopic techniques

The detection and analysis of *B. cereus* biofilms is a critical step in understanding their formation, structure, and potential impacts. Several advanced analytical techniques have been employed for this purpose. Microscopy methods, such as scanning electron microscopy (SEM) and confocal laser scanning microscopy (CLSM), allow for high-resolution visualization of biofilm architecture, cell morphology, and the extracellular matrix composition (Huang et al., 2020). Complementary techniques like atomic force microscopy (AFM) can provide nanoscale details of the biofilm surface topography and adhesive properties (Huang et al., 2020).

### 2.3.2 Spectroscopic techniques

Additionally, spectroscopic methods have been utilized to characterize the biochemical composition of *B. cereus* biofilms. Fourier-transform infrared (FTIR) spectroscopy and Raman spectroscopy enable the identification and quantification of specific biomolecules within the biofilm, such as proteins, polysaccharides, and lipids (Vatanshenassan et al., 2020). Mass spectrometry techniques like MALDI-TOF can analyze the molecular composition of biofilms. These techniques can provide insights into the extracellular matrix composition and changes in the biofilm's chemical profile under different environmental conditions (Vatanshenassan et al., 2020).

### 2.3.3 Quantitative techniques

Quantitative approaches, such as the crystal violet (CV) biofilm assay, have been employed to assess the biomass and relative abundance of *B. cereus* biofilms. Colorimetric methods like crystal violet, 1,9-dimethyl methylene blue, and fluorescein-di-acetate can quantify biofilm matrix. This colorimetric method allows for the rapid screening and comparison of biofilm formation across different strains or treatment conditions (Debroy et al., 2021). Resazurin, tetrazolium hydroxide salt, and LIVE/DEAD BacLight assays measure viable cells in biofilms (Haney et al., 2018).

### 2.3.4 Molecular Approaches

Molecular approaches, including quantitative PCR (qPCR) and transcriptomic analysis and fluorescence in situ hybridization (FISH), have also been utilized to elucidate the genetic regulation of biofilm formation by *B. cereus*. These techniques provide insights into the

underlying biological mechanisms driving biofilm development and adaptation (Mougin et al., 2020).

## 2.4 Techniques to eradicate biofilm

Given the tenacious nature of *B. cereus* biofilms and their potential impacts, various strategies have been explored for their prevention and removal.

### 2.4.1. Physical methods

Mechanical disruption techniques, such as scrubbing, sonication, and high-pressure water jetting, have shown some efficacy in dislodging *B. cereus* biofilms from surfaces (Ong & Chen, 2022). The combination of physical removal with thermal treatments, like steam or hot water exposure, can further enhance the effectiveness of these approaches (Park et al., 2017). Additionally, the use of ultrasound-assisted cleaning has been investigated as a means to disrupt biofilm integrity and facilitate their removal (Hussain et al., 2018).

### 2.4.2 Chemical approaches

Chemical disinfectants and antimicrobial compounds have been widely studied for their ability to inhibit *B. cereus* biofilm formation and eradicate established biofilms. Commonly tested agents include chlorine-based sanitizers, quaternary ammonium compounds, peracetic acid, and various essential oils. These compounds can target and disrupt the biofilm matrix, cell membranes, or intracellular processes to achieve biofilm control. The incorporation of chelating agents, such as EDTA, has also been explored to enhance the penetration and efficacy of antimicrobials against *B. cereus* biofilms (Camele et al., 2023; Liu et al., 2021).

### 2.4.3 Emerging technologies

Novel approaches, including the use of bacteriophages, QS inhibitors, and biofilm-dispersing enzymes, have shown promising results in controlling *B. cereus* biofilms (Yan et al., 2020). Bacteriophages can selectively target and lyse *B. cereus* cells within the biofilm, while QS inhibitors and dispersing enzymes can disrupt the signaling pathways and extracellular matrix, respectively, leading to biofilm destabilization. Additionally, the development of antimicrobial surfaces, such as those with micro- or nano-topographical features, has been investigated for their ability to prevent *B. cereus* biofilm formation (Yan et al., 2020).

# Chapter 3

# Materials & Methods

## 3.1 Stains and culture conditions

Two environmental isolates of *B. cereus* namely WGT1 and WGT2 isolated from soil were obtained from Plant biotechnology laboratory, Department of bioinformatics and biotechnology, GCUF. Both strains were streaked on LB agar medium (1% w/v tryptone, 1% w/v NaCl, 0.5% w/v yeast extract and 2% w/v agar) to obtain pure cultures. Inoculated agar plates were incubated for 24 h at 37℃. After 24 h, both agar LB plates were assessed for pure growth then were stored at 20℃.

## 3.2 Chemical preparations

Molar solutions of all the chemicals were made by calculating their molecular weights. Molar solutions were autoclaved at 120℃ for 20 min.

## 3.3 Abiotic surface adhesion test

Abiotic surface adhesion test was devised according to (Anderson et al., 2018) with some modifications. Bacterial strains were incubated up to 0.2 OD recorded by spectrophotometer. Four sterile 96 wells PVC plates were used for two bacterial strains, WGT1 and WGT2, 20 treatments each including positive and negative control. 198 µL (99% v/v) of LB medium containing inoculum was pipetted into each column of wells using a multichannel pipette. Afterwards, 2 µL (1%v/v) of molar solution of each of the molar solutions of the tested chemicals was pipetted into each well. Plates were then incubated at 37℃ for 48 h in a static incubator. After incubation, PVC plates were decanted and rinsed with distilled water three times to remove planktonic bacteria followed by pipetting 198 µL 0.001% CV dye into each well of all the plates followed by incubation for 15 min. Plates were then decanted again and rinsed with distilled water three times until extra CV dye was drained out. 198 µL of 95% ethanol was pipetted into 96 well of all four plates followed by recording absorbance at 570 nm in a microplate reader.

## 3.4 Biofilm culture

Biofilm culturing was intended for recording relative biofilm thickness, location, planktonic bacteria $OD_{600}$ and chiefly EPS encased bacteria $OD_{600}$. For these objectives, 4.9 mL or precisely 4950 µL (99% v/v) of LB broth medium was poured into 20 mL glass

tubes and each tube was supplemented with 50 µL (1% v/v) of each of the molar solutions of tested chemicals followed by autoclaving at 120℃ for 20 min. These tubes were inoculated from broth cultures of WGT1 and WGT2 strains. These inoculated tubes were then statically incubated at 37℃ for 48 h.

## 3.5 Biofilm live weight determination

Biofilm live weight refers to the weight of biofilm still attached to the surface. Live weight was recorded instead of fresh weight to prevent damage to EPS matrix, loss of water, loosing viability of bacteria and residual fragments of biofilm attached to surface; during detachment which can result in inaccurate measurements.

0.9 mL or precisely 990 µL of sterile LB broth medium was pipetted into sixty 1.5 mL sterile eppendorf tubes making up to 99% v/v of total makeup volume. 10 µL of molar solution of each of the molar solutions of tested compounds making up to 1% v/v of total volume was pipetted into each tube. Tubes for 18 treatments with 3 replicates each for both of the two bacterial strains WGT1 and WGT2 were prepared this way. Sixty tubes were inoculated with WGT1 and similarly 60 with WGT2. Negative control tubes were prepared separately for each treatment considering different chemicals have different weight. Total of 120 eppendorf tubes were incubated at 37℃ for 48 h for biofilm formation. After 48 h each tube was weighed against corresponding negative control.

## 3.6 Adherence visualization assay

Eppendorf tubes from above after recording relative biofilm live weights were decanted rinsed thoroughly with distilled water then stained with 0.001% CV dye, to visualize the comparative adherence levels of WGT1 and WGT2 to the tube walls under the influence of tested chemicals.

## 3.7 Swarming motility assay

Swarming motility assay was carried according to (Kearns & Losick, 2004) with some modifications Swarming plates were made by individually supplementing 29.7 mL 0r precisely 29,700 µL semisolid LB agar plate (0.5% agar) with 300 µL of 1 M solutions of tested compounds. Sixty swarming plates were prepared comprising of eighteen treatments, positive and negative control with three replicates, separately for WGT1 and WGT2. 5 µL of inoculum from broth cultures of WGT1 and WGT2 was spotted in the center of each

plate and dried with lid off for 30 min in laminar hood, followed by static incubation at 37℃ for 24 h.

## 3.8 Statistical analyses

To assess the relationships among various biofilm characteristics and bacterial behaviors, Pearson's correlation coefficients were calculated using Microsoft Excel 2020. The data included 20 observations for six variables: Abiotic adhesion represented as CV absorbance at 570nm, Biofilm Thickness, Planktonic Bacteria $OD_{600}$, EPS encased bacteria $OD_{600}$, Biofilm Live Weight, and Swarming Diameter for WGT1 and WGT2.

# Chapter 4

# Results

## 4.1 Distinct Biofilm morphotypes

Biofilm formed by WGT1 was characterized by grainy appearance whereas WGT2 formed appeared smooth.

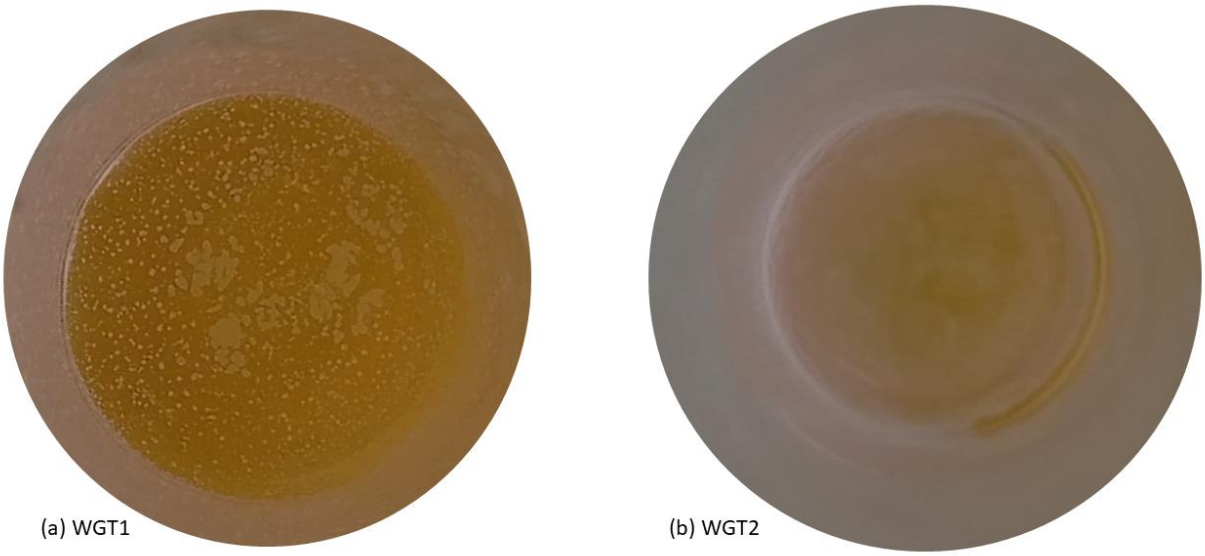


Figure 1. Distinct morphotypes of WGT1 and WGT2 formed on LB broth.

## 4.2 Abiotic surface adhesion test

The magnitude of quantified biofilm was evaluated by recording the absorbance of each PVC plate at 570 nm as shown in figure 4 and 5. After LB reference treatment, $OD_{570}$ recorded for WGT1 and WGT2 was 0.28 and 0.20 respectively (Table 1).

For WGT1 related treatments, increase in absorbance ranged from 41% to 457% compared to Reference LB treatment after supplementing with selected compounds. Ammonium sulfate, ascorbic acid and gelatine significantly augmented the biofilm quantification levels compared to other compounds and in a range from 300% to >600%. Calcium chloride, D glucose, glycine, manganese sulfate and pectin increased biofilm quantification levels in a range from 100% to 300%. Ammonium oxalate, boric acid, potassium chloride, potassium dihydrogen phosphate, magnesium sulfate and zinc oxide are the compounds that increased biofilm levels up to 100%.

For WGT2 treatment, biofilm quantification under the supplementation of selected compounds boosted in a range from 12% to 1516% compared to the reference LB treatment. Magnesium sulfate and gelatine increased the biofilm formation more than 1000%. Ammonium sulfate, ammonium oxalate, ascorbic acid and D glucose increased the biofilm levels more than 200%. Boric acid, calcium chloride, potassium chloride, potassium dihydrogen phosphate, molybdenum trioxide and pectin raised biofilm level more than 100%. Glycine, magnesium sulfate and zinc oxide increased biofilm level up to 100%. Oppositely, Citric acid, copper sulfate, iron (III) chloride and malic acid completely inhibited the biofilm formation as biofilm quantification levels recorded for these compounds were zero for both strains

Table 1 represents relative absorbance values at 579nm for WGT1 and WGT2. Figure 2 and 3 represent absorbance levels as bars. Figure 4 and 5 represents CV color produced by each treatment.

*Table 1. Relative absorbance levels of WGT1 and WGT2 biofilm formation at 570nm after multiclass compound treatments.*

| Treatments | Absorbance at 570nm (WGT1) | % Increase/ decrease | Absorbance at 570nm (WGT2) | % Increase/ decrease |
|---|---|---|---|---|
| LB + 1% Ammonium Oxalate | 0.44±0.08 | **53** | 1.10±0.21 | **483** |
| LB + 1% Ammonium Sulphate | 2.06±0.19 | **625** | 0.99±0.08 | **426** |
| LB + 1% Ascorbic Acid | 1.51±0.23 | **429** | 0.80±0.18 | **327** |
| LB + 1% Boric Acid | 0.56±0.03 | **98** | 0.41±0.03 | **118** |
| LB + 1% Calcium Chloride | 0.61±0.32 | **114** | 0.44±0.06 | **132** |
| LB + 1% Citric Acid | 0.00±0.00 | **-99** | 0.00±0.00 | **-95** |
| LB + 1% Copper Sulfate | 0.00±0.00 | **-98** | 0.00±0.00 | **-92** |
| LB + 1% D Glucose | 0.75±0.19 | **165** | 0.58±0.04 | **209** |
| LB + 1% Gelatin | 1.16±0.07 | **309** | 2.09±0.33 | **1010** |
| LB + 1% Glycine | 0.62±0.11 | **117** | 0.21±0.06 | **13** |
| LB + 1% Iron (III) Chloride | 0.00±0.00 | **-99** | 0.00±0.00 | **-99** |
| LB + 1% Magnesium Sulfate | 0.39±0.14 | **38** | 0.19±0.01 | **1** |
| LB + 1% Mallic Acid | 0.00±0.00 | **-98** | 0.00±0.00 | **-99** |
| LB + 1% Manganese Sulfate | 0.81±0.06 | **184** | 3.05±0.06 | **1516** |
| LB + 1% Molybdenum Trioxide | 0.25±0.06 | **-11** | 0.56±0.05 | **195** |
| LB + 1% Pectin | 0.67±0.11 | **137** | 0.38±0.06 | **104** |
| LB + 1% Potassium Chloride | 0.39±0.04 | **36** | 0.50±0.04 | **166** |
| LB + 1% Potassium Dihydrogen Phosphate | 0.50±0.09 | **77** | 0.52±0.09 | **175** |
| LB + 1% Zinc Oxide | 0.37±0.01 | **31** | 0.36±0.05 | **93** |
| LB | 0.28±0.02 | **0** | 0.19±0.00 | **0** |

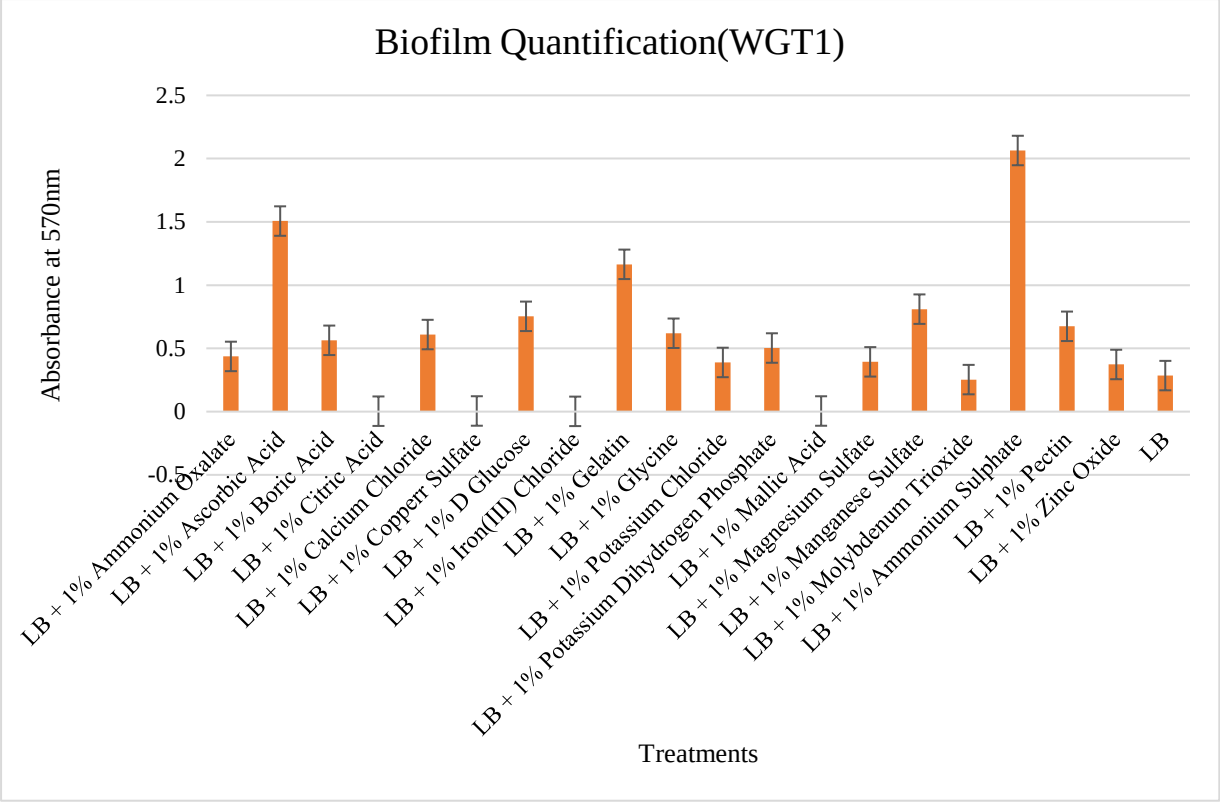


*Figure 2. Relative absorbance levels of biofilm formed by WGT1 at 570nm after multiclass compound treatments represented by bars.*

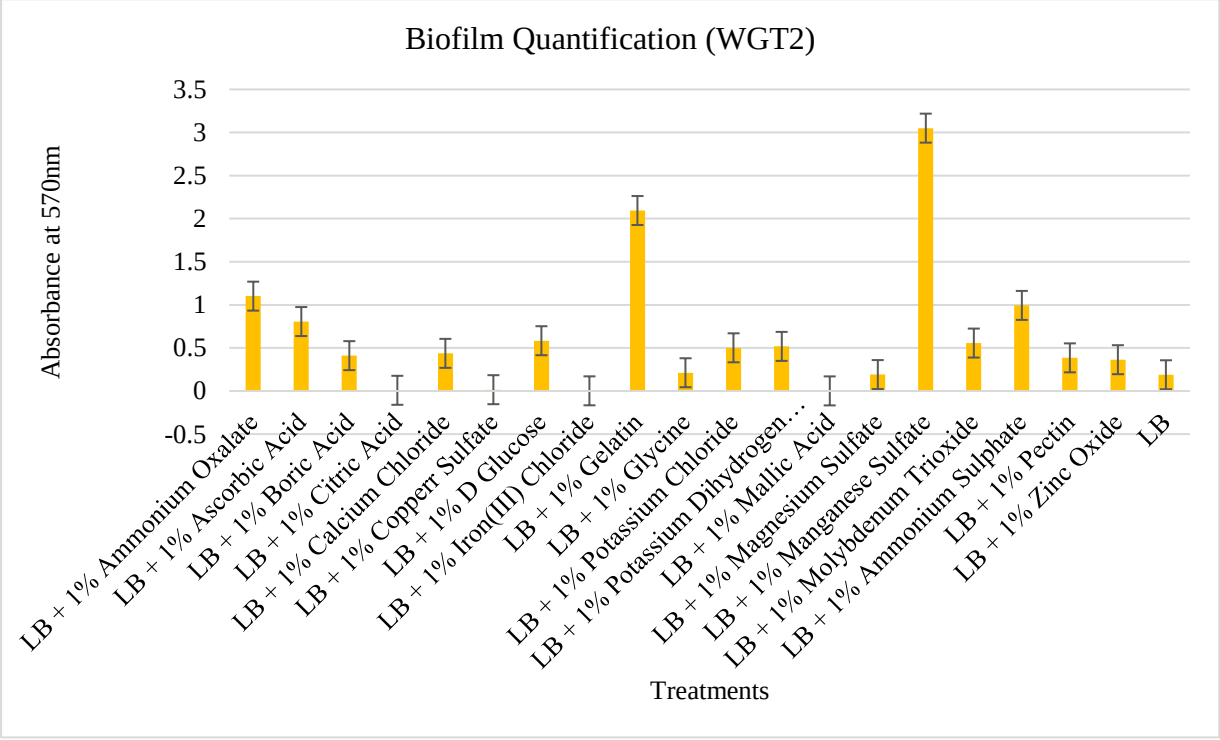


*Figure 3. Relative absorbance levels of biofilm formed by WGT2 at 570nm after multiclass compound treatments represented by bars.*

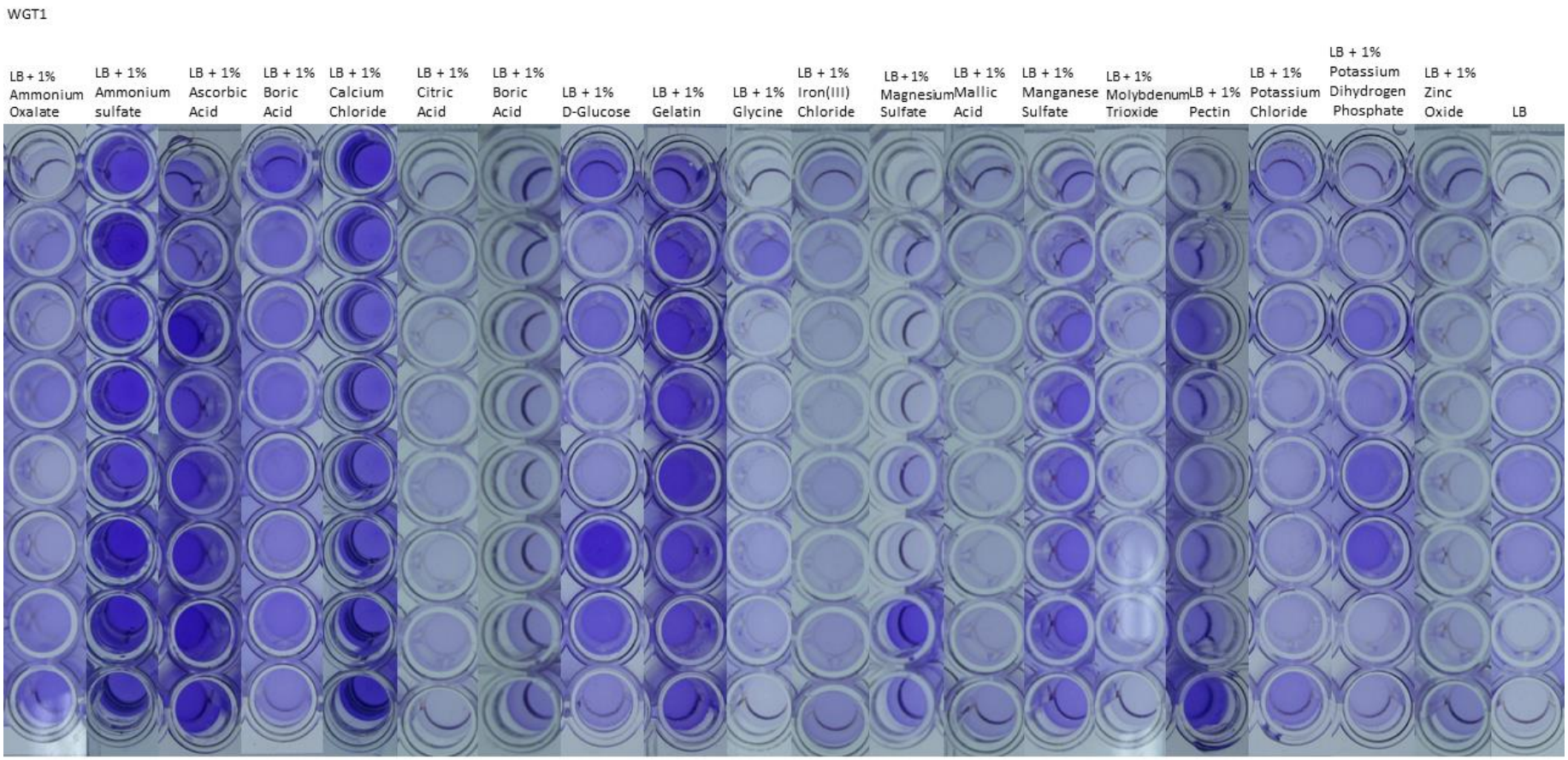
WGT1
LB + 1% Ammonium Oxalate
LB + 1% Ammonium sulfate
LB + 1% Ascorbic Acid
LB + 1% Boric Acid
LB + 1% Calcium Chloride
LB + 1% Citric Acid
LB + 1% Boric Acid
LB + 1% D-Glucose
LB + 1% Gelatin
LB + 1% Glycine
LB + 1% Iron(III) Chloride
LB + 1% Magnesium Sulfate
LB + 1% Mallic Acid
LB + 1% Manganese Sulfate
LB + 1% Molybdenum Trioxide
LB + 1% Pectin
LB + 1% Potassium Chloride
LB + 1% Potassium Dihydrogen Phosphate
LB + 1% Zinc Oxide
LB

*Figure 4. Calorimetric representation of relative absorbance levels of WGT1 biofilm at 570 nm after multiple compound treatments.*

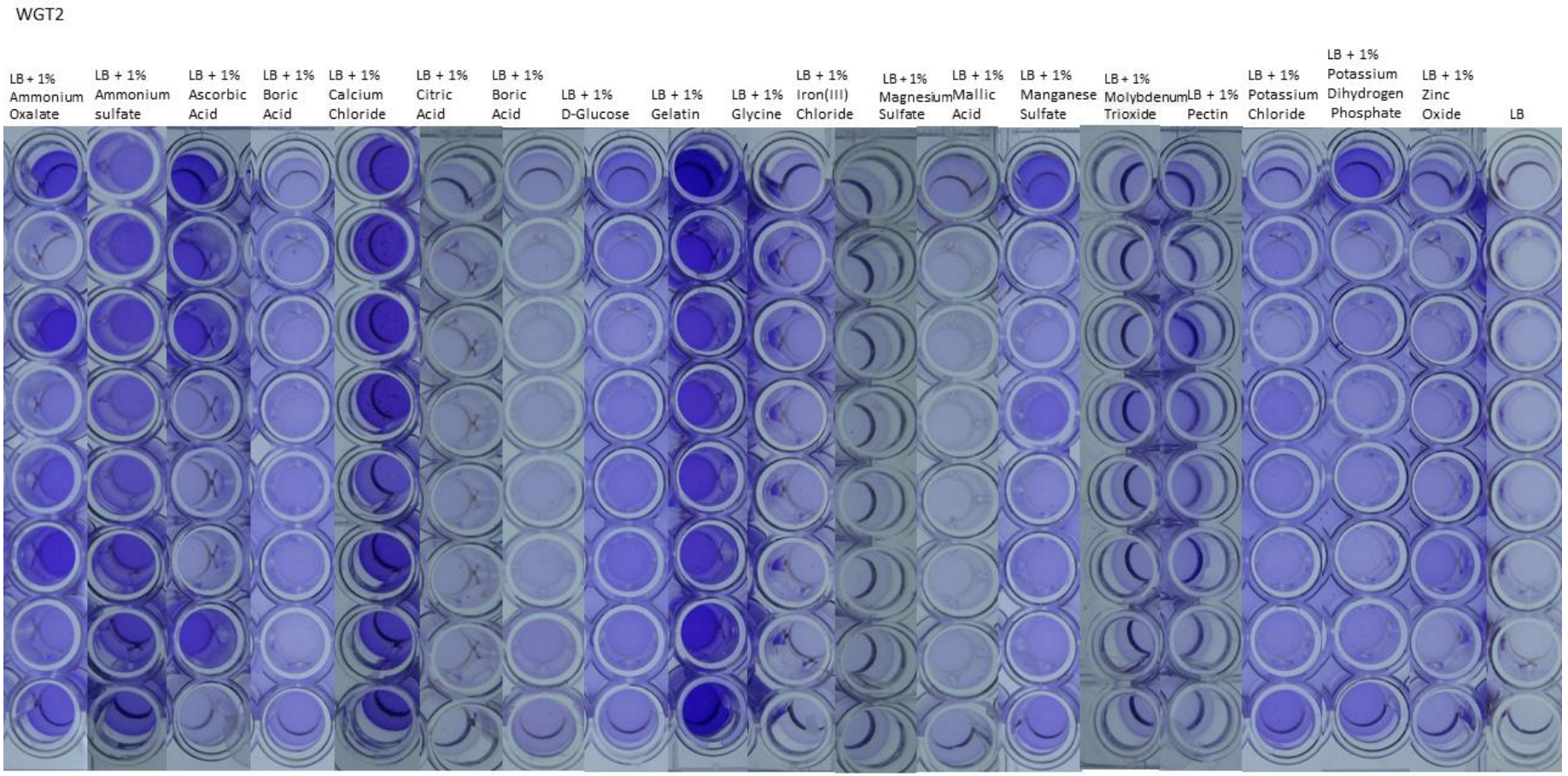
WGT2
LB + 1% Ammonium Oxalate
LB + 1% Ammonium sulfate
LB + 1% Ascorbic Acid
LB + 1% Boric Acid
LB + 1% Calcium Chloride
LB + 1% Citric Acid
LB + 1% Boric Acid
LB + 1% D-Glucose
LB + 1% Gelatin
LB + 1% Glycine
LB + 1% Iron(III) Chloride
LB + 1% Magnesium Sulfate
LB + 1% Mallic Acid
LB + 1% Manganese Sulfate
LB + 1% Molybdenum Trioxide
LB + 1% Pectin
LB + 1% Potassium Chloride
LB + 1% Potassium Dihydrogen Phosphate
LB + 1% Zinc Oxide
LB

*Figure 5. Calorimetric representation of relative absorbance of WGT2 biofilm at 570 nm after multiple compound treatments.*

## 4.3 Biofilm Thickness

Thickness of biofilm was measured by placing a centimeter scale against biofilm layer. Biofilm thickness measure for WGT1 and WGT2 after LB reference treatment was 0.23 cm and 0.30 cm respectively.

Tested compounds thickens the WGT1 biofilm in a range of 28%-157%. Ammonium sulfate, calcium chloride, D glucose, glycine, magnesium sulfate, manganese sulfate, potassium chloride and potassium dihydrogen phosphate, increase thickness of biofilm more than 100%. While Ammonium oxalate, ascorbic acid, boric acid, gelatin, molybdenum trioxide enhanced the biofilm thickness up to 100%.

Thickness of WGT2 biofilm increasingly ranged from 11% to 100%. Ammonium sulfate and calcium chloride increased WGT2 biofilm thickness up to 100%. D glucose, gelatin and magnesium sulfate boosted the thickness more than 80%. Boric acid, glycine, manganese sulfate, pectin and potassium chloride increased the thickness more than 50%. Ascorbic acid, molybdenum trioxide, potassium dihydrogen phosphate and zinc oxide caused less than 50% increase in WGT2 biofilm thickness.

Citric acid, copper sulfate, iron (III) chloride and malic acid completely inhibited the biofilm formation as thickness of biofilm measured for treatments including these compounds was zero for both strains

Table 2 represents the relative thickness levels of WGT1 and WGT2 biofilm. Figure 6 and 7 shows thickness levels of WGT1 and WGT2 represented as bars respectively. Figure 8 and 9 shows biofilms formed in glass tubes under different treatments for WGT1 and WGT2 respectively.

*Table 2. WGT1 and WGT2 Biofilm thickness in cm modulated by multiclass compound treatments.*

| Treatments | WGT1 Biofilm Thickness (cm) | % Increase/ decrease | WGT2 Biofilm Thickness (cm) | % Increase/ decrease |
|---|---|---|---|---|
| LB + 1% Ammonium Oxalate | 0.33±0.08 | **43** | 0.33±0.089 | **11** |
| LB + 1% Ammonium Sulphate | 0.53±0.03 | **129** | 0.60±0.06 | **100** |
| LB + 1% Ascorbic Acid | 0.33±0.03 | **43** | 0.37±0.03 | **22** |
| LB + 1% Boric Acid | 0.43±0.03 | **86** | 0.47±0.03 | **56** |
| LB + 1% Calcium Chloride | 0.57±0.03 | **143** | 0.60±0.06 | **100** |
| LB + 1% Citric Acid | 0.00±0.00 | **-100** | 0.00±0.00 | **-100** |
| LB + 1% Copperr Sulfate | 0.00±0.00 | **-100** | 0.00±0.00 | **-100** |
| LB + 1% D Glucose | 0.47±0.03 | **100** | 0.57±0.03 | **89** |
| LB + 1% Gelatin | 0.30.0.06 | **29** | 0.57±0.07 | **89** |
| LB + 1% Glycine | 0.57±0.03 | **143** | 0.47±0.03 | **56** |
| LB + 1% Iron(III) Chloride | 0.00±0.00 | **-100** | 0.00±0.00 | **-100** |
| LB + 1% Magnesium Sulfate | 0.60±0.06 | **157** | 0.57±0.03 | **89** |
| LB + 1% Mallic Acid | 0.00+0.00 | **-100** | 0.00±0.00 | **-100** |
| LB + 1% Manganese Sulfate | 0.57±0.09 | **143** | 0.53±0.03 | **78** |
| LB + 1% Molybdenum Trioxide | 0.30±0.06 | **29** | 0.43±0.09 | **44** |
| LB + 1% Pectin | 0.57±0.07 | **143** | 0.53±0.09 | **78** |
| LB + 1% Potassium Chloride | 0.57±0.03 | **143** | 0.53±0.03 | **78** |
| LB + 1% Potassium Dihydrogen Phosphate | 0.57±0.03 | **143** | 0.43±0.09 | **44** |
| LB + 1% Zinc Oxide | 0.23±0.03 | **0** | 0.33±0.03 | **11** |
| LB | 0.23+0.09 | **0** | 0.30±0.11 | **0** |

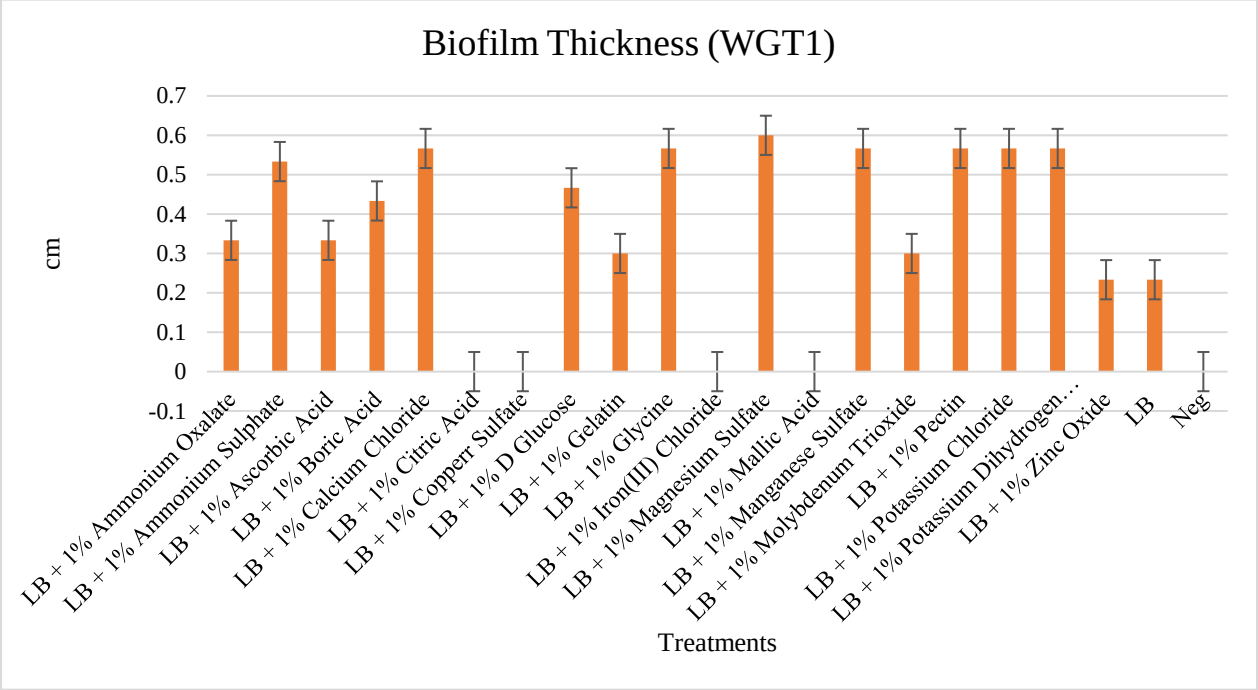


*Figure 6. Relative thickness of WGT1 biofilms measured in cm after multiclass compound treatments represented by bars.*

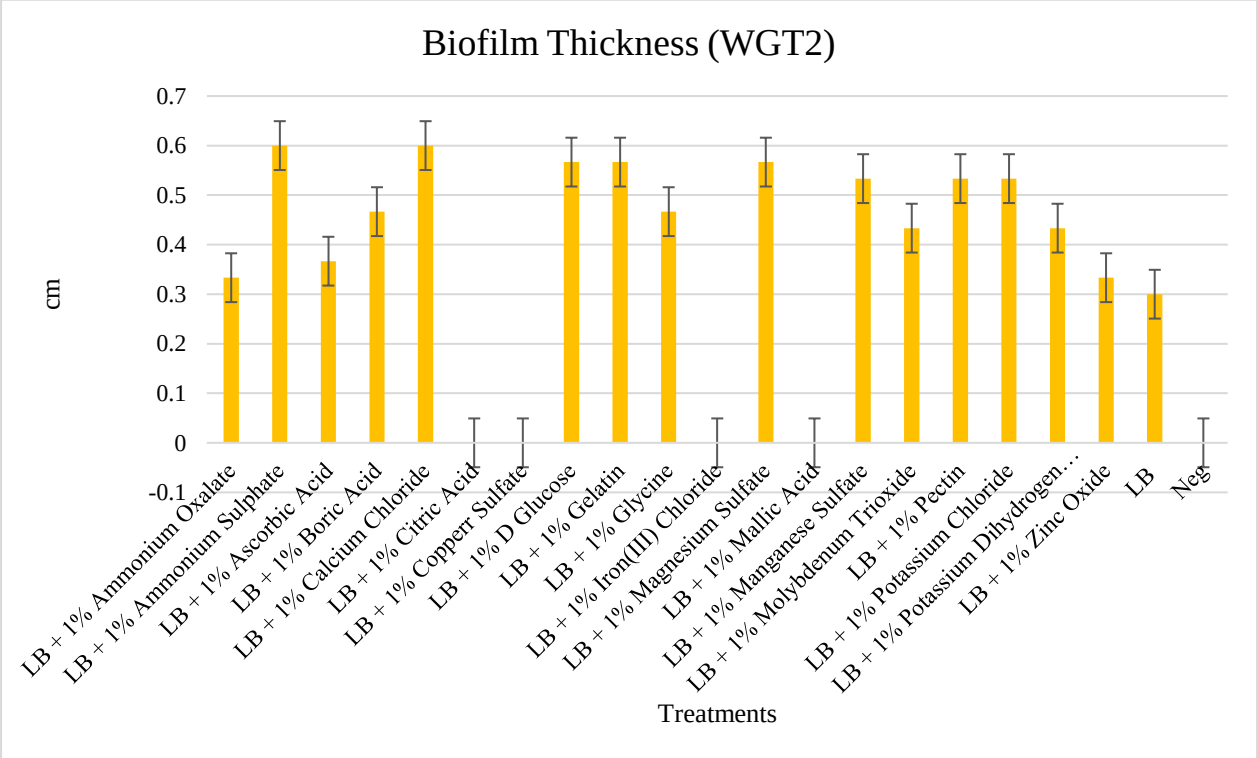


*Figure 7. Relative thickness of WGT2 biofilms measured in cm after multiclass compound treatments represented by bars.*

## 4.4 Biofilm location characterization

WGT1 and WGT2 was able to form pellicle, ring and submerged type biofilm. Table 3 represents Characterization of biofilms formed by WGT1 and WGT2 according to location which is shown in figure 8 and 9 respectively. Submerged biofilms are indicated by arrow head.

WGT1 formed pellicle and ring biofilm in the presence of all chemicals except citric acid, copper sulfate, iron (III) chloride and malic acid. WGT1 formed submerged biofilm in the presence of magnesium sulfate, pectin and zinc oxide.

WGT2 was able to form pellicle and ring biofilm in the presence of all compounds excepts citric acid, copper sulfate, iron (III) chloride and malic acid while submerged biofilm was formed in the presence of ammonium oxalate, ascorbic acid, gelatin, manganese sulfate, pectin and zinc oxide.

*Table 3. Characterization of biofilms formed by WGT1 and WGT2 according to location.*

| **Biofilm Location & Characterization** | **WGT1** | | | **WGT2** | | |
|---|---|---|---|---|---|---|
| **Treatments** | **Pellicle** | **Ring** | **Submerged** | **Pellicle** | **Ring** | **Submerged** |
| LB + 1% Ammonium Oxalate | (+) | (+) | (-) | (+) | (+) | **(+)** |
| LB + 1% Ammonium Sulphate | (+) | (+) | (-) | (+) | (+) | (-) |
| LB + 1% Ascorbic Acid | (+) | (+) | (-) | (+) | (+) | **(+)** |
| LB + 1% Boric Acid | (+) | (+) | (-) | (+) | (+) | (-) |
| LB + 1% Calcium Chloride | (+) | (+) | (-) | (+) | (+) | (-) |
| LB + 1% Citric Acid | (-) | (-) | (-) | (-) | (-) | (-) |
| LB + 1% Copper Sulfate | (-) | (-) | (-) | (-) | (-) | (-) |
| LB + 1% D Glucose | (+) | (+) | (-) | (+) | (+) | (-) |
| LB + 1% Gelatin | (+) | (+) | (-) | (+) | (+) | **(+)** |
| LB + 1% Glycine | (+) | (+) | (-) | (+) | (+) | (-) |
| LB + 1% Iron (III) Chloride | (-) | (-) | (-) | (-) | (-) | (-) |
| LB + 1% Magnesium Sulfate | (+) | (+) | **(+)** | (+) | (+) | (-) |
| LB + 1% Mallic Acid | (-) | (-) | (-) | (-) | (-) | (-) |
| LB + 1% Manganese Sulfate | (+) | (+) | (-) | (+) | (+) | **(+)** |
| LB + 1% Molybdenum Trioxide | (+) | (+) | (-) | (+) | (+) | (-) |
| LB + 1% Pectin | (+) | (+) | **(+)** | (+) | (+) | **(+)** |
| LB + 1% Potassium Chloride | (+) | (+) | (-) | (+) | (+) | (-) |
| LB + 1% Potassium Dihydrogen Phosphate | (+) | (+) | (-) | (+) | (+) | (-) |
| LB + 1% Zinc Oxide | (-) | (-) | **(+)** | (+) | (+) | **(+)** |
| LB | (+) | (+) | (-) | (+) | (+) | (-) |
| Neg | (-) | (-) | (-) | (-) | (-) | (-) |

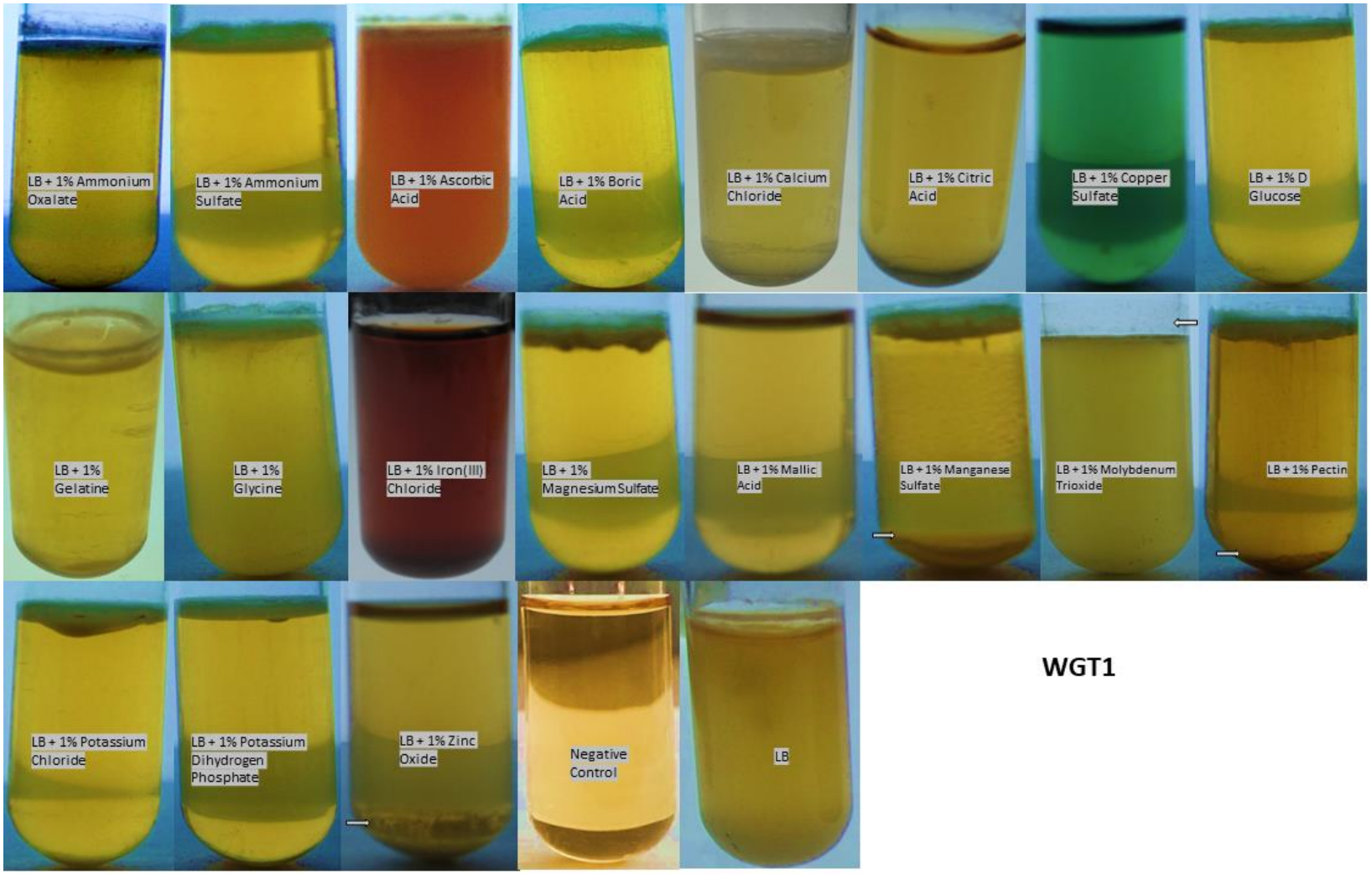
LB + 1% Ammonium Oxalate
LB + 1% Ammonium Sulfate
LB + 1% Ascorbic Acid
LB + 1% Boric Acid
LB + 1% Calcium Chloride
LB + 1% Citric Acid
LB + 1% Copper Sulfate
LB + 1% D Glucose
LB + 1% Gelatine
LB + 1% Glycine
LB + 1% Iron(III) Chloride
LB + 1% Magnesium Sulfate
LB + 1% Mallic Acid
LB + 1% Manganese Sulfate
LB + 1% Molybdenum Trioxide
LB + 1% Pectin
LB + 1% Potassium Chloride
LB + 1% Potassium Dihydrogen Phosphate
LB + 1% Zinc Oxide
Negative Control
LB
WGT1

*Figure 8. Biofilms formed by WGT1 modulated by multiclass chemical treatments.*

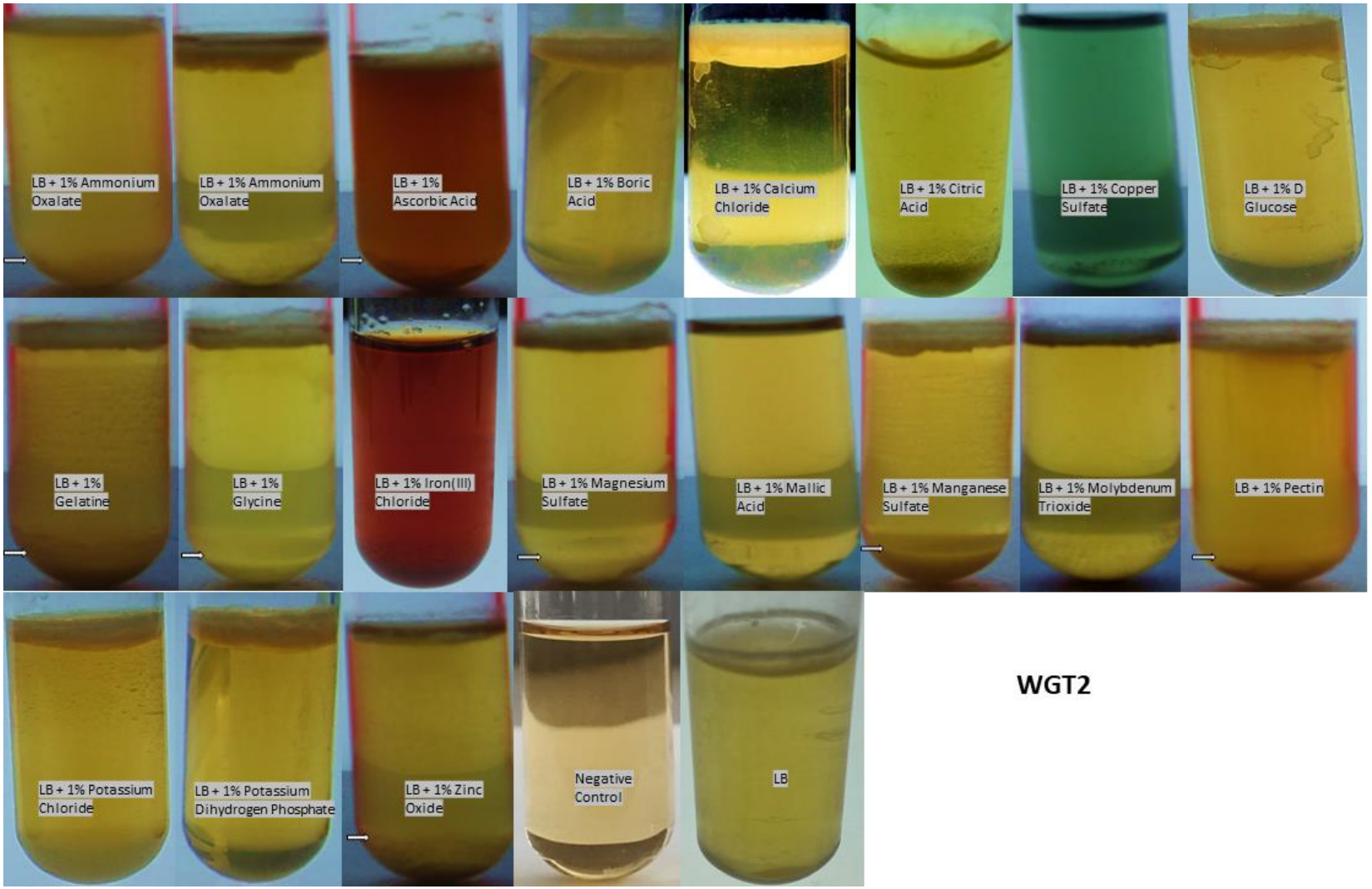
LB + 1% Ammonium Oxalate
LB + 1% Ammonium Oxalate
LB + 1% Ascorbic Acid
LB + 1% Boric Acid
LB + 1% Calcium Chloride
LB + 1% Citric Acid
LB + 1% Copper Sulfate
LB + 1% D Glucose
LB + 1% Gelatine
LB + 1% Glycine
LB + 1% Iron(III) Chloride
LB + 1% Magnesium Sulfate
LB + 1% Mallic Acid
LB + 1% Manganese Sulfate
LB + 1% Molybdenum Trioxide
LB + 1% Pectin
LB + 1% Potassium Chloride
LB + 1% Potassium Dihydrogen Phosphate
LB + 1% Zinc Oxide
Negative Control
LB
WGT2

*Figure 9. Biofilms formed by WGT2 modulated by multiclass chemical treatments.*

## 4.5 EPS encased bacteria $OD_{600}$

Absorbance of EPS encased bacteria at 600nm was calculated by subtracting planktonic bacteria $OD_{600}$ (table 5) from whole bacteria $OD_{600}$ ($OD_{600}$ after physically disrupting the biofilm). Planktonic bacterial $OD_{600}$ was generally lower than the whole $OD_{600}$. EPS encased bacteria $OD_{600}$ measured for LB reference treatment of WGT1 was 0.13 while for WGT2 it was 0.43.

Increase in WGT1 EPS encased bacteria $OD_{600}$, under the treatment of tested compounds ranged from 13% to 457%. Ammonium sulfate and magnesium sulfate caused an increase of more than 400%. Calcium chloride enhanced EPS encased bacteria $OD_{600}$ more than 300%. More than 200% increase was observed for boric acid, glycine, manganese sulfate and pectin. More than 100% increase was observed for ammonium oxalate, gelatin and potassium chloride; while less than 100% increase was ascorbic acid, d glucose, molybdenum trioxide and potassium dihydrogen phosphate. Zinc oxide caused 67% reduction in EPS encased bacteria $OD_{600}$.

Increase in WGT2 EPS encased bacteria $OD_{600}$ was recorded in a range of 55% - 311%. Manganese sulfate increases the EPS $OD_{600}$ more than 300%. More than 200% increase was observed for gelatine and magnesium sulfate. More than 100% increase in $OD_{600}$ was observed for ammonium oxalate, ammonium sulfate, ascorbic acid, calcium chloride, d glucose and potassium dihydrogen phosphate; while less than 100% increase was observed for glycine, molybdenum trioxide and pectin. Zinc oxide led to 53% reduction in EPS encased bacteria $OD_{600}$.

Citric acid, copper sulfate, iron (III) chloride and malic acid completely inhibited the biofilm formation. Therefore, zero planktonic $OD_{600}$ as well as whole $OD_{600}$ was recorded for both WGT1 and WGT2 after the treatments of these compounds.

Table 3 represents EPS encased bacteria $OD_{600}$ recorded in all treatments of treatments of WGT1 and WGT2. Figure 10 and 11 represents EPS bacteria $OD_{600}$ levels as bars respectively.

*Table 4. EPS encased bacteria $OD_{600}$ of WGT1 and WGT2 biofilms modulated by multiclass chemical treatments.*

| Treatments | WGT1 EPS encased bacteria $OD_{600}$ | % Increase/ decrease | WGT2 EPS encased bacteria $OD_{600}$ | % Increase/ decrease |
|---|---|---|---|---|
| LB + 1% Ammonium Oxalate | 0.31±0.05 | **143** | 1.00±0.30 | **687** |
| LB + 1% Ammonium Sulphate | 0.69±0.13 | **443** | 1.19±0.10 | **841** |
| LB + 1% Ascorbic Acid | 0.14±0.08 | **13** | 1.19±0.11 | **838** |
| LB + 1% Boric Acid | 0.49±0.05 | **288** | 0.24±0.13 | **89** |
| LB + 1% Calcium Chloride | 0.53±0.07 | **317** | 0.87±0.06 | **586** |
| LB + 1% Citric Acid | 0.00±0.00 | **-100** | 0.00±0.00 | **-100** |
| LB + 1% Copper Sulfate | 0.00±0.00 | **-100** | 0.00±0.00 | **-100** |
| LB + 1% D Glucose | 0.23±0.08 | **78** | 1.24±0.07 | **880** |
| LB + 1% Gelatin | 0.35±0.06 | **175** | 1.45±0.24 | **1045** |
| LB + 1% Glycine | 0.44±0.10 | **246** | 0.855333333 | **575** |
| LB + 1% Iron (III) Chloride | 0.00±0.00 | **-100** | 0.00±0.00 | **-100** |
| LB + 1% Magnesium Sulfate | 0.71±0.05 | **458** | 1.64±0.10 | **1194** |
| LB + 1% Mallic Acid | 0.00±0.00 | **-100** | 0.00±0.00 | **-100** |
| LB + 1% Manganese Sulfate | 0.39±0.03 | **205** | 1.78±0.09 | **1304** |
| LB + 1% Molybdenum Trioxide | 0.22±0.09 | **77** | 0.81±0.11 | **537** |
| LB + 1% Pectin | 0.39±0.26 | **212** | 0.84±0.21 | **567** |
| LB + 1% Potassium Chloride | 0.33±0.06 | **157** | 0.67±0.17 | **432** |
| LB + 1% Potassium Dihydrogen Phosphate | 0.18±0.04 | **42** | 1.00±0.17 | **694** |
| LB + 1% Zinc Oxide | 0.08±0.02 | **-34** | 0.23±0.09 | **80** |
| LB | 0.13±0.04 | **0** | 0.43±0.30 | **241** |
| Neg | 0 | **-100** | 0 | **-100** |

Table 5. Planktonic bacteria $OD_{600}$ of WGT1 and WGT2 biofilms modulated by multiclass chemical treatments

| Treatments | WGT1 Planktonic Bacteria $OD_{600}$ | WGT2 Planktonic bacteria $OD_{600}$ |
|---|---|---|
| LB + 1% Ammonium Oxalate | 0.41±0.08 | 0.37±0.11 |
| LB + 1% Ammonium Sulphate | 0.52±0.26 | 0.13±0.09 |
| LB + 1% Ascorbic Acid | 0.73±0.05 | 0.66±0.12 |
| LB + 1% Boric Acid | 0.45±0.02 | 0.52±0.09 |
| LB + 1% Calcium Chloride | 0.18±0.06 | 0.76±0.09 |
| LB + 1% Citric Acid | 0.10±0.00 | 0.05±0.01 |
| LB + 1% Copper Sulfate | 0.14±0.00 | 0.12±0.00 |
| LB + 1% D Glucose | 0.43±0.10 | 0.65±0.07 |
| LB + 1% Gelatin | 0.34±0.03 | 0.39±0.10 |
| LB + 1% Glycine | 0.14±0.05 | 0.60±0.13 |
| LB + 1% Iron (III) Chloride | 0.15±0.00 | 0.14±0.00 |
| LB + 1% Magnesium Sulfate | 0.08±0.02 | 0.15±0.01 |
| LB + 1% Mallic Acid | 0.12±0.01 | 0.10±0.01 |
| LB + 1% Manganese Sulfate | 0.33±0.01 | 0.20±0.05 |
| LB + 1% Molybdenum Trioxide | 0.43±0.09 | 0.38±0.12 |
| LB + 1% Pectin | 0.51±0.04 | 0.70±0.07 |
| LB + 1% Potassium Chloride | 0.35±0.12 | 1.20±0.15 |
| LB + 1% Potassium Dihydrogen Phosphate | 0.51±0.04 | 0.48±0.08 |
| LB + 1% Zinc Oxide | 0.59±0.01 | 0.44±0.09 |
| LB | 0.70±0.02 | 0.81±0.04 |
| Neg | 0.00±0.00 | 0.00±0.00 |

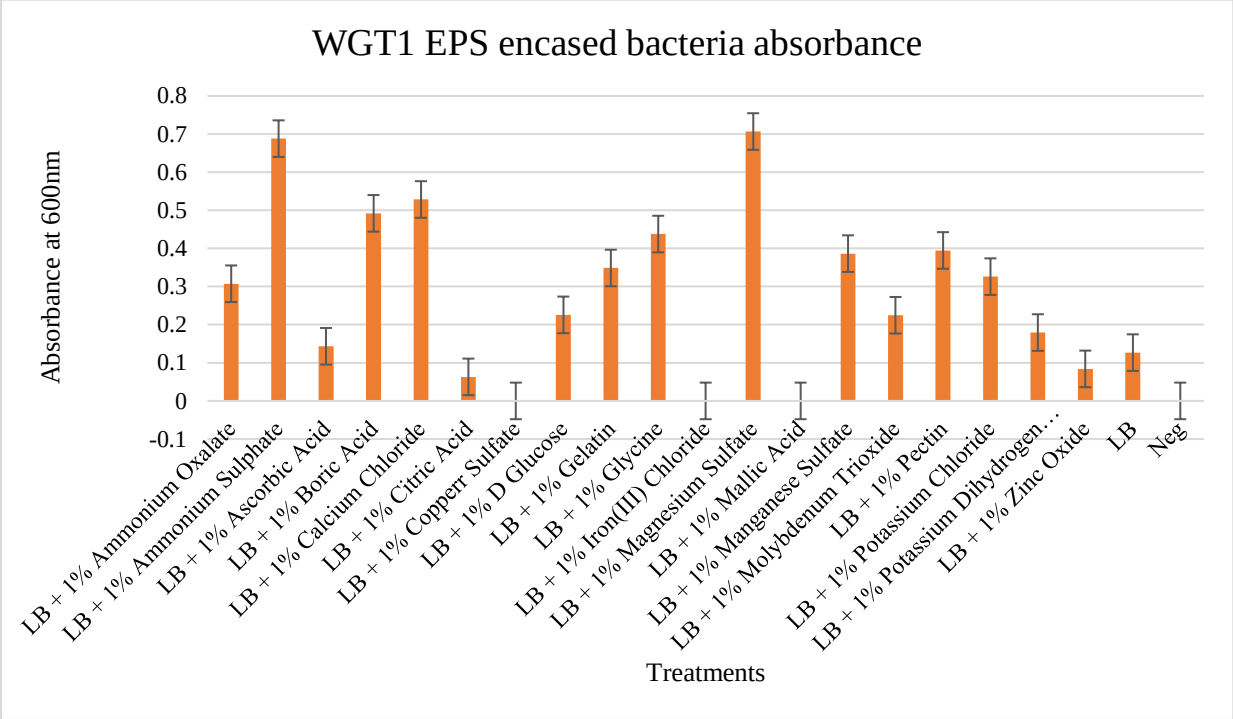


*Figure 10. Relative absorbance levels of WGT1 EPS bacterial population at 600nm represented by bars.*

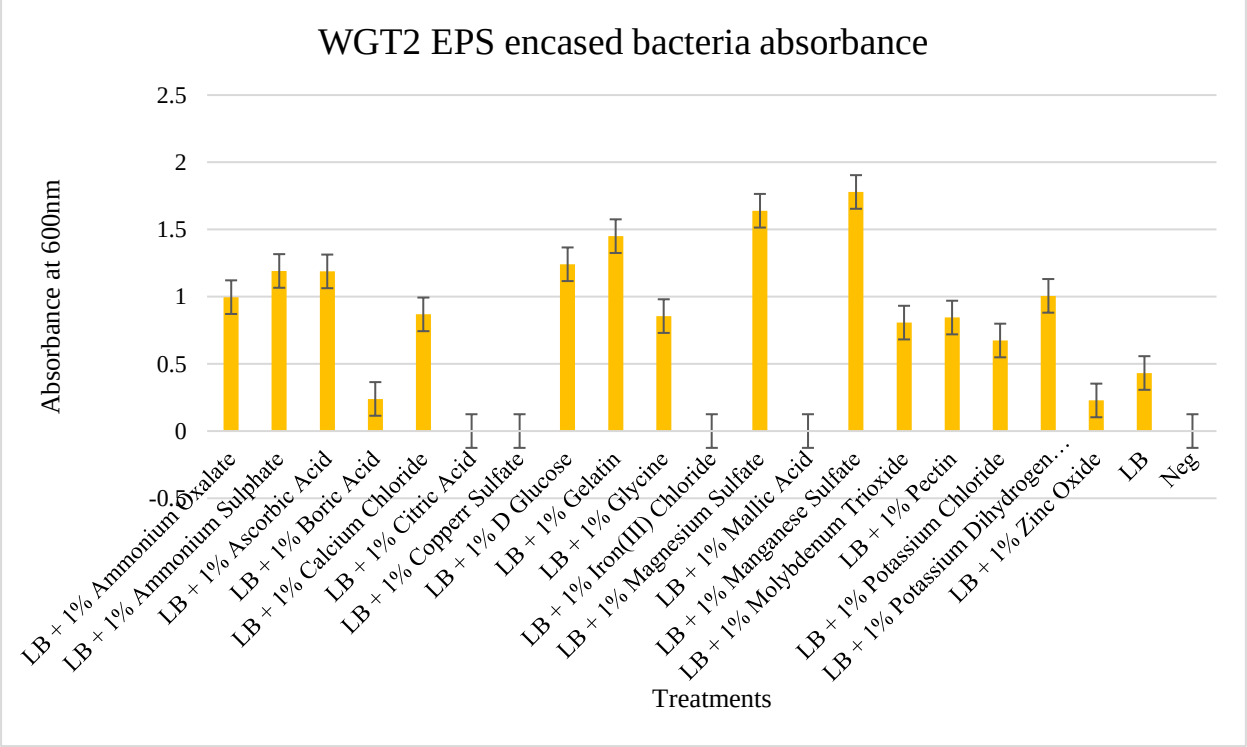


*Figure 11.Relative absorbance levels of WGT2 EPS bacterial population at 600nm represented by bars.*

## 4.6 Biofilm live weight

Live weight after each treatment was determined by weighing live biofilms on laboratory balance. Live weights recorded for WGT1 and WGT2 biofilm after LB reference treatment were 0.18g and 0.19g respectively.

Tested compounds causes increase in WGT1 biofilm live weight from 10% to 83%. Ammonium sulfate, manganese sulfate increased the live weight of WGT1 biofilm more than 50%, while ammonium oxalate, ascorbic acid, boric acid, calcium chloride, d- glucose, gelatin, glycine, magnesium sulfate, molybdenum trioxide, pectin, potassium chloride and potassium dihydrogen phosphate caused an increase of less than 50%. Whereas, zinc oxide reduced the live weight to 97%.

WGT1 biofilm live weight increased in a range of 9% to 103%. Ammonium sulfate, calcium chloride and magnesium sulfate caused an increase of more than 50% while ammonium oxalate, ascorbic acid, boric acid, d glucose, gelatin, glycine, manganese sulfate, molybdenum trioxide, pectin, potassium chloride, potassium dihydrogen phosphate and zinc oxide caused an increase of less than 50%.

Citric acid, copper sulfate, iron (III) chloride and malic acid completely inhibited the biofilm formation in both strains hence no live biofilm weight was recorded for these treatments.

Table 4 represents live weights of WGT1 and WGT2 biofilms modulated by multiclass compound treatments. Figure 12 and 13 represents live weights of WGT1 and WGT2 biofilms as bars.

*Table 6. Live weights of WGT1 and WGT2 biofilms modulated by multiclass compound treatments.*

| Treatments | WGT1 biofilm live weight (g) | % Increase/ decrease | WGT2 Biofilm live weight (g) | % Increase/ decrease |
|---|---|---|---|---|
| LB + 1% Ammonium Oxalate | 0.23±0.03 | **28** | 0.25±0.02 | **31** |
| LB + 1% Ammonium Sulphate | 0.27±0.01 | **51** | 0.31±0.05 | **61** |
| LB + 1% Ascorbic Acid | 0.20±0.02 | **10** | 0.21±0.01 | **10** |
| LB + 1% Boric Acid | 0.21±0.01 | **14** | 0.23±0.02 | **19** |
| LB + 1% Calcium Chloride | 0.26±0.05 | **45** | 0.29±0.03 | **52** |
| LB + 1% Citric Acid | 0.00±0.00 | **-100** | 0.22±0.02 | **-100** |
| LB + 1% Copper Sulfate | 0.00±0.00 | **-100** | 0.22±0.01 | **-100** |
| LB + 1% D Glucose | 0.24±0.03 | **32** | 0.26±0.04 | **34** |
| LB + 1% Gelatin | 0.26±0.01 | **42** | 0.29±0.01 | **34** |
| LB + 1% Glycine | 0.27±0.05 | **48** | 0.24±0.1 | **27** |
| LB + 1% Iron (III) Chloride | 0.00±0.00 | **-100** | 0.00±0.00 | **-100** |
| LB + 1% Magnesium Sulfate | 0.23±0.02 | **27** | 0.40±0.08 | **104** |
| LB + 1% Malic Acid | 0.00±0.00 | **-100** | 0.00±0.00 | **-100** |
| LB + 1% Manganese Sulfate | 0.33±0.03 | **84** | 0.29±0.03 | **50** |
| LB + 1% Molybdenum Trioxide | 0.24±0.05 | **31** | 0.22±0.01 | **14** |
| LB + 1% Pectin | 0.23±0.01 | **24** | 0.26±0.01 | **36** |
| LB + 1% Potassium Chloride | 0.25±0.01 | **36** | 0.25±0.01 | **27** |
| LB + 1% Potassium Dihydrogen Phosphate | 0.21±0.02 | **16** | 0.25±0.01 | **32** |
| LB + 1% Zinc Oxide | 0.17±0.01 | **-4** | 0.22±0.01 | **13** |
| LB | 0.18±0.04 | **0** | 0.20±0.02 | **0** |
| Negative control | 0 | **-100** | 0 | **-100** |

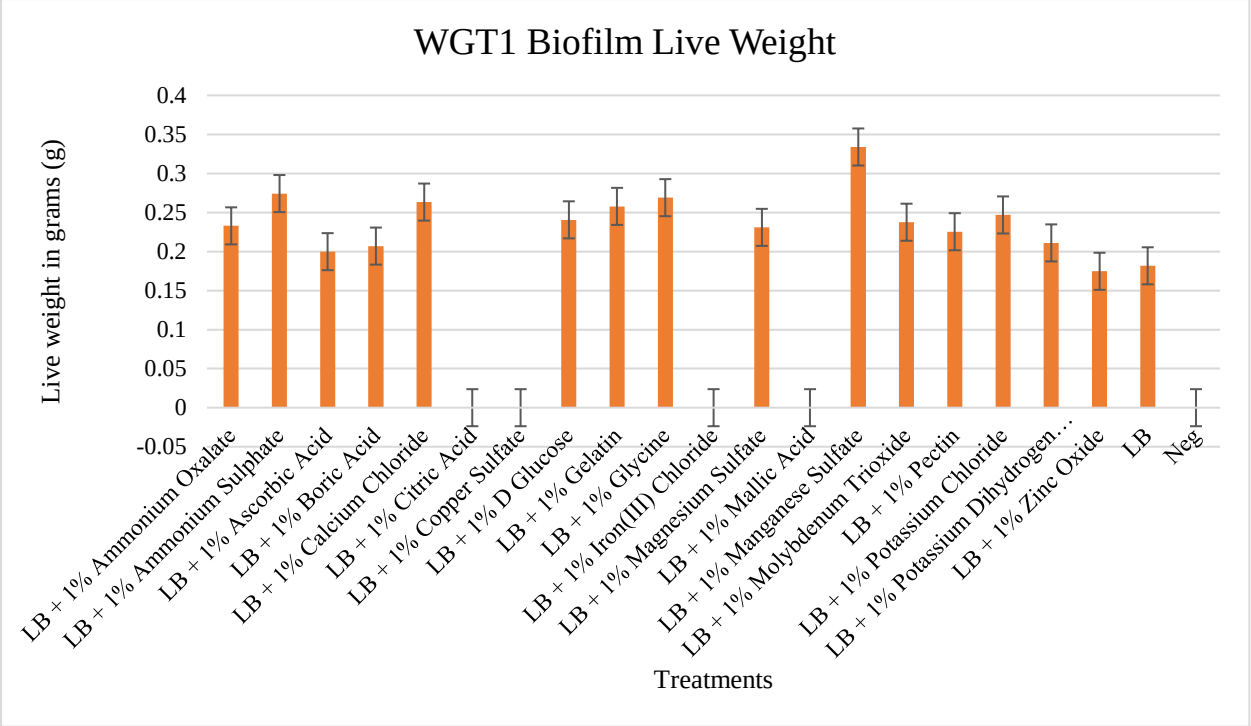


*Figure 12. Live weights of WGT1 biofilm modulated by multiclass compound treatments represented by bars.*

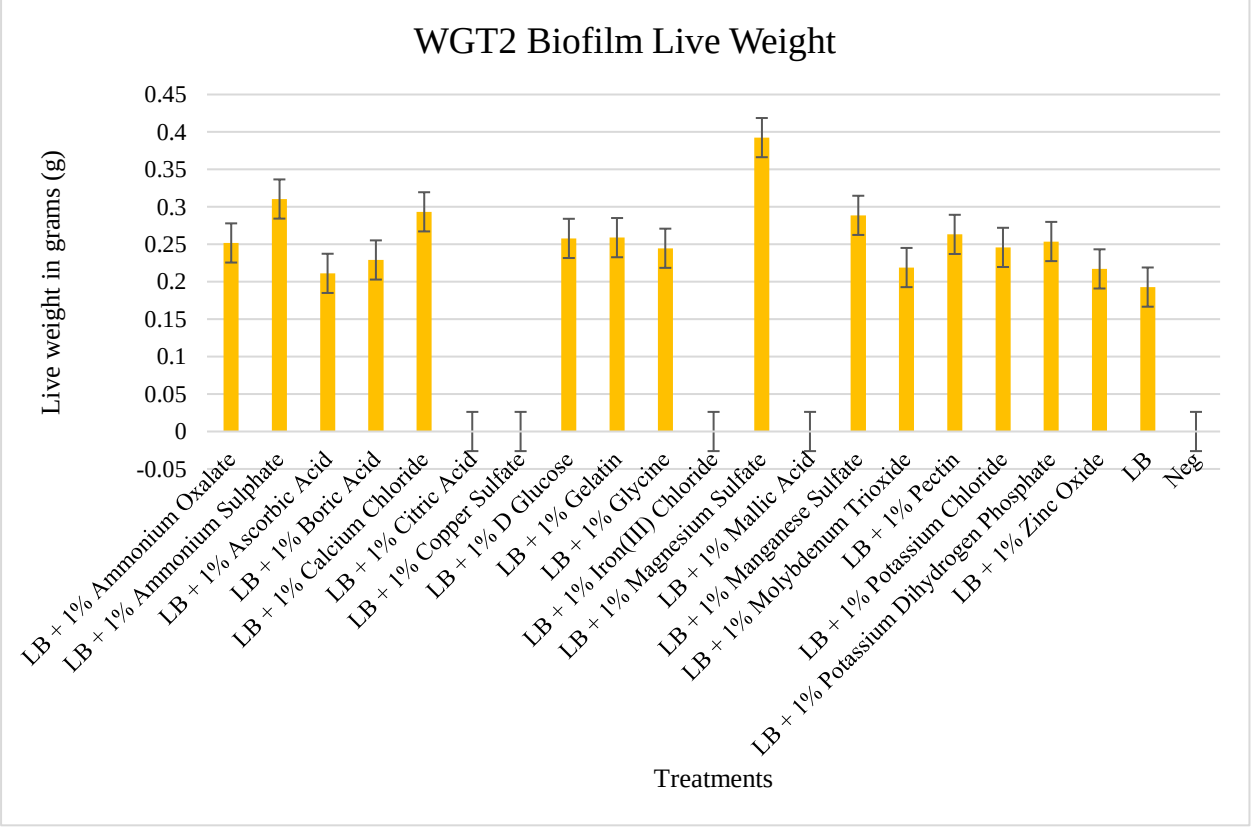


*Figure 13. Live weights of WGT2 biofilm modulated by multiclass compound treatments represented by bars.*

## 4.7 Adherence visualization assay

Stained regions of tubes represent bacterial adhesion sites. Both WGT1 and WGT2 showed robust levels of adherence in the presence of all compounds as compared to reference LB treatment. Citric acid, copper sulfate, iron (III) chloride and malic acid completely inhibited adherence of bacteria to the walls of Eppendorf tubes as no stained regions were observed for treatments involving these compounds for both strains.

Bacteria adhered randomly to a surface followed by flagellar movement towards air liquid interface. Chemicals showed pellicle or ring formation did not show bacteria attached to surface beneath air liquid interface while bacteria adhered to the surface beneath air liquid interface did not show pellicle or ring biofilm formation.

Figure 14 and 15 represents adherence of WGT1 and WGT2 influenced by multiclass compounds represented by stained regions respectively.

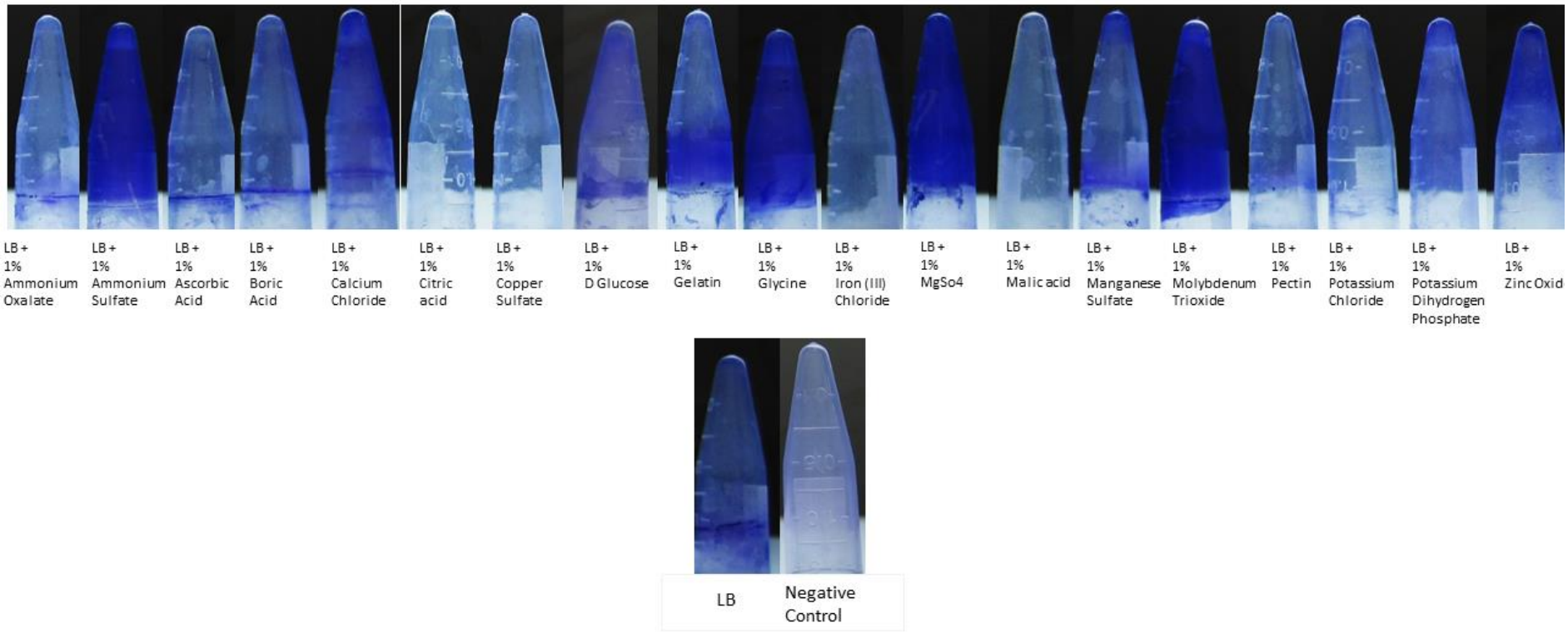
WGT1
LB + 1% Ammonium Oxalate
LB + 1% Ammonium Sulfate
LB + 1% Ascorbic Acid
LB + 1% Boric Acid
LB + 1% Calcium Chloride
LB + 1% Citric acid
LB + 1% Copper Sulfate
LB + 1% D Glucose
LB + 1% Gelatin
LB + 1% Glycine
LB + 1% Iron (III) Chloride
LB + 1% MgSo4
LB + 1% Malic acid
LB + 1% Manganese Sulfate
LB + 1% Molybdenum Trioxide
LB + 1% Pectin
LB + 1% Potassium Chloride
LB + 1% Potassium Dihydrogen Phosphate
LB + 1% Zinc Oxid
LB
Negative Control

*Figure 14. Adherence of WGT1 influenced by multiclass compounds represented by stained regions.*

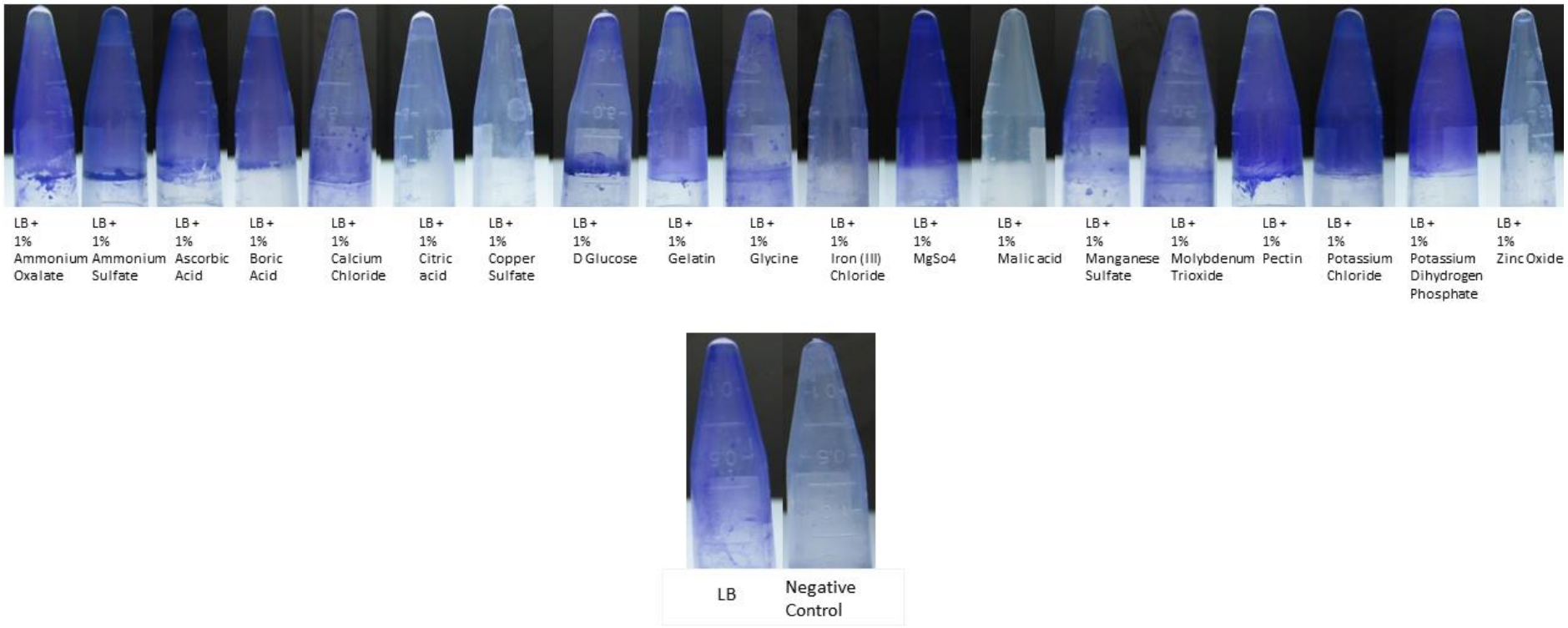
WGT2
LB + 1% Ammonium Oxalate
LB + 1% Ammonium Sulfate
LB + 1% Ascorbic Acid
LB + 1% Boric Acid
LB + 1% Calcium Chloride
LB + 1% Citric acid
LB + 1% Copper Sulfate
LB + 1% D Glucose
LB + 1% Gelatin
LB + 1% Glycine
LB + 1% Iron (III) Chloride
LB + 1% MgSo4
LB + 1% Malic acid
LB + 1% Manganese Sulfate
LB + 1% Molybdenum Trioxide
LB + 1% Pectin
LB + 1% Potassium Chloride
LB + 1% Potassium Dihydrogen Phosphate
LB + 1% Zinc Oxide
LB
Negative Control

*Figure 15. Adherence of WGT2 influenced by multiclass compounds represented by stained regions.*

## 4.8 Swarming motility assay

Tested compounds influenced the swarming of WGT1 and WGT2 within a vast spectrum. Swarming motility was numerically measured by recording swarming diameter in cm. Swarming diameter recorded after LB reference treatment for WGT1 was 1.93 cm while for WGT2 it was 2.53cm.

Tested compounds enhanced the swarming motility of WGT1 in a range of 6% to 303%. In the presence of calcium chloride, d glucose and potassium dihydrogen phosphate swarming diameter increased more than 300%. Ammonium oxalate, ammonium sulfate, magnesium sulfate, potassium chloride increased the swarming motility represented by diameter more than 200%. More than 100% increase in swarming diameter was observed in treatments of ascorbic acid, glycine, molybdenum trioxide and pectin; while less than 100% increase was observed for gelatin and manganese sulfate.

Swarming motility of WGT2, influenced by tested compounds, comes under the range of 15%-209%. More than 200% increase in swarming diameter was measured for calcium chloride, glycine and potassium chloride. More than 100% enhancement in swarming diameter was observed after treatment of ammonium sulfate, ascorbic acid, manganese sulfate, molybdenum trioxide, pectin and potassium dihydrogen phosphate; while, less than 100% increase in swarming diameter was observed for boric acid, d glucose and magnesium sulfate. Ammonium oxalate reduced the swarming diameter to 82%.

Citric acid, copper sulfate, iron (III) chloride, malic acid and zinc oxide completely inhibited the swarming activity as swarming diameter recorded for these compounds was zero for both WGT1 and WGT2.

Table 5 represents Swarming motility of WGT1 and WGT2 modulated by multiclass compound treatments represented by increase or decrease in swarming diameter (cm). Figure 16 and 17 represents relative swarming diameters due to WGT1 and WGT2 motility respectively, affected by multiclass chemical treatments represented by bars. Figure 18,19; 20, 21 shows WGT1 and WGT2 Swarming motility respectively, affected by multiclass compounds.

*Table 7. Swarming motility of WGT1 and WGT2 modulated by multiclass compound treatments represented by increase or decrease in swarming diameter (cm).*

| Treatments | WGT1 swarming Diameter (cm) | % Increase/ decrease | WGT2 swarming Diameter (cm) | % Increase/ decrease |
|---|---|---|---|---|
| LB + 1% Ammonium Oxalate | 6.50±0.29 | **236** | 2.07±0.15 | **-18** |
| LB + 1% Ammonium Sulphate | 7.50±0.50 | **288** | 7.33±0.44 | **189** |
| LB + 1% Ascorbic Acid | 4.50±0.29 | **133** | 5.27±0.62 | **108** |
| LB + 1% Boric Acid | 1.20±0.09 | **-40** | 2.93±1.28 | **16** |
| LB + 1% Calcium Chloride | 7.80±0.16 | **303** | 7.67±0.33 | **203** |
| LB + 1% Citric Acid | 0.00±0.00 | **-100** | 0.00±0.00 | **-100** |
| LB + 1% Copper Sulfate | 0.00±0.00 | **-100** | 0.00±0.00 | **-100** |
| LB + 1% D Glucose | 7.83±0.44 | **305** | 4.60±0.67 | **82** |
| LB + 1% Gelatin | 2.83±0.17 | **47** | 2.33±0.17 | **-8** |
| LB + 1% Glycine | 5.33±0.44 | **176** | 7.83±0.17 | **209** |
| LB + 1% Iron(III) Chloride | 0.00±0.00 | **-100** | 0.00±0.00 | **-100** |
| LB + 1% Magnesium Sulfate | 7.33±0.33 | **279** | 3.80±9.61 | **50** |
| LB + 1% Mallic Acid | 0.00±0.00 | **-100** | 0.00 | **-100** |
| LB + 1% Manganese Sulfate | 2.07±0.28 | **7** | 7.00±0.77 | **176** |
| LB + 1% Molybdenum Trioxide | 4.17±0.89 | **116** | 6.30±0.85 | **149** |
| LB + 1% Pectin | 5.10±0.38 | **164** | 7.33±0.67 | **189** |
| LB + 1% Potassium Chloride | 7.40±0.31 | **283** | 7.67±0.33 | **203** |
| LB + 1% Potassium Dihydrogen Phosphate | 7.83±0.17 | **305** | 6.33±0.89 | **150** |
| LB + 1% Zinc Oxide | 0.00 | **-100** | 0.00±0.00 | **-100** |
| LB | 1.93±0.12 | **0** | 2.53±0.26 | **0** |
| Negative Control | 0 | **-100** | 0 | **-100** |

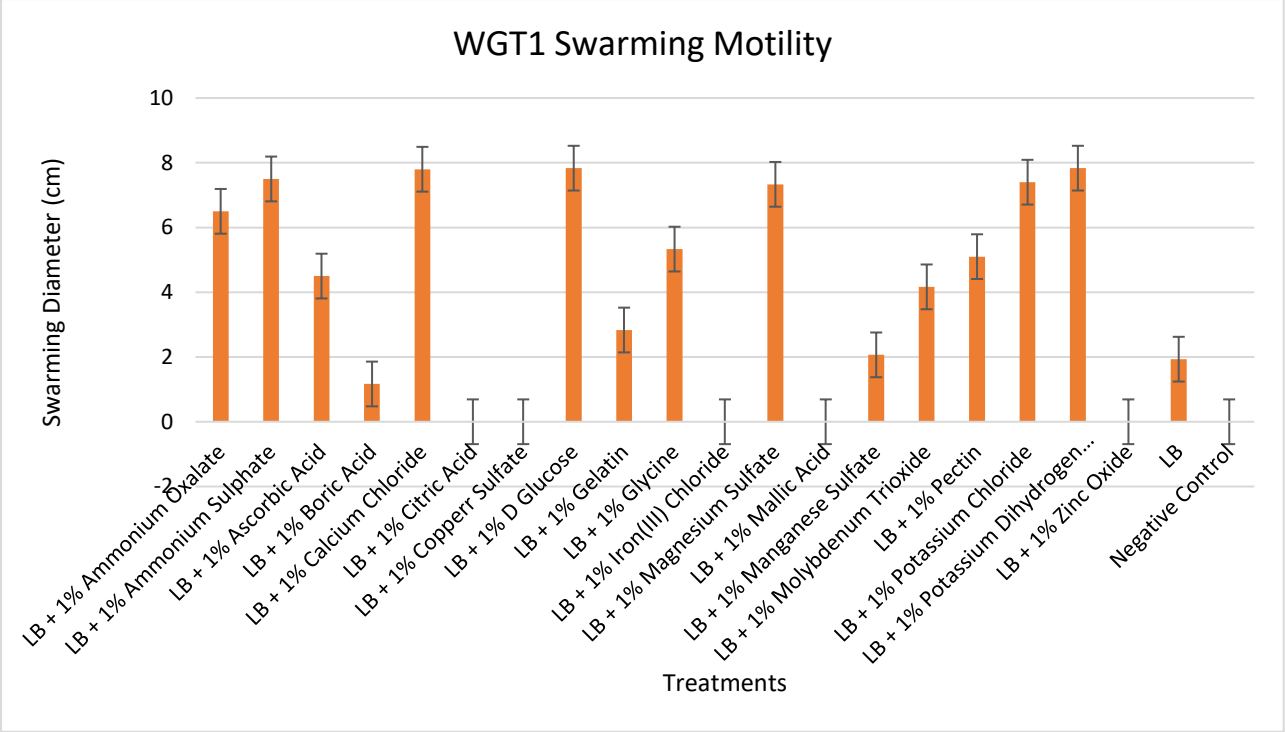


*Figure 16. Relative swarming diameters due to WGT1 motility affected by multiclass chemical treatments represented by bars.*

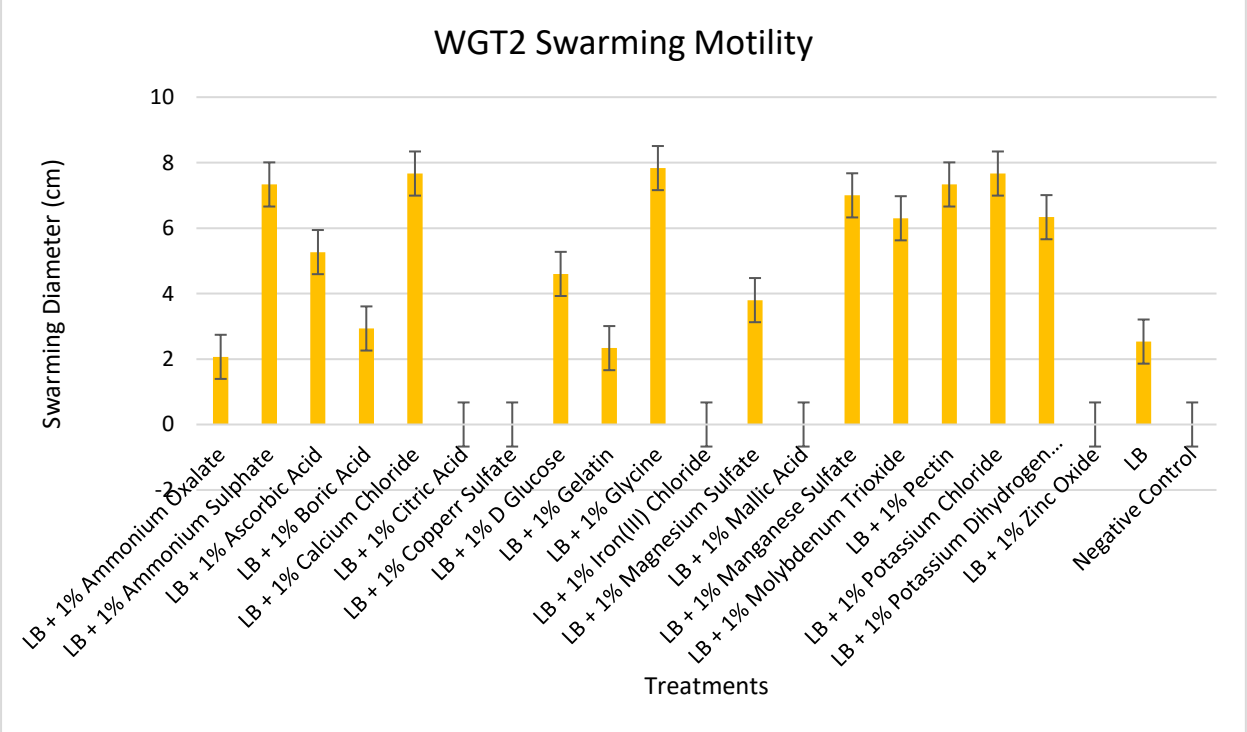


*Figure 17. Relative swarming diameters due to WGT2 motility affected by multiclass chemical treatments represented by bars.*

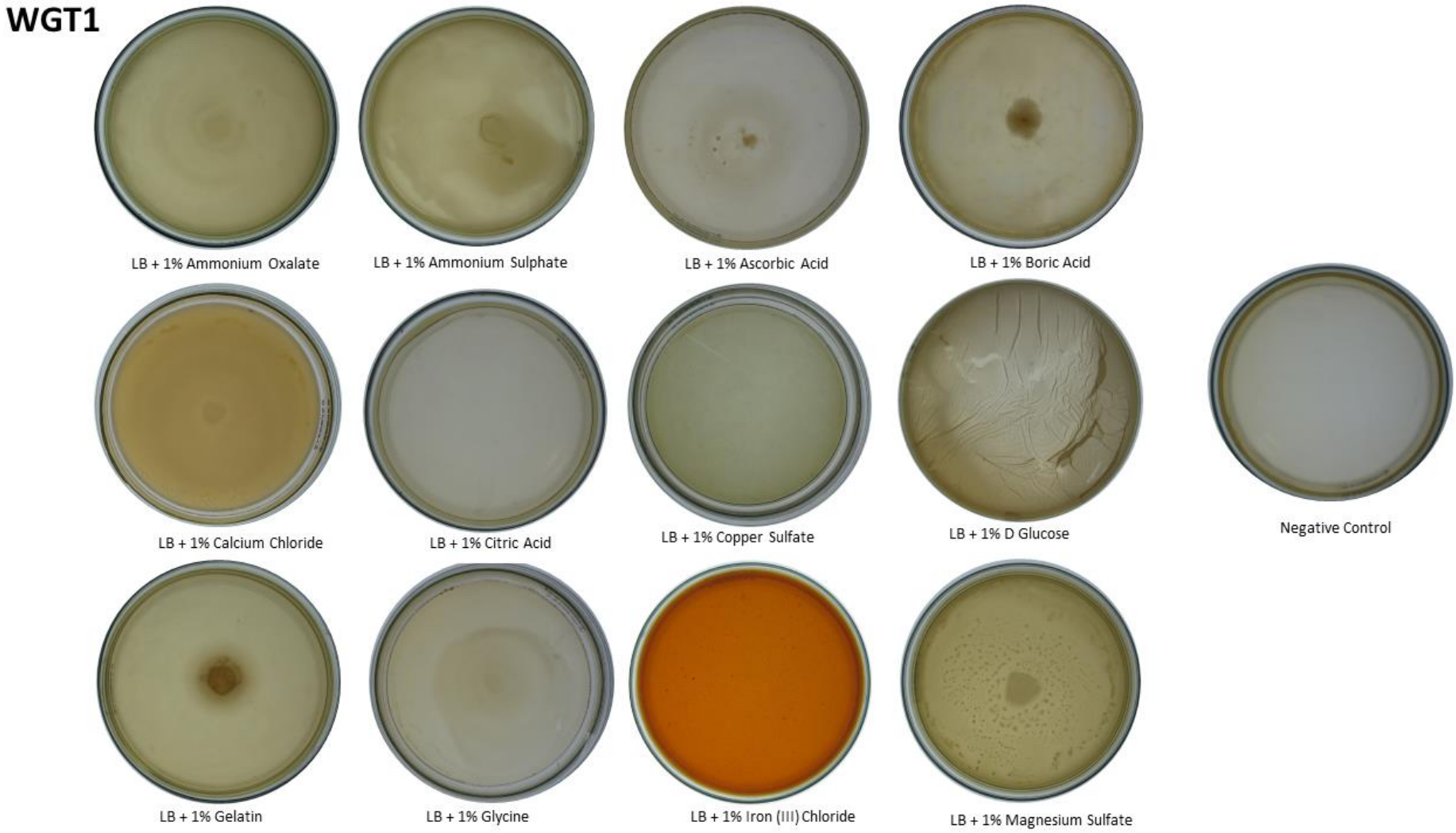
WGT1
LB + 1% Ammonium Oxalate
LB + 1% Ammonium Sulphate
LB + 1% Ascorbic Acid
LB + 1% Boric Acid
LB + 1% Calcium Chloride
LB + 1% Citric Acid
LB + 1% Copper Sulfate
LB + 1% D Glucose
Negative Control
LB + 1% Gelatin
LB + 1% Glycine
LB + 1% Iron (III) Chloride
LB + 1% Magnesium Sulfate

*Figure 18. WGT1 Swarming motility affected by multiclass compounds.*

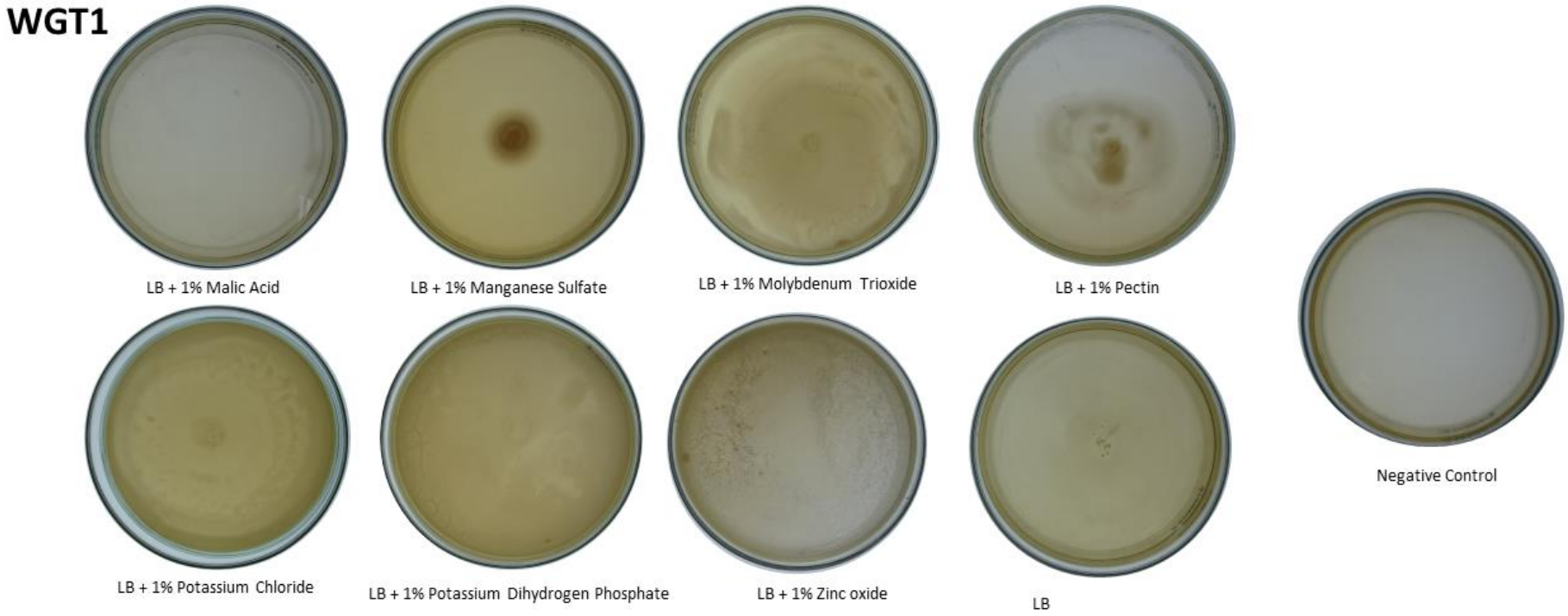


*Figure 19. WGT1 Swarming motility affected by multiclass compounds.*

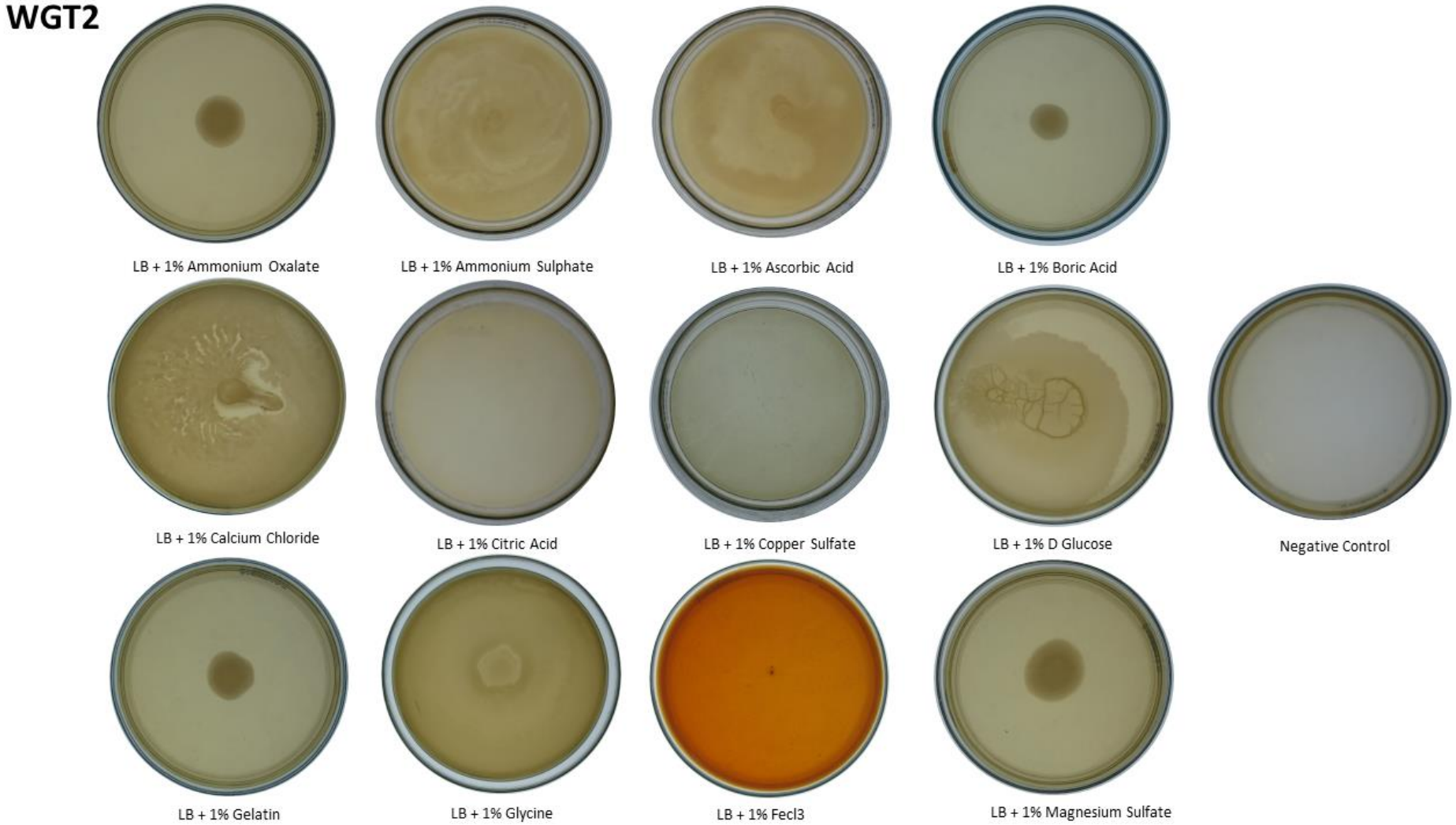
WGT2
LB + 1% Ammonium Oxalate
LB + 1% Ammonium Sulphate
LB + 1% Ascorbic Acid
LB + 1% Boric Acid
LB + 1% Calcium Chloride
LB + 1% Citric Acid
LB + 1% Copper Sulfate
LB + 1% D Glucose
Negative Control
LB + 1% Gelatin
LB + 1% Glycine
LB + 1% Fecl3
LB + 1% Magnesium Sulfate

*Figure 20. WGT2 Swarming motility affected by multiclass compounds.*

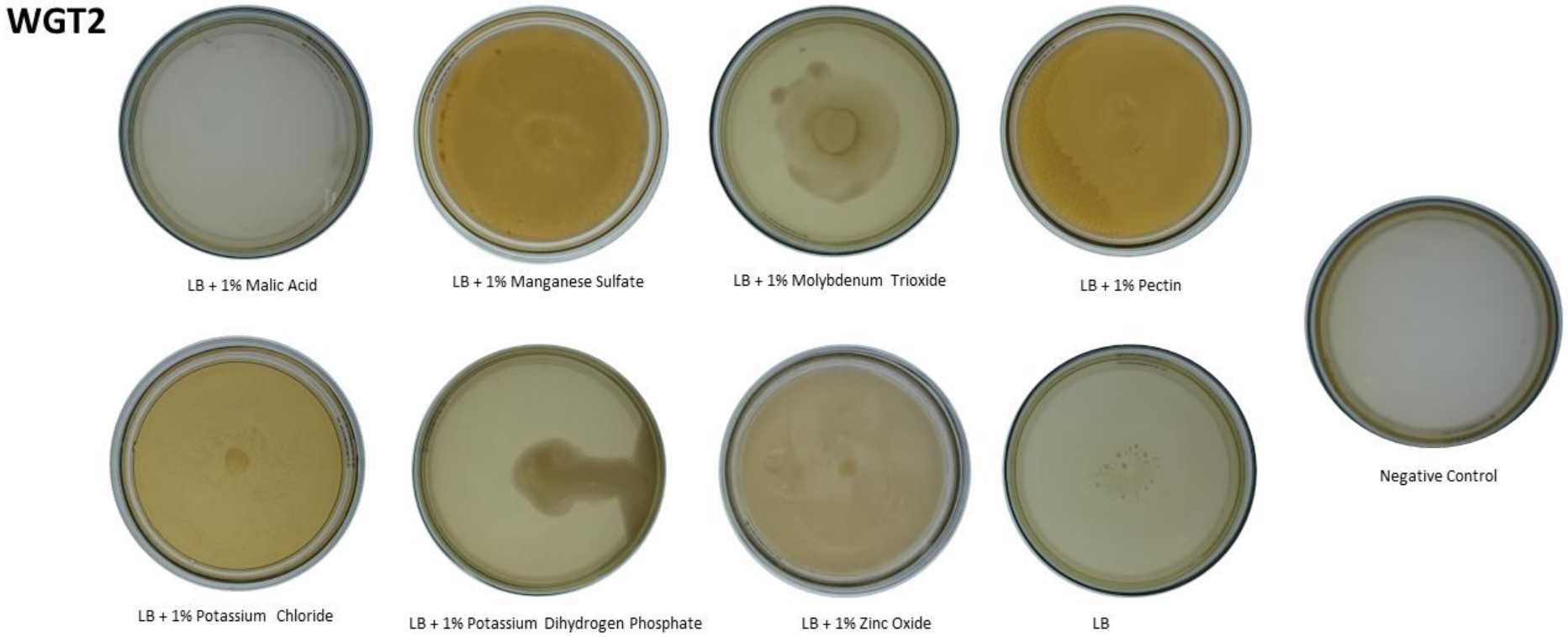


*Figure 21. WGT2 Swarming motility affected by multiclass compounds.*

## 4.9 Statistical analysis

The interpretation of the correlation matrix for six variables representing biofilm formation and swarming activities of strain WGT1: Abiotic adhesion represented as CV absorbance at 570nm, biofilm thickness, planktonic bacteria $OD_{600}$, EPS encased bacteria $OD_{600}$, biofilm live weight and swarming diameter reveals several important relationships.

For CV absorbance at 570nm, there is a moderate positive correlation with biofilm thickness ($r = 0.5$, $p < 0.05$), indicating that an increase bacterial adhesion is associated with an increase in biofilm thickness. Similarly, there is a moderate positive correlation with planktonic bacteria $OD_{600}$ ($r = 0.5$, $p < 0.05$), suggesting that higher adhesion is associated with higher planktonic bacteria $OD_{600}$. A strong positive correlation exists with EPS encased bacteria $OD_{600}$ ($r = 0.6$, $p < 0.01$), indicating a significant association between higher adhesion and larger EPS encased bacterial population. Additionally, there is a strong positive correlation with biofilm live weight ($r = 0.6$, $p < 0.01$), suggesting that an increase in CV absorbance is associated with an increase in biofilm live weight. Lastly, a moderate positive correlation with swarming diameter ($r = 0.5$, $p < 0.05$) indicates that as bacterial adhesion increases, the swarming activity also tends to increase.

Regarding biofilm thickness, there is a weak positive correlation with planktonic Bacteria $OD_{600}$ ($r = 0.2$), which is not statistically significant, suggesting little to no association between these variables. However, a strong positive correlation with EPS encased bacteria $OD_{600}$ ($r = 0.8$) indicates that thicker biofilms are associated with larger EPS encased bacterial population. There is a very strong positive correlation with biofilm live weight ($r = 0.9$), suggesting that thicker biofilms tend to have higher live weight. Additionally, a strong positive correlation with swarming diameter ($r = 0.8$, $p < 0.01$) indicates that thicker biofilms are associated with higher swarming activity.

For planktonic Bacteria $OD_{600}$, there is no significant correlation with EPS encased bacteria $OD_{600}$ ($r = 0.0$), suggesting no association between these variables. There is a weak positive correlation with biofilm Live weight ($r = 0.4$), which is not statistically significant, indicating little to no association between planktonic bacteria $OD_{600}$ and biofilm live weight. Furthermore, a weak positive correlation with swarming diameter ($r = 0.2$) is observed, suggesting little to no association between planktonic bacterial population and swarming diameter.

When examining EPS encased bacteria $OD_{600}$, a very strong positive correlation with biofilm live weight ($r = 0.7$, $p < 0.0001$) indicates that higher EPS encased bacteria $OD_{600}$ is significantly associated with higher biofilm live weight. A moderate positive correlation with swarming diameter ($r = 0.6$, $p < 0.01$) suggests that higher EPS bacteria $OD_{600}$ is associated with larger swarming diameters.

For biofilm live weight, there is a moderate positive correlation with swarming diameter ($r = 0.7$), indicating that higher biofilm live weight is associated with higher swarming.

Finally, swarming diameter shows significant positive correlations with CV absorbance at 570nm (adhesion) ($r = 0.5$, $p < 0.05$), biofilm thickness ($r = 0.8$, $p < 0.01$), EPS $OD_{600}$ ($r = 0.6$, $p < 0.01$), and biofilm live weight ($r = 0.7$). These correlations suggest that larger swarming diameters are associated with higher values of these variables.

Table 8. Correlation among biofilm and swarming properties of WGT1.

| **WGT1 variables** | *CV absorbance at 570nm* | *Biofilm Thickness* | *Planktonic Bacteria $OD_{600}$* | *EPS bacteriaO $D_{600}$* | *Biofilm live weight* | *Swarming Diameter* |
|---|---|---|---|---|---|---|
| *CV absorbance at 570nm* | 1.0 | | | | | |
| Biofilm Thickness | 0.5* | 1.0 | | | | |
| Planktonic bacteria $OD_{600}$ | 0.5* | 0.2 | 1.0 | | | |
| EPS bacteria $OD_{600}$ | 0.6** | 0.8 | 0.0 | 1.0 | | |
| Biofilm live weight | 0.6** | 0.9 | 0.4 | 0.7*** | 1.0 | |
| Swarming diameter | 0.5* | 0.8 | 0.2 | 0.6** | 0.7 | 1.0 |

*p<0.05, **p<0.01, ***p<0.0001

The interpretation of the correlation matrix for six variables representing biofilm formation and swarming activities of strain WGT2: Abiotic adhesion represented as CV absorbance at 570nm, biofilm thickness, planktonic bacteria $OD_{600}$, EPS encased bacteria $OD_{600}$, biofilm live weight and swarming diameter reveals several important relationships.

For CV absorbance at 570nm, there is a moderate positive correlation with biofilm thickness ($r = 0.5$, $p < 0.05$), indicating that an increase in bacterial adhesion is associated with an increase in biofilm thickness. There is a weak negative correlation with planktonic bacteria $OD_{600}$ ($r = -0.1$), which is not statistically significant, suggesting little to no

association between bacterial adhesion and planktonic bacteria $OD_{600}$. A strong positive correlation exists with EPS encased bacteria $OD_{600}$ ($r = 0.7$, $p < 0.01$), indicating a significant association between higher bacterial adhesion and higher EPS encased bacterial population. Additionally, a weak positive correlation with biofilm live Weight ($r = 0.4$, $p < 0.05$) suggests that an increase in bacterial adhesion is associated with an increase in biofilm live weight. There is a weak positive correlation with swarming diameter ($r = 0.3$), which is not statistically significant, indicating little to no association between adhesion and swarming activity.

Regarding biofilm thickness, there is a moderate positive correlation with planktonic bacteria $OD_{600}$ ($r = 0.5$, $p < 0.05$), suggesting that thicker biofilms are associated with larger planktonic bacterial population. A strong positive correlation with EPS encased bacteria $OD_{600}$ ($r = 0.8$) indicates that thicker biofilms are associated with larger EPS encased bacterial population. There is a very strong positive correlation with biofilm live weight ($r = 1.0$), suggesting that thicker biofilms tend to have higher live weight. Additionally, a strong positive correlation with swarming diameter ($r = 0.8$) indicates that thicker biofilms are associated with higher swarming activity.

For planktonic bacteria $OD_{600}$, there is a weak positive correlation with EPS encased bacteria $OD_{600}$ ($r = 0.1$), which is not statistically significant, suggesting little to no association between planktonic bacterial population and EPS encased bacterial population. A moderate positive correlation with biofilm live weight ($r = 0.4$) is observed, indicating that higher planktonic bacterial population is associated with higher biofilm live weight. Furthermore, a weak positive correlation with Swarming Diameter ($r = 0.5$) is observed, suggesting that larger planktonic bacterial population is associated with higher swarming activity.

When examining EPS encased bacteria $OD_{600}$, a strong positive correlation with biofilm live weight ($r = 0.8$) indicates that higher EPS encased bacterial population is associated with higher biofilm live weight. A moderate positive correlation with swarming diameter ($r = 0.6$, $p < 0.01$) suggests that larger EPS encased bacterial population is a result of higher swarming activity.

For biofilm live weight, there is a strong positive correlation with swarming diameter ($r = 0.7$, $p < 0.01$), indicating that higher biofilm live weight is associated with higher swarming activity.

Finally, swarming diameter, shows significant positive correlations with biofilm thickness ($r = 0.8$), EPS encased bacteria $OD_{600}$ ($r = 0.6$, $p < 0.01$), and biofilm live weight ($r = 0.7$, $p < 0.01$). These correlations suggest that higher swarming activities are associated with higher values of these variables

Table 9. Correlation among biofilm and swarming properties of WGT2.

| **WGT2 variables** | *CV absorbance at 570nm* | *Biofilm Thickness* | *Planktonic Bacteria $OD_{600}$* | *EPS encased bacteria $OD_{600}$* | *Biofilm live weight* | *Swarming Diameter* |
|---|---|---|---|---|---|---|
| *CV absorbance at 570nm* | *1.0* | | | | | |
| Biofilm Thickness | *0.5** | *1.0* | | | | |
| Planktonic bacteria $OD_{600}$ | *-0.1* | *0.5** | *1.0* | | | |
| EPS encased bacteria $OD_{600}$ | *0.7*** | *0.8* | *0.1* | *1.0* | | |
| Biofilm live weight | *0.4** | *1.0* | *0.4* | *0.8* | *1.0* | |
| Swarming diameter | *0.3* | *0.8* | *0.5** | *0.6*** | *0.7*** | *1.0* |

*p<0.05, **p<0.01, ***p<0.0001

# Chapter 5

## Discussion

Ammonium oxalate; ammonium sulphate; ascorbic acid; boric acid; calcium chloride; citric acid; copper sulfate; d glucose; gelatin; glycine; iron (iii) chloride; magnesium sulfate; malic acid; manganese sulfate; molybdenum trioxide; pectin; potassium chloride; potassium dihydrogen phosphate and zinc oxide were used in this study for investigating their influence on biofilm formation and swarming activities of *B. cereus.* Biofilm is multicellular community of microorganisms that adhere to biotic or abiotic surfaces and are encased in a self-produced gel like extracellular polymeric substance (EPS) matrix (Bello et al., 2023). Swarming is a collective type of flagellar motility of a large population of bacteria to colonize a surface. Biofilm formation and swarming motility are both interconnected and helps bacteria adapt to changing environment by allowing to move and colonize suitable niches by biofilm formation (Gloag et al., 2015).

Ammonium oxalate; ammonium sulphate; ascorbic acid; boric acid; calcium chloride; d glucose; gelatin; glycine; magnesium sulfate; manganese sulfate; molybdenum trioxide; pectin; potassium chloride; potassium dihydrogen phosphate and zinc oxide showed robust biofilm formation based on absorbance at $OD_{570}$ in PVC 96 wells plate for both *B. cereus* WGT1 and WGT2. citric acid; copper sulfate; iron (iii) chloride; mallic acid massively reduced biofilm formation in both strains. While molybdenum trioxide minimally reduced biofilm quantification of WGT1. Similar results were found in other studies where chemicals modulation affected the biofilm formation abilities of *B. cereus* during calorimetric biofilm quantification assays (Hayrapetyan et al., 2015; Kang et al., 2018; Lemos et al., 2014).

Ammonium oxalate; ammonium sulphate; ascorbic acid; boric acid; calcium chloride; d- glucose; gelatin; glycine; magnesium sulfate; manganese sulfate; molybdenum trioxide; pectin; potassium chloride; potassium dihydrogen phosphate thickened the biofilm layer by many folds for both WGT1 and WGT2. citric acid; copper sulfate; iron (iii) chloride; malic acid seemingly inhibited or impaired the biofilm formation in WGT1 as well as WGT2. Zinc oxide had negligible influence on the thickness of biofilm in both strains while Ammonium Oxalate negligibly affected WGT2 biofilm thickness. Previous studies agreeably reported the alteration in *B. cereus* thickness as a result of different chemical treatments (Huang et al., 2019; Wijman et al., 2007). Thickness of biofilm is

linearly correlated with its surface area (Gomes et al., 2021). Hence chemical compounds that increase or decreases the thickness of biofilm also affect the surface area in respective manner.

All of the compounds except, Citric Acid; Copper Sulfate; Iron (III) Chloride; Mallic Acid, favored formation of both pellicle and ring type biofilms. However, Magnesium Sulfate; Pectin; Zinc Oxide stimulated submerged biofilm formation of WGT1. While under the influence of, Ammonium Oxalate; Ascorbic Acid; Gelatin; Manganese Sulfate; Pectin; Zinc Oxide, WGT2 formed submerged biofilm. B. cereus has been shown to form ring, pellicle and submerged biofilms in the presence of distinct chemical compounds (Adame-Gómez et al., 2020).

EPS $OD_{600}$ represents the population of bacteria residing within the EPS or biofilm matrix. All of the tested compounds enhanced the EPS bacterial population except citric acid, copper sulfate, iron (III) chloride, malic acid and zinc oxide in WGT1 and WGT2 biofilms. Higher incorporation of bacterial population into the biofilm matrix can be interpreted by enhancement in flagellar movement stimulated by QS chemotactic signals released by biofilm host bacteria. Studies suggest that chemical treatments may stimulate QS signaling during biofilm formation (Saxena et al., 2018).

Biofilm live weight refers to the weight of biofilm still attached to the surface. Live weight was recorded instead of fresh weight to prevent damage to EPS matrix, loss of water, loosing viability of bacteria and residual fragments of biofilm attached to surface; during detachment which can result in inaccurate measurements. All of the compounds as stated above except, citric acid; copper sulfate; iron (iii) chloride; malic acid, supplemented the live weight of biofilm up to a massive extent for both WGT1 and WGT2 with exception of Zinc oxide which minimally reduced the biofilm live weight of WGT1, which implies that zinc oxide reduced the EPS synthesis. Weight and mass of *B. cereus* biofilms have been shown to be alterable depending on the presence of different chemical stimuli (Huang et al., 2019; Lemos et al., 2015).

All of the chemical treatments except citric acid, copper sulfate, iron (III) chloride, malic acid and zinc oxide showed wide range of adherence levels by WGT1 and WGT2; these chemicals inhibited the adherence of bacteria. However, it was observed from other treatments that bacteria reversibly adhere to the available site in a random manner followed by their flagellated swarm movement towards more suitable place for irreversible

adherence and biofilm formation. However, it was discovered in previous studies that swarming is a collective behavior of multiple bacterial cells and chemical treatments can influence the adhesive abilities of *B. cereus* (Huang et al., 2020).

Boric acid minimally reduced the swarming activity of WGT1 while ammonium oxalate and gelatine negligibly reduced the swarming activity of WGT2 as indicated by the swarming diameter measured in cm. Inversely, citric acid; copper sulfate; iron (iii) chloride; malic acid impaired the swarming ability of both strains. All other compounds as stated above boosted the swarming motility of both WGT1 and WGT2. Studies have agreeably shown that different chemical treatments can alter the swarming motility activity of *B. cereus* (N. Thampuran & P.K. Surendran, 1996; Zhao et al., 2021). Zinc chloride inhibited swarming without inhibiting biofilm formation in both WGT1 and WGT2 is a phenomenon resemblance of which has been reported previously that biofilm formation can happen without swarming activity (O'May et al., 2012).

A higher abiotic adhesion leads to dense biofilm formation and higher swarming activities. An enormous level of swarming leads to thicker and heavy biofilm due to higher EPS synthesis and incorporation of swarming bacteria into EPS layer. Planktonic bacteria do not block swarming and biofilm formation. A higher number of planktonic leads to enormous swarming which leads to robust and thick biofilm. The thickness of biofilm is positively correlated with population of EPS encased bacteria. Extent of swarming is not influenced by non-swarming planktonic bacteria population. These correllations are agreeably confirmed by previous studies that biofilm thickness and density is positively correlated to biomass and is a result of massive swarming activity (Dutt et al., 2022; Sahli et al., 2022).

Compounds which are widespread in environment and usually come in frequent interaction with microbial community were tested on B. cereus biofilm formation and swarming activities. Ammonium oxalate has been shown to influence stability of biofilm by altering its EPS architecture and composition (Donlan, 2002). Ammonium sulfate promotes swarming and EPS production which lead to robust biofilm formation (Rehman et al., 2016). Ammonium group as in ammonium oxalate and ammonium sulfate increases the adhesion of bacteria to the colonizing surface by increasing the surface hydrophobicity and which leads robust adhesion and biofilm formation (Choi et al., 2015). Ascorbic acid usually inhibits biofilm formation in bacterial species like *Staphylococcus aureus*,

*Escherichia coli*, *Listeria monocytogenes*, *Stenotrophomonas maltophilia*, and *Pseudomonas aeruginosa* in a concentration dependent manner as higher concentration can inhibit biofilm formation up to 94% in *E. coli.* However, some bacterial species have been shown to beresistant to antibiofilm effect of ascorbic acid as WGT1 and WGT2 in our study, ironically ascorbic acid reduces the swarming motility in several bacterial species (Ali Mirani et al., 2018; ElBaradei & Yakout, 2022; Przekwas et al., 2020; Rehman et al., 2016) the point which is in agreement with our study. Boric acid usually inhibits biofilm formation in dose dependent manner in many bacterial species but some bacterial species are resistant to its antibiofilm effect and form robust biofilm in an inverse manner as in our study WGT1 and WGT2 formed robust biofilm in the presence of boric acid. Boric acid also usually impairs swarming motility of bacteria due to disruption of chemotaxis system, (Ezhaveni Sathiyamoorthi et al., 2024; İnce, 2022; SYKES & REED, 1949) however in our study boric acid reduced swarming activity in the case of WGT1 but not WGT2. Calcium chloride leads to enhancement of both biofilm forming and swarming activity as reported in scientific literature (Fan et al., 2024). Calcium ions can promote biofilm formation and swarming by inducing the expression of lateral flagellar genes and type III secretion systems. Conversely, Higher concentrations of calcium ions i.e. higher than 2% w/v have been shown to inhibit both biofilm and swarming (Fan et al., 2024; Rajamma et al., 2020). Both citric acid and mallic acid have been reported to inhibit both biofilm formation and swarming which agrees with our study. Citric acid inhibits biofilm formation by altering the PH leading to truncation in EPS synthesis and inhibiting QS. Swarming is diminished by altering the surface charge properties of bacteria a property exhibited by mallic acid as well. Mallic acid also inhibit biofilm formation by similar mechanisms but studies have shown that it can serve as carbon source and ironically enhance biofilm formation in some bacteria like *P. aeruginosa* (Amrutha et al., 2017; Wu et al., 2017). Copper sulfate inhibits biofilm and swarming activity in many bacterial species (Falcón García et al., 2020; Mariano José Lacosegliaz et al., 2021) in a detrimental way. Copper sulfate interferes with QS diminishing cell to cell signaling and EPS synthesis. Swarming motility is reduced to negligible by inhibiting the expression of flagellar genes (Falcón García et al., 2020; Mariano José Lacosegliaz et al., 2021). Iron (III) Chloride is reported to enhance biofilm activity in *Serratia marcescens* and *P. aeruginosa* through iron (III) ions ($Fe^{3+}$) which leads to increase in biofilm biomass through QS regulation and EPS synthesis. Inversely, iron limitation or low amount of iron can reduce or even inhibit biofilm formation. However, iron (III) chloride is reported to inhibit swarming motility in many bacterial strains deficient

in iron acquisition mechanisms i.e. lacking siderophores (Lin et al., 2016; Patriquin et al., 2007). D- Glucose enhances the biofilm forming and swarming activity in bacteria by many folds (Ebru Sahin Kehribar et al., 2021; Solis & Sengupta, 2024). This has serious clinical implications in the case of diabetes in which biofilm contributes to diabetic periodontitis which is difficult to treat due to hyperglycemia-induced tissue dysfunction in diabetic patients. However, some studies have shown that higher concentrations of d- glucose leads to diminished biofilm formation due to decrease production of acyl-homoserine lactone (AHL) molecules that plays a central role in QS regulation. Swarming activity is reduced due higher concentrations of d- glucose due to down regulating the expression of genes involve in motility (Caiazza et al., 2007; Gatta et al., 2022). Gelatin reportedly shows antibiofilm activity against many bacterial species including *S. aureus* and *E. coli* through inhibiting EPS synthesis and QS inhibition. On the other hand, gelatin both promotes or reduce the swarming motility depending on conditions through nutritional influence and altering surface charge properties of the medium (Bessalah et al., 2024; de la Fuente-Núñez et al., 2012). Glycine is the simplest amino acid which modulate the biofilm formation and swarming motility depending on conditions (Shen et al., 2016). Glycine can act as carbon and nitrogen source which are essential nutrients for bacterial biofilm proteins and EPS structure. Glycine also alters the QS regulation by influencing the synthesis of signaling molecules deciding the fate of biofilm (Cleaver et al., 2021). Higher concentrations of glycine are reported to inhibit biofilm formation and swarming abilities of bacteria, inversely, lower concentrations seem to promote these abilities (O'Gara, 2007). Magnesium sulfate is a donor of Magnesium ions ($Mg^{2+}$) higher concentrations, 50mM or above, of which can alter the physical and chemical properties of biofilm matrix (Oknin et al., 2015). $Mg^{2+}$ inhibits biofilm activity in bacterial species particularly *B. subtilis* and *Enterobacter cloacae*. $Mg^{2+}$ influence electrostatic interactions between bacterial cells and surfaces altering the charge dynamic and ultimately reducing the surface adhesion of bacteria. By acting as cofactor for many constitutive enzymes $Mg^{2+}$ can regulation expression of genes related to QS sensing, EPS synthesis and flagellar genes involved in swarming motility (Demishtein et al., 2019) which is also influenced not only by $Mg^{2+}$ role stabilizing membrane structures and influencing ion transport across membranes (de la Fuente-Núñez et al., 2012). but also, Mg2+ mediated inhibition of type IV pili formation in bacteria like *Acidithiobacillus ferrooxidans*. (Tang et al., 2018). Manganese sulfate has been shown to promote biofilm formation in several bacteria including *B.cereus* (Hussain et al., 2018). LBGM is a widely used biofilm inducing nutrient medium constituents of

which include 200 uM concentration of manganese sulfate (Yan et al., 2017). Manganese sulfate has been shown to be utilized by manganese oxidizing bacteria like which are notoriously responsible for the corrosion of stainless steel (Balakrishnan et al., 2023). Manganese sulfate is a donor of manganese ions ($Mn^{2+}$) which has been shown to promote biofilm formation in lactic acid bacteria (LAB) (NOZAKA et al., 2014). Molybdenum Trioxide inhibits biofilm formation in bacterial species including *E. coli*, *S. aureus*, and *P. aeruginosa*, by generating reactive oxygen species (ROS) which causes damage to important cellular components including proteins, lipids and DNA leading to impaired metabolism and QS hence diminished biofilm formation. Molybdenum trioxide reduce the swarming ability by interfering with flagellar genes associated with swarming generally through ROS (Duan et al., 2021). Pectin is a plant polysaccharide that has been shown to promote biofilm formation in *Bacillus thuringenesis* (Rubinstein et al., 1992) and *Klebsiella oxytoca* (Li et al., 2021). Components of biofilm matrix are synthesized efficiently in the presence of pectin (Thérien et al., 2020). It has an important implication in agricultural sector that is PGPR when employed as biofertilizer are exposed to plant roots in the soil which are covered with glycoproteins like pectin which can not only act as adhesion site for beneficial PGPR but also induce robust biofilm formation a trait considered important in biofertilizer perspective. Potassium chloride when used in nutrient medium forms robust and wrinkly biofilm (Marsden et al., 2017). It donates potassium ions ($K^+$) which is a primary chemotactic signal secreted by biofilm forming bacterial cells for attracting swimming cells as an invitation (Zhang et al., 2024). Potassium chloride is used in the formulations of potassium fertilizers hence when applied to soil its components interacts with microbial community in soil (Castro-Suarez et al., 2022; Santos et al., 2016). Potassium Dihydrogen Phosphate donates phosphorus ions which are reported to lengthen the generation time of biofilm which has an impertinent implication in water distribution pipe walls and industrial effluent drainage pipelines (Kasahara et al., 2004). Phosphorus ions when not removed from water distribution pipelines lead to massive biofilm formation which results in deteriorated water quality due to bad taste and smell and corrosions in pipe walls (Okabe et al., 2002). Zinc Oxide is known for its antimicrobial, anti-biofilm and anti-swarming activity. Nanoparticle prepared from zinc are effective against biofilm and swarming of many bacterial species including *P. aeruginosa* and *S. aureus* through interfering with EPS synthesis and QS signaling (García-Lara et al., 2015). Nanoparticles prepared from zinc oxide are famous for their anti-biofilm, antimicrobial, anti-swarming, anti-QS activities (Mo Ahamad Khan et al., 2023). Exposure to zinc oxide nanoparticles

results in ROS production which culminates in oxidative damage to essential biomolecules in bacterial cell hence not only the synthesis of biofilm matrix components of maturing biofilm but also the structural integrity of matured biofilm can be deteriorated.

# Conclusion

Presence of chemical compounds influence biofilm formation and swarming activities in both stimulatory and inhibitory ways. Compounds inhibited biofilm formation either by inhibiting adherence and swarming or by limiting EPS synthesis which results in reduced biofilm thickness and vice versa. Our results emphasize the adaptive nature of *B. cereus* biofilms in response to chemical stimuli manifested by multiclass compounds. Bacteria reversely adhere to random places to travel towards suitable place for irreversible adherence and biofilm formation. Correlation analyses inferred that lack of adherence resulted in inhibition of both swarming activity and biofilm formation. Motility of swarming bacteria is independent of non-swarming bacteria. A large population of planktonic bacteria lead to massive swarming, which results in vigorous adherence, more EPS synthesis and incorporation of a large population of bacteria into the biofilm hence increasing the thickness of biofilm. Biofilm-promoting compounds can be utilized in various applications: Biofilm-inducing nutrient media for research and development, Inoculants in biofertilizers to enhance root colonization by PGPR, Nutrient media formulations for industrial biofilm reactors to foster robust biofilm formation and bioremediation processes that require the development of robust biofilms. Conversely, biofilm-inhibiting compounds could be incorporated into sanitizer formulations to eradicate undesirable biofilms.

# References


Abdelraheem, W. M., Refaie, M. M. M., Yousef, R. K. M., Abd El Fatah, A. S., Mousa, Y. M., & Rashwan, R. (2022). Assessment of Antibacterial and Anti-biofilm Effects of Vitamin C Against *Pseudomonas aeruginosa* Clinical Isolates. Frontiers in Microbiology, 13. https://doi.org/10.3389/fmicb.2022.847449

Abebe, G. M. (2020). The Role of Bacterial Biofilm in Antibiotic Resistance and Food Contamination. International Journal of Microbiology, 2020, 1–10. https://doi.org/10.1155/2020/1705814

Adame-Gómez, R., Cruz-Facundo, I.-M., García-Díaz, L.-L., Ramírez-Sandoval, Y., Pérez-Valdespino, A., Ortuño-Pineda, C., Santiago-Dionisio, M.-C., & Ramírez-Peralta, A. (2020). Biofilm Production by Enterotoxigenic Strains of *Bacillus cereus* in Different Materials and under Different Environmental Conditions. Microorganisms, 8(7), 1071. https://doi.org/10.3390/microorganisms8071071

Ahmad, A., Banat, F., & Taher, H. (2022, January 1). Chapter 1 - Algal engineering for bioremediation, bioenergy production, and biomedical applications (A. Ahmad, F. Banat, & H. Taher, Eds.). ScienceDirect; Elsevier. https://www.sciencedirect.com/science/article/abs/pii/B9780323904766000157

Ali Mirani, Z., Khan, M. N., Siddiqui, A., Khan, F., Aziz, M., Naz, S., Ahmed, A., & Khan, S. I. (2018). Ascorbic acid augments colony spreading by reducing biofilm formation of methicillin-resistant *Staphylococcus aureus*. Iranian Journal of Basic Medical Sciences, 21(2), 175–180. https://doi.org/10.22038/IJBMS.2018.20714.5398

Alipal, J. (2021). A review of gelatin: Properties, sources, process, applications, and commercialisation. Materials Today: Proceedings, 42, 240–250. https://doi.org/10.1016/j.matpr.2020.12.922

Alper Solmaz, Ömer Saltuk Bölükbaşi, & Zeynel Abidin Sari. (2024). Green industry work: production of FeCl3 from iron and steel industry waste (mill scale) and its use in wastewater treatment. Environmental Science and Pollution Research International, 31(13), 19795–19814. https://doi.org/10.1007/s11356-024-32451-6

Amrutha, B., Sundar, K., & Shetty, P. H. (2017). Effect of organic acids on biofilm formation and quorum signaling of pathogens from fresh fruits and vegetables. Microbial Pathogenesis, 111, 156–162. https://doi.org/10.1016/j.micpath.2017.08.042

Anderson, M., Schaaf, E., Breshears, L., Wallis, H., Johnson, J., Tkaczyk, C., Sellman, B., Sun, J., & Peterson, M. (2018). Alpha-Toxin Contributes to Biofilm Formation among *Staphylococcus aureus* Wound Isolates. Toxins, 10(4), 157. https://doi.org/10.3390/toxins10040157

Armbruster, C. R., & Parsek, M. R. (2018). New insight into the early stages of biofilm formation. Proceedings of the National Academy of Sciences, 115(17), 4317–4319. https://doi.org/10.1073/pnas.1804084115

Assefa, M., & Amare, A. (2022). Biofilm-Associated Multi-Drug Resistance in Hospital-Acquired Infections: A Review. Infection and Drug Resistance, Volume 15, 5061–5068. https://doi.org/10.2147/idr.s379502

Balakrishnan, A., Dhaipule, K., & Philip, J. (2023). Microbiologically influenced corrosion of AISI 202 and 316L stainless steels under manganese-oxidizing biofilms. 3 Biotech, 14(1). https://doi.org/10.1007/s13205-023-03845-z

Bello, O. O., Martins, F. T., Bello, T. K., I.A. Anuoluwa, M.M. Anyakudo, O.A. Amolegbe, & A.M. Ilemobayo. (2023). Occurrence and Role of Bacterial Biofilms in Different Systems. Acta Microbiologica Bulgarica, 39(3), 239–248. https://doi.org/10.59393/amb23390304

Bessalah, S., Faraz, A., D bara, M., Khorcheni, T., Hammadi, M., Ajose, D. J., & Saeed, S. I. (2024). Antibacterial, Anti-Biofilm, and Anti-Inflammatory Properties of Gelatin-Chitosan-Moringa-Biopolymer-Based Wound Dressings towards *Staphylococcus aureus* and *Escherichia coli*. Pharmaceuticals (Basel, Switzerland), 17(5), 545. https://doi.org/10.3390/ph17050545

Bianco, A., Capozzi, L., Monno, M. R., Del Sambro, L., Manzulli, V., Pesole, G., Loconsole, D., & Parisi, A. (2021). Characterization of *Bacillus cereus* Group Isolates from Human Bacteremia by Whole-Genome Sequencing. Frontiers in Microbiology, 11. https://doi.org/10.3389/fmicb.2020.599524

Borriss, R. (2020, January 1). Chapter 7 - *Bacillus* (N. Amaresan, M. Senthil Kumar, K. Annapurna, K. Kumar, & A. Sankaranarayanan, Eds.). ScienceDirect; Academic Press. https://www.sciencedirect.com/science/article/abs/pii/B9780128234143000071

Caiazza, N. C., Merritt, J. H., Brothers, K. M., & O'Toole, G. A. (2007). Inverse Regulation of Biofilm Formation and Swarming Motility by *Pseudomonas aeruginosa* PA14. Journal of Bacteriology, 189(9), 3603–3612. https://doi.org/10.1128/jb.01685-06

Caldara, M., Belgiovine, C., Secchi, E., & Rusconi, R. (2022). Environmental, Microbiological, and Immunological Features of Bacterial Biofilms Associated with Implanted Medical Devices. Clinical Microbiology Reviews, 35(2). https://doi.org/10.1128/cmr.00221-20

Camele, I., Sadeek, S. A., Racioppi, R., & Elshafie, H. S. (2023). Antimicrobial Activity of Diffusible and Volatile Metabolites Emitted by *Beauveria bassiana*: Chemical Profile of Volatile Organic Compounds (VOCs) Using SPME-GC/MS Analysis. Plants, 12(15), 2854. https://doi.org/10.3390/plants12152854

Candela, T., Maes, E., Garénaux, E., Yoann Rombouts, Krzewinski, F., Gohar, M., & Yann Guérardel. (2011). Environmental and Biofilm-dependent Changes in a *Bacillus cereus* Secondary Cell Wall Polysaccharide. Journal of Biological Chemistry, 286(36), 31250–31262. https://doi.org/10.1074/jbc.m111.249821

Carezzano, M. E., Alvarez Strazzi, F. B., Pérez, V., Bogino, P., & Giordano, W. (2023). Exopolysaccharides Synthesized by Rhizospheric Bacteria: A Review Focused on Their Roles in Protecting Plants against Stress. Applied Microbiology, 3(4), 1249–1261. https://doi.org/10.3390/applmicrobiol3040086

Carrascosa, C., Raheem, D., Ramos, F., Saraiva, A., & Raposo, A. (2021). Microbial Biofilms in the Food Industry—A Comprehensive Review. International Journal of Environmental Research and Public Health, 18(4), 2014. https://doi.org/10.3390/ijerph18042014

Carroll, L. M., Cheng, R. A., Wiedmann, M., & Kovac, J. (2021). Keeping up with the *Bacillus cereus* group: taxonomy through the genomics era and beyond. Critical Reviews in Food Science and Nutrition, 1–26. https://doi.org/10.1080/10408398.2021.1916735

Castro-Suarez, J. R., Colpas-Castillo, F., & Taron-Dunoyer, A. (2022). Chemical and Morphologic Characterization of Sylvite (KCl) Mineral from Different Deposits Used in the Production of Fertilizers. Agronomy, 13(1), 52. https://doi.org/10.3390/agronomy13010052

Chan, S., Pullerits, K., Keucken, A., Persson, K. M., Paul, C. J., & Rådström, P. (2019). Bacterial release from pipe biofilm in a full-scale drinking water distribution system. Npj Biofilms and Microbiomes, 5(1). https://doi.org/10.1038/s41522-019-0082-9

Chateau, A., Alpha-Bazin, B., Armengaud, J., & Duport, C. (2022). Heme A Synthase Deficiency Affects the Ability of *Bacillus cereus* to Adapt to a Nutrient-Limited Environment. International Journal of Molecular Sciences, 23(3), 1033. https://doi.org/10.3390/ijms23031033

Chien, S. H., Gearhart, M. M., & Villagarcía, S. (2011). Comparison of Ammonium Sulfate with Other Nitrogen and Sulfur Fertilizers in Increasing Crop Production and Minimizing Environmental Impact. Soil Science, 176(7), 327–335. https://doi.org/10.1097/ss.0b013e31821f0816

Cho, W.-I., & Chung, M.-S. (2020). *Bacillus* spores: a review of their properties and inactivation processing technologies. Food Science and Biotechnology, 29(11), 1447–1461. https://doi.org/10.1007/s10068-020-00809-4

Choi, N.-Y., Bae, Y.-M., & Lee, S.-Y. (2015). Cell surface properties and biofilm formation of pathogenic bacteria. Food Science and Biotechnology, 24(6), 2257–2264. https://doi.org/10.1007/s10068-015-0301-y

Cleaver, L. M., Moazzez, R. V., & Carpenter, G. H. (2021). Evidence for Proline Utilization by Oral Bacterial Biofilms Grown in Saliva. Frontiers in Microbiology, 11. https://doi.org/10.3389/fmicb.2020.619968

Cui, Z.-Q., Wei, Z., Chen, C., Sun, Y.-Y., Deng, Z.-P., Xu, Y.-M., Huo, L.-H., & Gao, S. (2024). Waste cigarette butts-templated synthesis of in-situ graphitic carbon-doped ZnO fibers boosting dual-selectivity NO2/butanone at different temperatures. Chemical Engineering Journal, 487, 150717–150717. https://doi.org/10.1016/j.cej.2024.150717

Danish, M., Shahid, M., Altaf, M., Tyagi, A., & Ali, S. (2024). Plant growth-promoting rhizobacteria and biocontrol agents triggered plant defense responses against phytopathogenic fungi and improved rice growth. Physiological and Molecular Plant Pathology, 133, 102337. https://doi.org/10.1016/j.pmpp.2024.102337

de la Fuente-Núñez, C., Korolik, V., Bains, M., Nguyen, U., Breidenstein, E. B. M., Horsman, S., Lewenza, S., Burrows, L., & Hancock, R. E. W. (2012). Inhibition of Bacterial Biofilm Formation and Swarming Motility by a Small Synthetic Cationic Peptide. Antimicrobial Agents and Chemotherapy, 56(5), 2696–2704. https://doi.org/10.1128/aac.00064-12

Debroy, A., George, N., & Mukherjee, G. (2021). Role of biofilms in the degradation of microplastics in aquatic environments. Journal of Chemical Technology & Biotechnology. https://doi.org/10.1002/jctb.6978

Del Pozo, J. L. (2017). Biofilm-related disease. Expert Review of Anti-Infective Therapy, 16(1), 51–65. https://doi.org/10.1080/14787210.2018.1417036

Demishtein, K., Reifen, R., & Shemesh, M. (2019). Antimicrobial Properties of Magnesium Open Opportunities to Develop Healthier Food. Nutrients, 11(10), 2363. https://doi.org/10.3390/nu11102363

Di, G., Oliva, A., & María Guembe. (2022). The Current Knowledge on the Pathogenesis of Tissue and Medical Device-Related Biofilm Infections. Microorganisms, 10(7), 1259–1259. https://doi.org/10.3390/microorganisms10071259

Dong, W., Liu, H., Ning, Z., Bian, Z., Zeng, L., & Xie, D. (2023). Inoculation with *Bacillus cereus* DW019 Modulates Growth, Yield and Rhizospheric Microbial Community of Cherry Tomato. Agronomy, 13(6), 1458. https://doi.org/10.3390/agronomy13061458

Donlan, R. M. (2002). Biofilms: Microbial Life on Surfaces. Emerging Infectious Diseases, 8(9), 881–890. https://doi.org/10.3201/eid0809.020063

Duan, G., Wen, L., Sun, X., Wei, Z., Duan, R., Zeng, J., Cui, J., Liu, C., Yu, Z., Xie, X., & Gao, M. (2021). Healing Diabetic Ulcers with MoO 3− X Nanodots Possessing

Intrinsic ROS-Scavenging and Bacteria-Killing Capacities. Small, 2107137. https://doi.org/10.1002/smll.202107137

Dutt, Y., Dhiman, R., Singh, T., Vibhuti, A., Gupta, A., Pandey, R. P., Raj, V. S., Chang, C.-M., & Priyadarshini, A. (2022). The Association between Biofilm Formation and Antimicrobial Resistance with Possible Ingenious Bio-Remedial Approaches. *Antibiotics*, *11*(7), 930. https://doi.org/10.3390/antibiotics11070930

Dutta, B., Nag, M., Lahiri, D., Ghosh, S., Dey, A., Joshi, S., & Rina Rani Ray. (2022). Biofilms for Biofuel Production. Clean Energy Production Technologies, 219–237. https://doi.org/10.1007/978-981-16-8094-6_13

Dutton, M. V., Evans, C. S., Atkey, P. T., & Wood, D. A. (1993). Oxalate production by Basidiomycetes, including the white-rot species *Coriolus versicolor* and *Phanerochaete chrysosporium*. Applied Microbiology and Biotechnology, 39(1), 5–10. https://doi.org/10.1007/bf00166839

Ebru Sahin Kehribar, Musa Efe Isilak, Eray Ulas Bozkurt, Adamcik, J., Raffaele Mezzenga, & Urartu Ozgur Safak Seker. (2021). Engineering of biofilms with a glycosylation circuit for biomaterial applications. Biomaterials Science, 9(10), 3650–3661. https://doi.org/10.1039/d0bm02192j

Ehling-Schulz, M., Lereclus, D., & Koehler, T. M. (2019). The *Bacillus cereus* Group: *Bacillus* Species with Pathogenic Potential. Microbiology Spectrum, 7(3). https://doi.org/10.1128/microbiolspec.gpp3-0032-2018

ElBaradei, A., & Yakout, M. A. (2022). *Stenotrophomonas maltophilia*: Genotypic Characterization of Virulence Genes and The Effect of Ascorbic Acid on Biofilm Formation. Current Microbiology, 79(6). https://doi.org/10.1007/s00284-022-02869-7

Elumalai, P., AlSalhi, M. S., Mehariya, S., Karthikeyan, O. P., Devanesan, S., Parthipan, P., & Rajasekar, A. (2020). Bacterial community analysis of biofilm on API 5LX carbon steel in an oil reservoir environment. Bioprocess and Biosystems Engineering, 44(2), 355–368. https://doi.org/10.1007/s00449-020-02447-w

Ezhaveni Sathiyamoorthi, Lee, J.-H., & Lee, J. (2024). Antibacterial and antibiofilm activity of halogenated phenylboronic acids against *Vibrio parahaemolyticus* and *Vibrio harveyi*. Frontiers in Cellular and Infection Microbiology, 14. https://doi.org/10.3389/fcimb.2024.1340910

Falcón García, C., Kretschmer, M., Lozano-Andrade, C. N., Schönleitner, M., Dragoŝ, A., Kovács, Á. T., & Lieleg, O. (2020). Metal ions weaken the hydrophobicity and antibiotic resistance of *Bacillus subtilis* NCIB 3610 biofilms. Npj Biofilms and Microbiomes, 6(1). https://doi.org/10.1038/s41522-019-0111-8

Fan, L., Dai, H., Zhou, W., Yuan, L., Yang, J., Yang, Z., & Jiao, X. (2024). Unraveling the significance of calcium as a biofilm promotion signal for *Bacillus licheniformis* strains isolated from dairy products. Food Research International, 182, 114145. https://doi.org/10.1016/j.foodres.2024.114145

Flint, S., Bremer, P., Brooks, J., Palmer, J., Sadiq, F. A., Seale, B., Teh, K. H., Wu, S., & Md Zain, S. N. (2020). Bacterial fouling in dairy processing. International Dairy Journal, 101, 104593. https://doi.org/10.1016/j.idairyj.2019.104593

Floyd, K. A., Eberly, A. R., & Hadjifrangiskou, M. (2017). Adhesion of bacteria to surfaces and biofilm formation on medical devices. Biofilms and Implantable Medical Devices, 47–95. https://doi.org/10.1016/b978-0-08-100382-4.00003-4

Fukushima, A., Kobayashi, T., Otsuka, Y., Hosokawa, N., Moody, S., Takagi, M., & Yoshida, A. (2024). A case of prosthetic valve endocarditis and aortic abscess due to *Bacillus cereus*. IDCases, 36, e01940–e01940. https://doi.org/10.1016/j.idcr.2024.e01940

Gadd, G. M. (1999, January 1). Fungal Production of Citric and Oxalic Acid: Importance in Metal Speciation, Physiology and Biogeochemical Processes (R. K. Poole, Ed.). ScienceDirect; Academic Press. https://www.sciencedirect.com/science/article/abs/pii/S0065291108601654

García-Lara, B., Saucedo-Mora, M. Á., Roldán-Sánchez, J. A., Pérez-Eretza, B., Ramasamy, M., Lee, J., Coria-Jimenez, R., Tapia, M., Varela-Guerrero, V., & García-Contreras, R. (2015). Inhibition of quorum-sensing-dependent virulence factors and biofilm formation of clinical and environmental *Pseudomonas aeruginosa* strains by ZnO nanoparticles. Letters in Applied Microbiology, 61(3), 299–305. https://doi.org/10.1111/lam.12456

Gatta, R., Wiese, A., Iwanicki, A., & Obuchowski, M. (2022). Influence of glucose on swarming and quorum sensing of Dickeya solani. PLoS ONE, 17(2), e0263124. https://doi.org/10.1371/journal.pone.0263124

Gerasimov, A., Chugunova, M., & Polyak, Y. (2021). Changes in Salinity and Toxicity of Soil Contaminated with De-icing Agents during Growing Season. Environmental Research, Engineering and Management, 77(2), 53–62. https://doi.org/10.5755/j01.erem.77.2.23633

Gloag, E. S., Turnbull, L., & Whitchurch, C. B. (2015). Bacterial Stigmergy: An Organising Principle of Multicellular Collective Behaviours of Bacteria. Scientifica, 2015, 1–8. https://doi.org/10.1155/2015/387342

Gomes, I. B., Lemos, M., Fernandes, S., Borges, A., Simões, L. C., & Simões, M. (2021). The Effects of Chemical and Mechanical Stresses on *Bacillus cereus* and *Pseudomonas fluorescens* Single- and Dual-Species Biofilm Removal.

Microorganisms, 9(6), 1174–1174. https://doi.org/10.3390/microorganisms9061174

Griffiths, M. W., & Schraft, H. (2017, January 1). Chapter 20 - *Bacillus cereus* Food Poisoning (C. E. R. Dodd, T. Aldsworth, R. A. Stein, D. O. Cliver, & H. P. Riemann, Eds.). ScienceDirect; Academic Press. https://www.sciencedirect.com/science/article/abs/pii/B9780123850072000206

H.G. Gowtham, Sudarshana Brijesh Singh, Natarajamurthy Shilpa, Aiyaz, M., Kalegowda Nataraj, Udayashankar, A. C., Kestur Nagaraj Amruthesh, Murali, M., Mirza, B., Gafur, A., Almalki, W. H., & Sayyed, R. Z. (2022). Insight into Recent Progress and Perspectives in Improvement of Antioxidant Machinery upon PGPR Augmentation in Plants under Drought Stress: A Review. Antioxidants, 11(9), 1763–1763. https://doi.org/10.3390/antiox11091763

Haas, K. T., Wightman, R., Peaucelle, A., & Höfte, H. (2021). The role of pectin phase separation in plant cell wall assembly and growth. The Cell Surface, 7, 100054. https://doi.org/10.1016/j.tcsw.2021.100054

Hadrup, N., Frederiksen, M., & Sharma, A. K. (2021). Toxicity of boric acid, borax and other boron containing compounds: A review. Regulatory Toxicology and Pharmacology, 121, 104873. https://doi.org/10.1016/j.yrtph.2021.104873

Hall, C. W., & Mah, T.-F. (2017). Molecular mechanisms of biofilm-based antibiotic resistance and tolerance in pathogenic bacteria. FEMS Microbiology Reviews, 41(3), 276–301. https://doi.org/10.1093/femsre/fux010

Haney, E. F., Trimble, M. J., Cheng, J. T., Vallé, Q., & Hancock, R. E. W. (2018). Critical Assessment of Methods to Quantify Biofilm Growth and Evaluate Antibiofilm Activity of Host Defence Peptides. Biomolecules, 8(2). https://doi.org/10.3390/biom8020029

Hayrapetyan, H., Muller, L., Tempelaars, M., Abee, T., & Nierop Groot, M. (2015). Comparative analysis of biofilm formation by *Bacillus cereus* reference strains and undomesticated food isolates and the effect of free iron. International Journal of Food Microbiology, 200, 72–79. https://doi.org/10.1016/j.ijfoodmicro.2015.02.005

Hsueh, Y.-H., Somers, E. B., Lereclus, D., & Wong, A. C. L. (2006). Biofilm Formation by *Bacillus cereus* Is Influenced by PlcR, a Pleiotropic Regulator. Applied and Environmental Microbiology, 72(7), 5089–5092. https://doi.org/10.1128/AEM.00573-06

Hu, Y., Chen, C., Liu, S., Zhou, Y., Jia, W., & Cao, Y. (2022). Biofilm-induced corrosion inhibition of Q235 carbon steel by anaerobic *Bacillus cereus* inoculum in simulated cooling water. Environmental Science and Pollution Research International, 30(8), 20833–20848. https://doi.org/10.1007/s11356-022-23561-0

Huang, Y., Chakraborty, S., & Liang, H. (2020). Methods to probe the formation of biofilms: applications in foods and related surfaces. Analytical Methods, 12(4), 416–432. https://doi.org/10.1039/C9AY02214G

Huang, Y., Flint, S. H., & Palmer, J. S. (2020). *Bacillus cereus* spores and toxins – The potential role of biofilms. Food Microbiology, 90, 103493. https://doi.org/10.1016/j.fm.2020.103493

Huang, Z., Lin, Y., Ren, F., Song, S., & Guo, H. (2019). Benzalkonium bromide is effective in removing *Bacillus cereus* biofilm on stainless steel when combined with cleaning-in-place. Food Control, 105, 13–20. https://doi.org/10.1016/j.foodcont.2019.05.017

Hussain, M. S., Kwon, M., & Oh, D.-H. (2018). Impact of manganese and heme on biofilm formation of *Bacillus cereus* food isolates. PLOS ONE, 13(7), e0200958. https://doi.org/10.1371/journal.pone.0200958

Hussain, M. S., Kwon, M., & Oh, D.-H. (2018). Impact of manganese and heme on biofilm formation of *Bacillus cereus* food isolates. PLOS ONE, 13(7), e0200958. https://doi.org/10.1371/journal.pone.0200958

Hussain, M. S., Kwon, M., Tango, C. N., & Oh, D. H. (2018). Effect of Electrolyzed Water on the Disinfection of *Bacillus cereus* Biofilms: The Mechanism of Enhanced Resistance of Sessile Cells in the Biofilm Matrix. Journal of Food Protection, 81(5), 860–869. https://doi.org/10.4315/0362-028x.jfp-17-450

Hwang, J., Lee, S., Ho Geon Lee, Choi, D., & Kyung Min Lim. (2022). Evaluation of Skin Irritation of Acids Commonly Used in Cleaners in 3D-Reconstructed Human Epidermis Model, KeraSkinTM. Toxics, 10(10), 558–558. https://doi.org/10.3390/toxics10100558

İnce, G. (2022). In vitro Activity of Boric Acid against Biofilm Formation and Biofilm Viability in Medically Important Microorganisms. Erciyes Medical Journal. https://doi.org/10.14744/etd.2022.78910

Iryna Kulkova, Jakub Dobrzyński, Kowalczyk, P., Grzegorz Bełżecki, & Kramkowski, K. (2023). Plant Growth Promotion Using *Bacillus cereus*. International Journal of Molecular Sciences, 24(11), 9759–9759. https://doi.org/10.3390/ijms24119759

Isakova, O. M., Turayev, Z., Ergasheva, Z. S., Mamayunusova, M. G., & Ikramov, M. X. (2024). Solubility in manganese sulfate-ammonium sulfate-water system. E3S Web of Conferences, 486, 05019. https://doi.org/10.1051/e3sconf/202448605019

Jiao, H., Xu, W., Hu, Y., Tian, R., & Wang, Z. (2022). Citric Acid in Rice Root Exudates Enhanced the Colonization and Plant Growth-Promoting Ability of *Bacillus altitudinis* LZP02. Microbiology Spectrum, 10(6). https://doi.org/10.1128/spectrum.01002-22

Johnson, A. A., & Cuellar, T. L. (2023). Glycine and aging: Evidence and mechanisms. Ageing Research Reviews, 87, 101922. https://doi.org/10.1016/j.arr.2023.101922

Jovanovic, J., Ornelis, V. F. M., Madder, A., & Rajkovic, A. (2021). *Bacillus cereus* food intoxication and toxicoinfection. Comprehensive Reviews in Food Science and Food Safety, 20(4), 3719–3761. https://doi.org/10.1111/1541-4337.12785

Kang, J., Liu, L., Wu, X., Sun, Y., & Liu, Z. (2018). Effect of thyme essential oil against *Bacillus cereus* planktonic growth and biofilm formation. Applied Microbiology and Biotechnology, 102(23), 10209–10218. https://doi.org/10.1007/s00253-018-9401-y

Kasahara, S., Maeda, K., & Ishikawa, M. (2004). Influence of phosphorus on biofilm accumulation in drinking water distribution systems. Water Science and Technology: Water Supply, 4(5-6), 389–398. https://doi.org/10.2166/ws.2004.0130

Kearns, D. B., & Losick, R. (2004). Swarming motility in undomesticated *Bacillus subtilis*. Molecular Microbiology, 49(3), 581–590. https://doi.org/10.1046/j.1365-2958.2003.03584.x

Kenichiro Yaita, Kenji Gotoh, Nakano, R., Iwahashi, J., Sakai, Y., Horita, R., Yano, H., & Watanabe, H. (2019). Biofilm-Forming by Carbapenem Resistant *Enterobacteriaceae* May Contribute to the Blood Stream Infection. International Journal of Molecular Sciences, 20(23), 5954–5954. https://doi.org/10.3390/ijms20235954

Kim, M.-J., Kim, S., Shin, S., & Kim, G. (2021). Production of high-purity MgSO4 from seawater desalination brine. Desalination, 518, 115288. https://doi.org/10.1016/j.desal.2021.115288

Koizumi, Y., Okuno, T., Hitoshi Minamiguchi, Hodohara, K., Hiroshige Mikamo, & Andoh, A. (2020). Survival of a case of *Bacillus cereus* meningitis with brain abscess presenting as immune reconstitution syndrome after febrile neutropenia – a case report and literature review-. BMC Infectious Diseases, 20(1). https://doi.org/10.1186/s12879-019-4753-1

Kwon, M., Hussain, M. S., & Oh, D. H. (2017). Biofilm formation of *Bacillus cereus* under food-processing-related conditions. Food Science and Biotechnology, 26(4), 1103–1111. https://doi.org/10.1007/s10068-017-0129-8

Lapeyrie, F., Chilvers, G. A., & Bhem, C. A. (1987). Oxalic Acid Synthesis by The Mycorrhizal Fungus *Paxillus Involutus* (Batsch. Ex Fr.) Fr. New Phytologist, 106(1), 139–146. https://doi.org/10.1111/j.1469-8137.1987.tb04797.x

Leire Goñi-Ciaurriz, & Itziar Vélaz. (2023). Chapter 4. Antibacterial properties of polylactic acid composites for food packaging. De Gruyter EBooks, 73–100. https://doi.org/10.1515/9783111067285-004

Lemos, M., Borges, A., Teodósio, J., Araújo, P., Filipe Mergulhão, Melo, L., & Simões, M. (2014). The effects of ferulic and salicylic acids on *Bacillus cereus* and *Pseudomonas fluorescens* single- and dual-species biofilms. International Biodeterioration & Biodegradation, 86, 42–51. https://doi.org/10.1016/j.ibiod.2013.06.011

Lemos, M., Mergulhão, F., Melo, L., & Simões, M. (2015). The effect of shear stress on the formation and removal of *Bacillus cereus* biofilms. Food and Bioproducts Processing, 93, 242–248. https://doi.org/10.1016/j.fbp.2014.09.005

Li, C., Chen, X., Guo, H., Zhou, X., & Cao, J. (2021). Production of Potash and N-Mg Compound Fertilizer via Mineral Shoenite from Kunteyi Salt Lake: Phase Diagrams of Quaternary System $(NH_4)_2SO_4$-$MgSO_4$-$K_2SO_4$-$H_2O$ in the Isothermal Evaporation and Crystallization Process. Acta Geologica Sinica/Acta Geologica Sinica, 95(3), 1016–1023. https://doi.org/10.1111/1755-6724.14409

Li, M., Shu, C., Ke, W., Li, X., Yu, Y., Guan, X., & Huang, T. (2021). Plant Polysaccharides Modulate Biofilm Formation and Insecticidal Activities of *Bacillus thuringiensis* Strains. Frontiers in Microbiology, 12. https://doi.org/10.3389/fmicb.2021.676146

Li, Y., Chen, N., Wu, Q., Liang, X., Yuan, X., Zhu, Z., Zheng, Y., Yu, S., Chen, M., Zhang, J., Wang, J., & Ding, Y. (2022). A Flagella Hook Coding Gene flgE Positively Affects Biofilm Formation and Cereulide Production in Emetic *Bacillus cereus*. Frontiers in Microbiology, 13. https://doi.org/10.3389/fmicb.2022.897836

Li, Y., Liao, C., & Tjong, S. C. (2020). Recent Advances in Zinc Oxide Nanostructures with Antimicrobial Activities. International Journal of Molecular Sciences, 21(22), 8836. https://doi.org/10.3390/ijms21228836

Lin, C.-S., Tsai, Y.-H., Chang, C.-J., Tseng, S.-F., Wu, T.-R., Lu, C.-C., Wu, T.-S., Lu, J.-J., Horng, J.-T., Martel, J., Ojcius, D. M., Lai, H.-C., & Young, J. D. (2016). An iron detection system determines bacterial swarming initiation and biofilm formation. Scientific Reports, 6(1), 36747. https://doi.org/10.1038/srep36747

Lin, Y., Briandet, R., & Kovács, Á. T. (2022). *Bacillus cereus* sensu lato biofilm formation and its ecological importance. Biofilm, 4, 100070. https://doi.org/10.1016/j.bioflm.2022.100070

Liu, M. M., Coleman, S., Wilkinson, L., Smith, M. L., Hoang, T., Niyah, N., Mukherjee, M., Huynh, S., Parker, C. T., Kovac, J., Hancock, R. E. W., & Gaynor, E. C. (2020). Unique inducible filamentous motility identified in pathogenic *Bacillus cereus* group species. The ISME Journal, 14(12), 2997–3010. https://doi.org/10.1038/s41396-020-0728-x

Liu, X.-Y., Hu, Q., Xu, F., Ding, S.-Y., & Zhu, K. (2020). Characterization of *Bacillus cereus* in Dairy Products in China. Toxins, 12(7), 454. https://doi.org/10.3390/toxins12070454

Liu, Y., Wu, L., Han, J., Dong, P., Luo, X., Zhang, Y., & Zhu, L. (2021). Inhibition of Biofilm Formation and Related Gene Expression of Listeria monocytogenes in Response to Four Natural Antimicrobial Compounds and Sodium Hypochlorite. Frontiers in Microbiology, 11. https://doi.org/10.3389/fmicb.2020.617473

Lu, L., Hu, X., Zeng, R., Lin, Q., Huang, X., Wei, Q., Tang, D., & Knopp, D. (2023). Ag/MoO3–Pd-mediated gasochromic reaction: An efficient dual-mode photoelectrochemical and photothermal immunoassay. Biosensors and Bioelectronics, 230, 115267–115267. https://doi.org/10.1016/j.bios.2023.115267

M Rollán-Martínez Herrera, P González-Urdiales, A Zubizarreta-Zamalloa, E Rodríguez-Merino, & F Martínez-Dubarbie. (2022). Infección del sistema nervioso central por *Bacillus cereus*: descripción de un caso y revisión de la bibliografía. Https://Www.sciencedirect.com/Science/Article/Pii/S2214250922001536, 75(08), 239–239. https://doi.org/10.33588/rn.7508.2021412

Ma, H., & Katzenmeyer-Pleuss, K. N. (2017). Molecular Approaches for Studying Medical Device-Associated Biofilms: Techniques, Challenges, and Future Prospects. Springer EBooks, 97–126. https://doi.org/10.1007/978-3-319-57494-3_4

Ma, Q., Wang, X., Yuan, W., Tang, H., & Luan, M. (2021). The Optimal Concentration of KH2PO4 Enhances Nutrient Uptake and Flower Production in Rose Plants via Enhanced Root Growth. Agriculture, 11(12), 1210. https://doi.org/10.3390/agriculture11121210

Machado, I., Silva, L. R., Giaouris, E. D., Melo, L. F., & Simões, M. (2020). Quorum sensing in food spoilage and natural-based strategies for its inhibition. Food Research International, 127, 108754. https://doi.org/10.1016/j.foodres.2019.108754

Majed, R., Faille, C., Kallassy, M., & Gohar, M. (2016). *Bacillus cereus* Biofilms—Same, Only Different. Frontiers in Microbiology, 7. https://doi.org/10.3389/fmicb.2016.01054

Malik-Tabassum, K., Hussain, Y. S., Scott, K. S., & Farndon, M. (2017). *Bacillus cereus*: A causative organism for deep soft tissue infection to forearm following trauma. Journal of Arthroscopy and Joint Surgery, 4(2), 100–102. https://doi.org/10.1016/j.jajs.2017.05.001

María Gabriela Paraje. (2023). Biofilms: the Achilles' Heel of Antimicrobial Resistance. Bentham Science Publishers E Books, 225–241. https://doi.org/10.2174/9789815049428123010011

Mariano José Lacosegliaz, Mariela Analía Torres, Carolina, A., Bertani, I., Venturi, V., Castellanos, I., Pablo Marcelo Fernández, & Carlos Gabriel Nieto-Peñalver. (2021). Copper sulfate inhibition of quorum sensing in Pseudomonas capeferrum is

dependent on biotic interactions. Rhizosphere, 20, 100434–100434. https://doi.org/10.1016/j.rhisph.2021.100434

Marsden, A. E., Grudzinski, K., Ondrey, J. M., DeLoney-Marino, C. R., & Visick, K. L. (2017). Impact of Salt and Nutrient Content on Biofilm Formation by *Vibrio fischeri*. PLOS ONE, 12(1), e0169521. https://doi.org/10.1371/journal.pone.0169521

Martinko, K., Ivanković, S., Lazarević, B., Đermić, E., & Đermić, D. (2022). Control of Early Blight Fungus (*Alternaria alternata*) in Tomato by Boric and Phenylboronic Acid. Antibiotics, 11(3), 320. https://doi.org/10.3390/antibiotics11030320

McDowell, R. H., Friedman, H., & Sands, E. M. (2023, January 23). *Bacillus Cereus*. Nih.gov; StatPearls Publishing. https://www.ncbi.nlm.nih.gov/books/NBK459121/

Messelhäußer, U., & Ehling-Schulz, M. (2018). *Bacillus cereus*—a Multifaceted Opportunistic Pathogen. Current Clinical Microbiology Reports, 5(2), 120–125. https://doi.org/10.1007/s40588-018-0095-9

Mo Ahamad Khan, Showkat Ahmad Lone, Shahid, M., Mohammad Tarique Zeyad, Syed, A., Aquib Ehtram, Elgorban, A. M., Verma, M., & Danish, M. (2023). Phytogenically Synthesized Zinc Oxide Nanoparticles (ZnO-NPs) Potentially Inhibit the Bacterial Pathogens: In Vitro Studies. Toxics, 11(5), 452–452. https://doi.org/10.3390/toxics11050452

Mougin, J., Roquigny, R., Travers, M.-A., Grard, T., Bonnin-Jusserand, M., & Le Bris, C. (2020). Development of a mreB-targeted real-time PCR method for the quantitative detection of *Vibrio harveyi* in seawater and biofilm from aquaculture systems. Aquaculture, 525, 735337. https://doi.org/10.1016/j.aquaculture.2020.735337

N. Thampuran, & P.K. Surendran. (1996). Effect of chemical agents on swarming of *Bacillus* species. Journal of Applied Bacteriology, 80(3), 296–302. https://doi.org/10.1111/j.1365-2672.1996.tb03223.x

Nagrale, D. T., Aalok Ranjan Chaurasia, Kumar, S., Gawande, S. P., Hiremani, N. S., Shankar, R., Nandini Gokte-Narkhedkar, Renu, & Prasad, Y. G. (2023). PGPR: the treasure of multifarious beneficial microorganisms for nutrient mobilization, pest biocontrol and plant growth promotion in field crops. World Journal of Microbiology & Biotechnology, 39(4). https://doi.org/10.1007/s11274-023-03536-0

Newman, P., Garcia, M., Ward, R., Killian, J., & Mayberry, S. (2022). A Rare Case of *Bacillus cereus* Septic Arthritis. Cureus. https://doi.org/10.7759/cureus.33148

NOZAKA, S., FURUKAWA, S., SASAKI, M., HIRAYAMA, S., OGIHARA, H., & MORINAGA, Y. (2014). Manganese Ion Increases LAB-yeast Mixed-species

Biofilm Formation. Bioscience of Microbiota, Food and Health, 33(2), 79–84. https://doi.org/10.12938/bmfh.33.79

O'Gara, J. P. (2007). Ica and beyond: biofilm mechanisms and regulation in *Staphylococcus epidermidis* and *Staphylococcus aureus*. FEMS Microbiology Letters, 270(2), 179–188. https://doi.org/10.1111/j.1574-6968.2007.00688.x

O'May, C., Ciobanu, A., Lam, H., & Tufenkji, N. (2012). Tannin derived materials can block swarming motility and enhance biofilm formation in *Pseudomonas aeruginosa*. Biofouling, 28(10), 1063–1076. https://doi.org/10.1080/08927014.2012.725130

Odeyemi, O. A., Alegbeleye, O. O., Strateva, M., & Stratev, D. (2020). Understanding spoilage microbial community and spoilage mechanisms in foods of animal origin. Comprehensive Reviews in Food Science and Food Safety, 19(2), 311–331. https://doi.org/10.1111/1541-4337.12526

Okabe, S., Kokazi, T., & Watanabe, Y. (2002). Biofilm formation potentials in drinking waters treated by different advanced treatment processes. Water Science and Technology: Water Supply, 2(4), 97–104. https://doi.org/10.2166/ws.2002.0126

Oknin, H., Steinberg, D., & Shemesh, M. (2015). Magnesium ions mitigate biofilm formation of *Bacillus* species via downregulation of matrix genes expression. Frontiers in Microbiology, 6. https://doi.org/10.3389/fmicb.2015.00907

Oliveira, G. S., Lopes, D. R. G., Andre, C., Silva, C. C., Baglinière, F., & Vanetti, M. C. D. (2019). Multispecies biofilm formation by the contaminating microbiota in raw milk. Biofouling, 35(8), 819–831. https://doi.org/10.1080/08927014.2019.1666267

Ong, C. C., & Chen, Y.-H. (2022). Investigation on Cell Disruption Techniques and Supercritical Carbon Dioxide Extraction of *Mortierella alpina* Lipid. Foods, 11(4), 582. https://doi.org/10.3390/foods11040582

Pa, A., Pavan, D., & Jacob, L. (2023). Biofilm Formation by *Staphylococcus Aureus* and Detection Of Biofilm Producing *Staphylococci*. International Journal of Scientific and Research Publications, 13(3). https://doi.org/10.29322/ijsrp.13.03.2023.p13535

Park, E., Hussain, M. S., Wei, S., Kwon, M., & Oh, D.-H. (2019). Genotypic and phenotypic characteristics of biofilm formation of emetic toxin producing *Bacillus cereus* strains. Food Control, 96, 527–534. https://doi.org/10.1016/j.foodcont.2018.10.008

Park, H. S., Yang, J., Choi, H. J., & Kim, K. H. (2017). Effective Thermal Inactivation of the Spores of *Bacillus cereus* Biofilms Using Microwave. Journal of Microbiology and Biotechnology, 27(7), 1209–1215. https://doi.org/10.4014/jmb.1702.02009

Patriquin, G. M., Banin, E., Gilmour, C., Tuchman, R., Greenberg, E. P., & Poole, K. (2007). Influence of Quorum Sensing and Iron on Twitching Motility and Biofilm Formation in *Pseudomonas aeruginosa*. Journal of Bacteriology, 190(2), 662–671. https://doi.org/10.1128/jb.01473-07

Pei, K., Xiao, K., Hou, H., Tao, S., Xu, Q., Liu, B., Yu, Z., Yu, W., Wang, H., Xue, Y., Liang, S., Hu, J., Deng, H., & Yang, J. (2020). Improvement of sludge dewaterability by ammonium sulfate and the potential reuse of sludge as nitrogen fertilizer. Environmental Research, 191, 110050. https://doi.org/10.1016/j.envres.2020.110050

Przekwas, J., Wiktorczyk, N., Budzyńska, A., Wałecka-Zacharska, E., & Gospodarek-Komkowska, E. (2020). Ascorbic Acid Changes Growth of Food-Borne Pathogens in the Early Stage of Biofilm Formation. Microorganisms, 8(4), 553. https://doi.org/10.3390/microorganisms8040553

Qin, Y., Leticia Lima Angelini, & Chai, Y. (2022). *Bacillus subtilis* Cell Differentiation, Biofilm Formation and Environmental Prevalence. Microorganisms, 10(6), 1108–1108. https://doi.org/10.3390/microorganisms10061108

Qin, Y., Li, Z., Sun, J., Xu, M., Gu, M., Wei, Y., & Lei, J. (2023). Manganese (II) sulfate affects the formation of iron-manganese oxides in soil and the uptake of cadmium and arsenic by rice. Ecotoxicology and Environmental Safety, 263, 115360–115360. https://doi.org/10.1016/j.ecoenv.2023.115360

Quinn, L., Barros, C., Vitale, S., & Casey, E. (2019). Extraction and identification of components of the biofilm matrix in *Pseudomonas* species biofilms. Access Microbiology, 1(1A). https://doi.org/10.1099/acmi.ac2019.po0219

Rajamma, S. B., Raj, A., Kalampalath, V., & Eapen, S. J. (2020). Elucidation of antibacterial effect of calcium chloride against *Ralstonia pseudosolanacearum* race 4 biovar 3 infecting ginger (Zingiber officinale Rosc.). Archives of Microbiology, 203(2), 663–671. https://doi.org/10.1007/s00203-020-02052-1

Rao, T. S. (2023, January 1). Chapter 40 - Industrial applications and implications of biofilms (S. Das & N. A. Kungwani, Eds.). ScienceDirect; Academic Press. https://www.sciencedirect.com/science/article/abs/pii/B9780323999779000296

Rehman, S., Mujtaba Ghauri, S., & Sabri, A. N. (2016). Impact of Plant Extracts and Antibiotics on Biofilm Formation of Clinical Isolates from Otitis Media. Jundishapur Journal of Microbiology, 9(1). https://doi.org/10.5812/jjm.29483

Rubinstein, A., Ezra, M., & Rokem, J. S. (1992). Adhesion of bacteria on pectin casted films. Microbios, 70(284-285), 163–170. https://pubmed.ncbi.nlm.nih.gov/1406337/

Sahli, C., Moya, S. E., Lomas, J. S., Gravier-Pelletier, C., Briandet, R., & Hémadi, M. (2022). Recent advances in nanotechnology for eradicating bacterial biofilm. *Theranostics*, *12*(5), 2383–2405. https://doi.org/10.7150/thno.67296

Saini, S., Tewari, S., Dwivedi, J., & Sharma, V. (2023). Biofilm Mediated Wastewater Treatment: A Comprehensive Review. Materials Advances. https://doi.org/10.1039/d2ma00945e

Sanchez-Vizuete, P., Dergham, Y., Bridier, A., Deschamps, J., Dervyn, E., Hamze, K., Aymerich, S., Le Coq, D., & Briandet, R. (2022). The coordinated population redistribution between *Bacillus subtilis* submerged biofilm and liquid-air pellicle. Biofilm, 4, 100065. https://doi.org/10.1016/j.bioflm.2021.100065

Sandra Pamela Cangui-Panchi, Anahí Lizbeth Ñacato-Toapanta, Leonardo Joshué Enríquez-Martínez, Reyes, J., Garzon-Chavez, D., & Liles, A. (2022). Biofilm-forming microorganisms causing hospital-acquired infections from intravenous catheter: A systematic review. Current Research in Microbial Sciences, 3, 100175–100175. https://doi.org/10.1016/j.crmicr.2022.100175

Santos, W. O., Mattiello, E. M., Vergutz, L., & Costa, R. F. (2016). Production and evaluation of potassium fertilizers from silicate rock. Journal of Plant Nutrition and Soil Science, 179(4), 547–556. https://doi.org/10.1002/jpln.201500484

Saxena, P., Joshi, Y., Rawat, K., & Bisht, R. (2018). Biofilms: Architecture, Resistance, Quorum Sensing and Control Mechanisms. Indian Journal of Microbiology, 59(1), 3–12. https://doi.org/10.1007/s12088-018-0757-6

Shao, T., Liu, L., Li, Y., Zhang, X., Deng, Z., Huo, L., & Gao, S. (2021). Highly Sensitive and Selective Detection of Long-Chain Alcohol Vapors Based on Keel-Type ZnO Fibers Derived from Waste Cigarette Butts. ACS Sustainable Chemistry & Engineering, 9(17), 5838–5848. https://doi.org/10.1021/acssuschemeng.0c08767

Sharma, P., Thakur, D., & Kumar, D. (2023). Novel Enzymatic Biosensor Utilizing a $MoS_2/MoO_3$ Nanohybrid for the Electrochemical Detection of Xanthine in Fish Meat. ACS Omega, 8(35), 31962–31971. https://doi.org/10.1021/acsomega.3c03776

Shen, Y., Zhu, W., Chen, C., Nie, Y., & Lin, X. (2016). Biofilm formation in attached microalgal reactors. Bioprocess and Biosystems Engineering, 39(8), 1281–1288. https://doi.org/10.1007/s00449-016-1606-9

Smith, V., Josefsen, M., Lindbäck, T., Hegna, I. K., Finke, S., Tourasse, N. J., Nielsen-LeRoux, C., Økstad, O. A., & Fagerlund, A. (2020). MogR Is a Ubiquitous Transcriptional Repressor Affecting Motility, Biofilm Formation and Virulence in *Bacillus thuringiensis*. Frontiers in Microbiology, 11. https://doi.org/10.3389/fmicb.2020.610650

Solis, R., & Sengupta, B. (2024). Abstract 1855 The Significance of Glucose Concentration on Bacterial Biofilm Formation. Journal of Biological Chemistry/□the □Journal of Biological Chemistry, 300(3), 105867–105867. https://doi.org/10.1016/j.jbc.2024.105867

Suparna DuttaSinha, Madhumita Choudhuri, Basu, T., Gupta, D., & Datta, A. (2021). Decisive Role of Polymer-BSA Interactions in Biofilm Substrates on “Philicity” and EPS Composition. BioRxiv (Cold Spring Harbor Laboratory). https://doi.org/10.1101/2021.02.26.433004

SYKES, J. A., & REED, R. (1949). The Control of the Swarming of *Proteus vulgaris* by Boric Acid. Journal of General Microbiology, 3(1), 117–121. https://doi.org/10.1099/00221287-3-1-117

Tamm, L., Thuerig, B., Apostolov, S., Blogg, H., Borgo, E., Corneo, P. E., Fittje, S., de Palma, M., Donko, A., Experton, C., Alcázar Marín, É., Morell Pérez, Á., Pertot, I., Rasmussen, A., Steinshamn, H., Vetemaa, A., Willer, H., & Herforth-Rahmé, J. (2022). Use of Copper-Based Fungicides in Organic Agriculture in Twelve European Countries. Agronomy, 12(3), 673. https://doi.org/10.3390/agronomy12030673

Tang, D., Gao, Q., Zhao, Y., Li, Y., Chen, P., Zhou, J., Xu, R., Wu, Z., Xu, Y., & Li, H. (2018). Mg2+ reduces biofilm quantity in *Acidithiobacillus ferrooxidans* through inhibiting Type IV pili formation. FEMS Microbiology Letters, 365(4). https://doi.org/10.1093/femsle/fnx266

Thérien, M., Kiesewalter, H. T., Auria, E., Charron-Lamoureux, V., Wibowo, M., Maróti, G., Kovács, Á. T., & Beauregard, P. B. (2020). Surfactin production is not essential for pellicle and root-associated biofilm development of *Bacillus subtilis*. Biofilm, 2, 100021. https://doi.org/10.1016/j.bioflm.2020.100021

Tirloni, E., Stella, S., Celandroni, F., Mazzantini, D., Bernardi, C., & Ghelardi, E. (2022). *Bacillus cereus* in Dairy Products and Production Plants. Foods, 11(17), 2572. https://doi.org/10.3390/foods11172572

Vatanshenassan, M., Boekhout, T., Mauder, N., Robert, V., Maier, T., Meis, J. F., Berman, J., Then, E., Kostrzewa, M., & Hagen, F. (2020). Evaluation of Microsatellite Typing, ITS Sequencing, AFLP Fingerprinting, MALDI-TOF MS, and Fourier-Transform Infrared Spectroscopy Analysis of *Candida auris*. Journal of Fungi, 6(3), 146. https://doi.org/10.3390/jof6030146

Vestby, L. K., Grønseth, T., Simm, R., & Nesse, L. L. (2020). Bacterial Biofilm and Its Role in the Pathogenesis of Disease. Antibiotics, 9(2), 59. https://doi.org/10.3390/antibiotics9020059

Vishwakarma, V. (2019). Impact of environmental biofilms: Industrial components and its remediation. Journal of Basic Microbiology. https://doi.org/10.1002/jobm.201900569

Vittoria, M., Saggese, A., Di Gregorio Barletta, G., Castaldi, S., Isticato, R., Baccigalupi, L., & Ricca, E. (2023). Sporulation efficiency and spore quality in a human intestinal isolate of *Bacillus cereus*. Research in Microbiology, 174(6), 104030. https://doi.org/10.1016/j.resmic.2023.104030

Wang, P., Zeng, W., Xu, S., Du, G., Zhou, J., & Chen, J. (2018). Current challenges facing one-step production of l-ascorbic acid. Biotechnology Advances, 36(7), 1882–1899. https://doi.org/10.1016/j.biotechadv.2018.07.006

Wijman, J. G. E., de Leeuw, P. P. L. A., Moezelaar, R., Zwietering, M. H., & Abee, T. (2007). Air-Liquid Interface Biofilms of *Bacillus cereus*: Formation, Sporulation, and Dispersion. Applied and Environmental Microbiology, 73(5), 1481–1488. https://doi.org/10.1128/aem.01781-06

Wu, H., Wu, L., Zhu, Q., Wang, J., Qin, X., Xu, J., Kong, L., Chen, J., Lin, S., Muhammad Umar Khan, Amjad, H., & Lin, W. (2017). The role of organic acids on microbial deterioration in the *Radix pseudostellariae* rhizosphere under continuous monoculture regimes. Scientific Reports, 7(1). https://doi.org/10.1038/s41598-017-03793-8

Xue, Y., Yu, C., Ouyang, H., Huang, J., & Kang, X. (2024). Uncovering the Molecular Composition and Architecture of the *Bacillus subtilis* Biofilm via Solid-State NMR Spectroscopy. Journal of the American Chemical Society, 146(17), 11906–11923. https://doi.org/10.1021/jacs.4c00889

Yan, F., Yu, Y., Gozzi, K., Chen, Y., Guo, J.-H., & Chai, Y. (2017). Genome-Wide Investigation of Biofilm Formation in *Bacillus cereus*. Applied and Environmental Microbiology, 83(13), e00561-17. https://doi.org/10.1128/AEM.00561-17

Yan, Z., Huang, M.-C., Melander, C., & Kjellerup, B. V. (2020). Dispersal and inhibition of biofilms associated with infections. Journal of Applied Microbiology, 128(5), 1279–1288. https://doi.org/10.1111/jam.14491

Yaron, S., & Römling, U. (2014). Biofilm formation by enteric pathogens and its role in plant colonization and persistence. Microbial Biotechnology, 7(6), 496–516. https://doi.org/10.1111/1751-7915.12186

Yasmeen, T., Ahmad, A., Arif, M. S., Mubin, M., Rehman, K., Shahzad, S. M., Iqbal, S., Rizwan, M., Ali, S., Alyemeni, M. N., & Wijaya, L. (2020). Biofilm forming rhizobacteria enhance growth and salt tolerance in sunflower plants by stimulating antioxidant enzymes activity. Plant Physiology and Biochemistry, 156, 242–256. https://doi.org/10.1016/j.plaphy.2020.09.016

Yu, Z., & Guo, J. (2022). Non-caloric artificial sweeteners exhibit antimicrobial activity against bacteria and promote bacterial evolution of antibiotic tolerance. Journal of Hazardous Materials, 433, 128840. https://doi.org/10.1016/j.jhazmat.2022.128840

Zhang, C., Zhang, R., & Yuan, J. (2024). Potassium-mediated bacterial chemotactic response. ELife, 12, RP91452. https://doi.org/10.7554/eLife.91452

Zhao, L., Duan, F., Gong, M., Tian, X., Guo, Y., Jia, L., & Deng, S. (2021). (+)-Terpinen-4-ol Inhibits *Bacillus cereus* Biofilm Formation by Upregulating the Interspecies Quorum Sensing Signals Diketopiperazines and Diffusing Signaling Factors. Journal of Agricultural and Food Chemistry, 69(11), 3496–3510. https://doi.org/10.1021/acs.jafc.0c07826

Zheng, J., Lin, L., Liao, J., Zhao, X., Lin, J., & Duan, F. (2024). Endophthalmitis Caused by *Bacillus cereus*: Clinical Characteristics, Outcomes and Antibiotic Susceptibility. Antibiotics, 13(7), 658. https://doi.org/10.3390/antibiotics13070658